Development of Orientation-Birefringence-Controlled Optical Polymers via Synthesis and Combination of Bottlebrush Polymers

January 2025

Masaki Tamura

A Thesis for the Degree of Ph.D. in Engineering

Development of Orientation-Birefringence-Controlled Optical Polymers via Synthesis and Combination of Bottlebrush Polymers

January 2025

Graduate School of Science and Technology

Keio University

Masaki Tamura

CONTENTS

FIGURE LIST

TABLE LIST

Chapter 1

Introduction

1.1 Optical polymer

1.1.1 Background

1.1.1.1 Definition of optical polymers

An optical polymer is a type of polymeric material designed specifically for optical applications where the transmission, reflection, or control of light is critical. These materials have optical properties that make them suitable for use in applications as shown in Figure 1.1.

Figure 1.1 Applications of optical polymers

1.1.1.2 Properties and characteristics of optical polymers

The usage of optical polymers originally started as an alternative to optical glass, therefore, optical polymers were required to have properties and characteristics similar to those of optical glass. Optical polymers are currently used as not only alternatives to optical glass but also unique materials for a wide variety of optical applications. However, the key properties and characteristics remain consistent, and they are as follows:

a) Transparency

Optical polymers are highly transparent and allow light to pass through with minimal scattering or absorption over a wide range of wavelengths, mainly in the visible light range. The high transparency makes them ideal for use in lenses, optical fibers, and display films.

b) Refractive Index

The refractive index is a measure of how much light bends as it passes through the material. Optical polymers with inherent refractive indices are engineered to perform the desired function on their own, or to match or complement other materials in an optical system. In many cases, a high refractive index is desirable. This is because optical polymers with high refractive indices can make lenses in eyeglasses and cameras thinner.

c) Mechanical Properties

In addition to the above optical properties, optical polymers must also have mechanical properties such as toughness, hardness, and flexibility, depending on each application. In evaluating the mechanical properties, items such as the tensile modulus (Young's modulus), tensile strength, and elongation at break are often emphasized.

d) Chemical Resistance

Many optical applications require that optical polymers are resistant to chemicals, particularly in environments where they might be exposed to solvents, oils, or other substances that could degrade their performance.

e) Durability

To ensure that optical devices using optical polymers maintain their functionality for a certain period of time, the optical polymers are required to possess durability to environmental factors such as ultraviolet light, humidity, and temperature changes.

f) Thermal Stability

Optical polymers need to maintain their optical and mechanical properties over a range of temperatures. This is particularly important in applications such as automotive lenses, where the material might be exposed to both high and low temperatures.

1.1.1.3 Types of optical polymers

A variety of practical optical polymers are limited compared to optical glass, because only some polymeric materials possess the properties and characteristics mentioned in the previous section. Typical optical polymers are as follows:

a) Poly(methyl methacrylate) (PMMA)

PMMA, which is commonly known as acrylic resin, is most widely used in various optical applications due to its high transparency and durability against ultraviolet light. It is also easy to process and a low-cost material. It is still fresh in our minds that PMMA was used as partitions (acrylic panels) between people during the time of COVID-19.

b) Polystyrene (PS)

PS, which is known as a very low-cost material, has relatively high refractive index in optical polymers. It is used as light diffusers in liquid crystal displays due to its lower cost and lower moisture-absorption than PMMA.

c) Polycarbonate (PC)

PC, which is known for its toughness and high impact resistance, is used in optical applications, where toughness, hardness and durability to thermal change are critical. As an example, it is used as lenses for eyeglasses and substrates for CDs / DVDs.

d) Cyclo-olefin polymer (COP) and Cyclo-olefin copolymer (COC)

COP and COC are comparatively new materials offering high optical transparency, extremely low moisture-absorption, and excellent chemical resistance, which make them suitable for advanced optical devices such as imaging lens systems with high resolution.

e) Optical epoxy resins

Optical epoxy resins are used in coatings and adhesives for optics, these resins provide strong bonds while maintaining transparency.

1.1.1.4 Advantages of optical polymers

Optical polymers possessed some advantages over optical glass, so they have generated remarkable developments in optical devises. The representative advantages are as follows:

a) Lightweight

Compared to optical glass, optical polymers are significantly light weight, which is very beneficial in portable devices such as smartphone cameras. Specifically, the specific gravity of optical polymers is 1.0 to 1.2 g/cm^3, while that of optical glass is more than 2.5 g/cm^3. Therefore, optical polymers can make optical devices considerably lighter.

b) Low cost

Many optical polymers are less expensive to manufacture and process than traditional optical materials such as optical glass. For example, in the case of lens elements used in the imaging lens systems of smartphone cameras, the cost of a lens made from an optical polymer is less than one-fifth that of optical glass after processing. The low cost can make them suitable for mass-production.

c) High flexibility in optical design

Optical polymers can be molded into complex shapes such as aspherical surfaces and freeform surfaces. Optical glass can also be molded into aspherical or freeform surfaces using low-melting-point glass; however, it is extremely difficult to process optical glass into complex shapes with inflection points that change from convex to concave or from concave to convex. Optical polymers, on the other hand, can be molded into such complex shapes because of their good moldability. Thus, optical polymers allow the use of such complex shapes in optical design, enabling innovative optical design that could not be realized before.

These advantages have made optical polymers indispensable to modern technology. Especially, since the usage of optical polymers for lenses of smartphone cameras has recently skyrocketed, high interest has been focused on the application of optical polymers to lenses for imaging lens systems.

1.1.2 Application of optical polymers to lenses

With the global proliferation of smartphones, the application of optical polymers to lenses for smartphone cameras has attracted much attention. In order to properly understand this background, this section covers the history of the development of optical polymers for lenses, the specific application of optical polymers to lenses for mobile-phone and smartphone cameras, and an issue on optical polymers in high-resolution imaging lens systems.

1.1.2.1 History of optical polymers for lenses in imaging lens systems

Table 1.1 shows the history of developments related to optical polymers for lenses in imaging lens systems.[1] Serious research on polymers as optical materials began in 1940 at Polaroid under contract with the U.S. National Defense Commission. This was before the development of injection molding technology, so the research was conducted primarily through cast molding. However, various material studies and a number of optical devices were developed in this research. The systematic and practical research conducted at this time, including measures to prevent degradation of performance due to moisture-absorption, is considered to be the starting point for the development of optical polymers. Shortly thereafter, injection molding technology and acrylic resins compatible with the injection molding were developed. In the 1960s, cameras (Instamatic, Kodak) equipped with a single lens with F-number 8 (f/8), made of injection-molded PMMA, began to appear on the market. Initially, the use of lenses made of optical polymers in imaging lens systems was limited to low-end cameras, however, in 1978, a high-performance f/1.9 imaging lens system combining glass and plastic lenses was used in the camera (Ektramax, Kodak). This lens system, which included an aspherical lens made of poly(cyclohexyl methacrylate) with low moisture-absorption, had a major impact on the subsequent development of lenses made of optical polymers.

Thereafter, successful examples of development that actively utilized the advantages of optical polymers, such as lightweight, low cost for mass production, and high flexibility in optical design, appeared in optical pickup lenses, eyeglass lenses, and contact lenses. In the area of imaging lens systems, optical polymers were used for the

lenses of lens-equipped films (Utsurundesu, Fujifilm) launched in 1986, and other competitors subsequently entered this category (Fujifilm achieved a cumulative production of one billion lens-equipped films in 2002). In materials, alicyclic polyolefin resins with low moisture-absorption and heat resistance, such as COP and COC, were developed in 1990, and the COP (Zeonex, ZEON) with high transparency began to be used as a material for lenses in imaging lens systems. In 1994, digital cameras were launched, and optical polymers were used in combination with optical glass in the lens systems of low-end compact digital cameras. By this time, a considerable amount of optical polymers were on the market, and the market changed even more significantly after the year 2000. That was the advent of mobile phones equipped with cameras.

Table 1.1 History of optical polymers for lenses in imaging lens systems

Year	Event
1940	Serious research on optical polymers for lenses started at Polaroid.
1943	Acrylic resins for injection molding were developed.
1963	The camera “Instamatic” (Kodak) equipped with a single plastic lens with f/8 was launched.
1978	The camera “Ektramax” (Kodak) with the f/1.9 imaging lens system combining glass and plastic lenses was released.
1986	The lens-equipped film “Utsurundesu” (Fujifilm) was launched.
1990	Alicyclic polyolefin resins were developed.
1994	Digital cameras were released.
2000	Mobile phones equipped with cameras were released.

1.1.2.2 Application of optical polymers to lenses for mobile-phone cameras

Since the introduction of camera-equipped mobile phones in 2000, their camera performance has evolved dramatically. As the lens system for mobile-phone cameras was required to be compact, lightweight, and low cost, optical glass could hardly be used as the lens material, especially due to its high cost. As a result, optical polymers got used for most of the lens materials. Then, as the number of pixels in the camera increased, the number of lenses composed of the lens system increased.

The lens system that initially consisted of only a single lens was replaced by a two-element lens system for cameras with more than 1 million pixels launched in 2003, a three-element lens system for cameras with 2 to 3 million pixels released around 2004, and a four-element lens system for cameras with more than 5 million pixels released in 2007 and later. This led to a large increase in shipments of optical polymers, but the increase was not yet dramatic. This was because although camera-equipped mobile phones were common in Japan and Korea, they were globally limited to high-end mobile phones, and camera-equipped mobile phones were not yet common worldwide. This situation was dramatically changed with the introduction of the smartphone developed by Apple.

1.1.2.3 Application of optical polymers to lenses for smartphone cameras

The first iPhone, which was the smartphone developed by Apple, was announced in 2007 and launched in the United States. Since the first iPhone adopted only a quad-band global system for mobile communications (GSM), it could not be used in countries and regions that did not adopt GSM as their communication method, it was not sold in such countries and regions. In addition, since the applications on the original iPhone were limited to Apple products and did not have many functions, the first iPhone did not spread worldwide in the beginning. However, the iPhone 3G, released the following year, was compatible with the 3rd generation mobile communication system (3G) and was launched in 22 regions, including North America, Europe, Australia, Japan, and Hong Kong. From this point on, smartphones began to spread throughout the world.

From its first model, the iPhone was equipped with a 2-megapixel rear camera,

and the iPhone made it standard for smartphones to have a camera. Since then, performance in smartphone cameras has evolved dramatically. Table 1.2 summarizes the development of cameras on major iPhones. The main camera of iPhone 14 Pro, introduced in 2022, finally reached 48 megapixels. As of 2024, the latest iPhone 16 Pro has three rear cameras with different angles of view and one front camera for the selfie, making it the flagship smartphone with multiple cameras. Other competitors have also released smartphones with multiple cameras with similar features, and flagship smartphones with multiple cameras have become commonplace around the world.

Table 1.2 Development of cameras on major iPhones

Year	Model	Feature of camera
2007	iPhone (Original)	2-megapixel main camera
2009	iPhone 3GS	3-megapixel main camera
2010	iPhone 4	5-megapixel main camera 0.3-megapixel selfie camera
2012	iPhone 5	8-megapixel main camera 1.2-megapixel selfie camera
2015	iPhone 6s	12-megapixel main camera 5-megapixel selfie camera
2016	iPhone 7 Plus	12-megapixel main camera 12-megapixel 2× telephoto camera 7-megapixel selfie camera
2019	iPhone 11 Pro	12-megapixel main camera 12-megapixel ultra-wide camera 12-megapixel 2× telephoto camera 12-megapixel selfie camera
2022	iPhone 14 Pro	48-megapixel main camera 12-megapixel ultra-wide camera 12-megapixel 3× telephoto camera 12-megapixel selfie camera
2024	iPhone 16 Pro	48-megapixel main camera 48-megapixel ultra-wide camera 12-megapixel 5× telephoto camera 12-megapixel selfie camera

In the lens systems for these cameras, the number of lenses that composed the lens system increased significantly as the number of pixels in the camera increased (i.e., the required resolution became higher). In addition, multiple lens systems were used for multi-cameras with different angles of view. As a result, the demand for optical polymers, which were the materials of the lenses used in these lens systems, increased dramatically. Since the use of optical polymers skyrocketed, a further technological interest turned to optical polymers.

1.1.2.4 Optical polymers for high-resolution imaging lens systems

Since the number of pixels in smartphone cameras increased, higher resolution was required for the lens systems used in the cameras. Therefore, optical polymers used as optical materials for the high-resolution imaging lens systems were also required to have greater optical properties.

Recently, special polycarbonates and fluorene polyesters with high refractive index and high chromatic dispersion were developed to compensate chromatic aberration with high precision while maintaining the transparency.[2, 3] The usage of these materials in combination with COP and COC has resulted in lens systems with high-resolution performance, greatly improving the camera performance of smartphones. Despite these developments, however, there remains one potential problem with polymer materials that can degrade resolution performance. That is birefringence. If a lens material in an imaging lens system has high birefringence, a light ray incident on the lens material is affected by the birefringence, gets split and refracted in different directions. As a result, the imaging point is slightly shifted, creating an image blur and degrading the resolution performance. Thus, lens materials used in high-resolution imaging lens systems are required to possess extremely low birefringence. In the case of utilizing optical polymers as lens materials for high-resolution imaging lens systems, the birefringence inherent in polymers must be carefully considered, unlike the case of utilizing glass materials.

1.2 Birefringence

1.2.1 Background

1.2.1.1 Definition of birefringence

Birefringence is an optical property of a material in which light propagates at different speeds depending on its direction of polarization, also known as double refraction. When a ray of light enters a birefringent material, it splits into two rays and travels through the material, following different paths. This is because the material with optical anisotropy has refractive indices which depend on polarization direction of light, indicating that there is difference in the refractive index along different axes within the material.

In isotropic materials like glass or water, the refractive index is uniform in all directions, and light travels at the same speed regardless of its orientation. However, in anisotropic materials such as calcite and quartz, the refractive index varies with direction. Figure 1.2 shows how unpolarized light incident slantingly passes through a birefringent material of uniaxial crystal, which means that optical anisotropy is exhibited in a single direction while optical isotropy is demonstrated in all directions perpendicular to it. This specific direction is identified as the optic axis of the birefringent material.

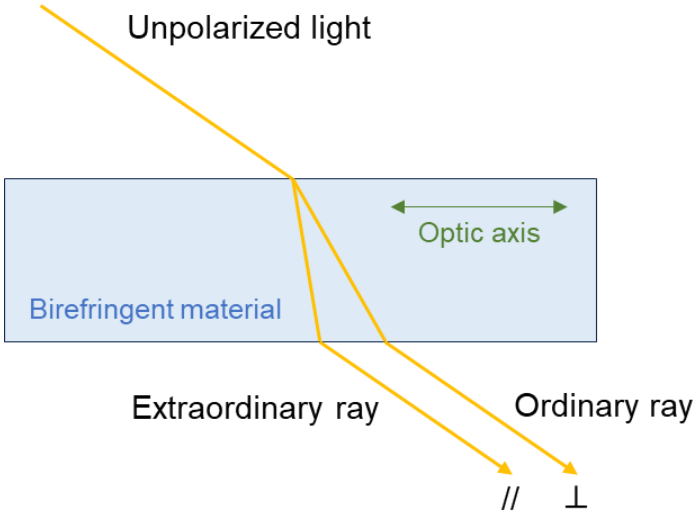

Figure 1.2 Behavior of unpolarized light incident to a birefringent material

When unpolarized light enters the birefringent material slantingly, it undergoes effect of birefringence from the material and splits into two rays. One is the ray polarized perpendicular to the optic axis, called the ordinary ray, which follows Snell's law[4] and behaves according to the material's ordinary refractive index. The other is the ray polarized parallel to the optic axis, called the extraordinary ray, which does not follow Snell's law because its refractive index varies with an incident angle. This is why an image appears double when looking at an object through a birefringent material such as calcite. In this case, birefringence (Δn) is calculated by the following equation.

$$\Delta n = n_e - n_o \tag{1.1}$$

where n_e is the refractive index of the extraordinary ray and n_o is that of the ordinary ray. As also recognized from this equation, birefringence can be two different values, positive or negative. Positive birefringence occurs when n_e is larger than n_o, i.e., the ordinary ray travels faster than the extraordinary ray in a material. It is often observed in materials such as quartz. Negative birefringence occurs when n_e is smaller than n_o, i.e., the ordinary ray travels slower than the extraordinary ray in a material. This is less common but can be found in materials such as calcite.

1.2.1.2 Birefringence of optical polymers

In optical polymers, birefringence occurs macroscopically due to orientation of the polymer chains, and direction of its orientation performs an optic axis of the birefringent material. Therefore, light incident on an optical polymer with oriented polymer chains is divided into a ray with polarization perpendicular to the orientation direction and another ray with polarization parallel to the orientation direction, each propagating through the optical polymer at a different speed. Figure 1.3 shows an example of an oriented main chain of PC and Figure 1.4 shows an example of an oriented main chain of PS. In Figure 1.3, the aromatic groups composing the main chains of PC oriented along the z-axis have a large optical anisotropy and illustrate a large polarizability in this direction. It results in $n_z > n_x = n_y$, where n_x, n_y, n_z are refractive indices along the

respective axes. When unpolarized light go through this PC material along y-axis, its birefringence is represented as $\Delta n = n_e - n_o = n_z - n_x > 0$, which denotes a positive value. In Figure 1.4, while the main chain of PS orients along the z-axis, the aromatic groups composing the side chains of PS orient perpendicular to z-axis. Thus, a large polarizability appears in the x-direction and the y-direction, resulting in $n_z < n_x = n_y$. In this case, when unpolarized light go through this PS material along y-axis, its birefringence is represented as $\Delta n = n_e - n_o = n_z - n_x < 0$, which denotes a negative value. Birefringence of optical polymers displays various values depending on their molecular structure. In addition, birefringence of optical polymers is generally classified into orientation birefringence and photoelastic birefringence. The details are described in the following sub-sections.

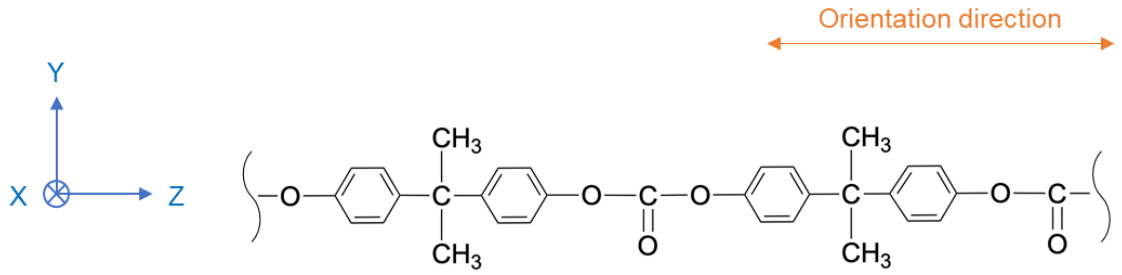

Figure 1.3 Example of an oriented main chain of polycarbonate

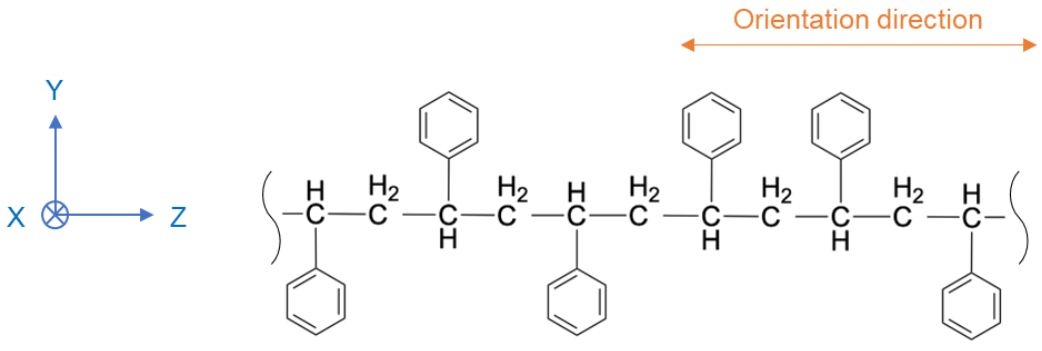

Figure 1.4 Example of an oriented main chain of polystyrene

1.2.1.3 Orientation birefringence

Orientation birefringence of optical polymers is generated by plastic deformation of a polymer in the molten state under shear or tensile stress in injection molding or extrusion, resulting in macroscopic alignment of polarization direction of atomic groups comprising the polymer. Since each monomer unit composing the polymer chain has some extent of anisotropy of molecular polarizability, the polarizability is maximum in a certain angular direction from a tangential direction of the polymer chain. Figure 1.5 shows the case where polarizability of a monomer unit is perpendicular to a polymer chain. A polarizability ellipsoid in Figure 1.5 is a schematic diagram to illustrate the anisotropy of molecular polarizability in the monomer unit. When the polymer chain is random, the polarizability ellipsoids of the monomer units are oriented in a random direction. The anisotropies of polarizability then cancel each other out, resulting in zero birefringence. When the polymer chain is oriented, the polarizability ellipsoids of the monomer units are macroscopically oriented in a certain direction, and birefringence appears. Birefringence generated by orientation of the polymer chain (Δn) is generally represented by the following equation,

$$\Delta n = n_{//} - n_{\perp} \tag{1.2}$$

where $n_{//}$ and $n_{\perp}$ are refractive indices of lights polarized parallel and perpendicular to the orientation of the polymer chain, respectively, corresponding to n_e and n_o in Equation 1.1.

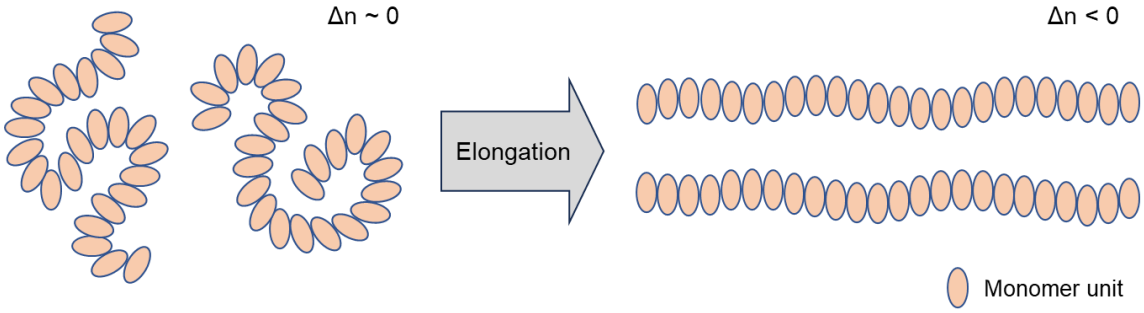

Figure 1.5 Appearance of birefringence due to orientation of polymer chains

When intrinsic birefringence, which is birefringence of a polymer oriented perfectly, is defined as Δn^0, the orientation birefringence (Δn_o) is calculated by the following equation,[5]

$$\Delta n_o = f \times \Delta n^0 \tag{1.3}$$

where f is the Hermans orientation function representing degree of orientation of the polymer chain.[6] The intrinsic birefringence is obtained by differentiating the Lorentz-Lorenz equation which represents relation between a refractive index and polarizability of a material,[7] represented as

$$\Delta n^0 = \frac{2\pi}{9} \times \frac{(\bar{n}^2 + 2)^2}{\bar{n}} \times \frac{\rho}{M} \times N_A \times \Delta\alpha \tag{1.4}$$

where $\bar{n}$ is an average refractive index, ρ is density of the polymer, M is molecular weight of a monomer unit composing the polymer, N_A is Avogadro's number, and $\Delta\alpha$ is difference in polarizability of the monomer unit for each direction. In the case that the polymer is uniaxially stretched to orient the polymer chain, the orientation function is defined as the following equation,[6]

$$f = \frac{3 < \cos^2\theta > -1}{2} \tag{1.5}$$

where θ is the angle between the stretching direction and a tangential direction of the polymer chain as shown in Figure 1.6. The orientation function can be acquired by the following equation via measurements of the infrared dichroic ratio $D = A_{//} / A_{\perp}$.[5]

$$f = \frac{D-1}{D+2} \times \frac{2\cot^2\varphi + 2}{2\cot^2\varphi - 1} \tag{1.6}$$

where $A_{//}$ and $A_{\perp}$ are the absorbances measured with radiation polarized parallel and perpendicular to the stretching direction, respectively, and φ is the angle between the transition moment vector of the absorbing group and the tangential direction of the polymer chain as shown in Figure 1.6. Thus, the intrinsic birefringence of the polymer can be evaluated by measuring the orientation function and the corresponding orientation birefringence. Table 1.3 shows the intrinsic birefringence values of the representative optical polymers.[8] The intrinsic birefringence of PC and PS is 20 times or more higher than that of PMMA, even though they are all used as optical polymers.

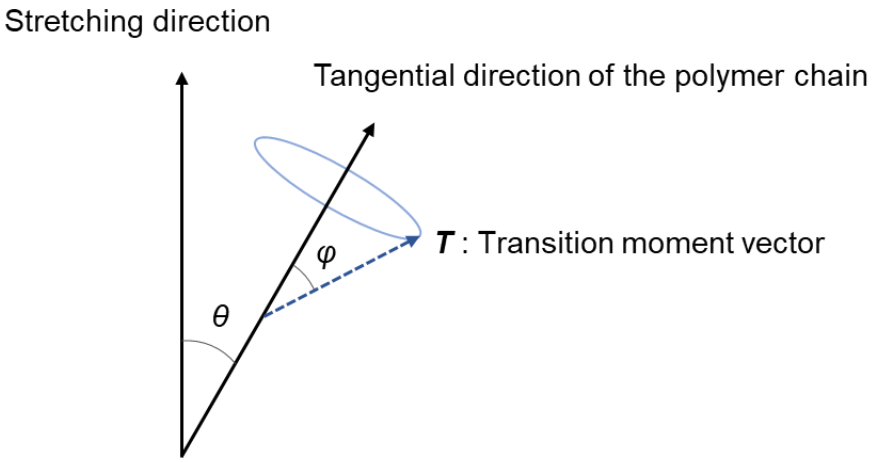

Figure 1.6 Relationship among stretching direction, polymer chain's direction, and the transition moment vector

Table 1.3 Intrinsic birefringence of PMMA, PS, and PC

Optical polymer	Intrinsic birefringence
PMMA	-0.004
PS	-0.100
PC	0.106

1.2.1.4 Photoelastic birefringence

Photoelastic birefringence of optical polymers results from residual stress in the solid polymer after manufacture and elastic deformation due to external forces. As well as the appearance of orientation birefringence, it is considered that certain atomic groups are slightly arranged along a direction of the stress or the deformation, generating photoelastic birefringence. In this case, the photoelastic birefringence (Δn_p) is represented by the following equation,

$$\Delta n_p = c \times \delta \tag{1.3}$$

where c is photoelastic coefficient, and δ is stress. Generally, if a polymer is under external forces and is made elastic deformation at lower temperature than its glass transition temperature (T_g), photoelastic birefringence will disappear after removing the external forces. In addition, if a polymer with residual stress is appropriately annealed at a little lower temperature than T_g, most of the residual stress can be removed and photoelastic birefringence can be sufficiently reduced. Therefore, in practical optical polymers, reducing photoelastic birefringence tends not to be as important as reducing orientation birefringence. Table 1.4 shows the photoelastic coefficients of PMMA, PS, and PC.[9, 10] It is known that PC has a much larger photoelastic coefficient than PMMA and PS.

Table 1.4 Photoelastic coefficient of PMMA, PS, and PC

Optical polymer	Photoelastic coefficient ($\times 10^{-12}$ Pa^{-1})
PMMA	-4.3
PS	9.4
PC	110

1.2.2 Previous studies on birefringence

In order to process optical polymers into desired shape while keeping orientation birefringence as low as possible, the following two methods can be considered:

a) To process a polymer so that the polymer chains are not oriented as much as possible.
b) To process a polymer which demonstrates little birefringence even if the polymer chains are oriented.

Initially, the method of processing polymers without making the polymer chains oriented was mainly developed. However, since shapes of polymer products became more complex and required higher precision, it had become rather difficult to reduce birefringence with this approach. Therefore, it became mainstream to develop polymers showing low birefringence even if the polymer chains are oriented, and many various studies have been conducted to investigate and control birefringence to date.

A method performed from the initial phase is to blend two polymers with positive and negative birefringence.[11-17] In this method called "polymer blend", blends with low birefringence can be produce even if the polymer chains are oriented after processing, because positive birefringence of a polymer can be appropriately offset by negative birefringence of another polymer. As transparency of the blend, which is an important property of an optical polymer, largely depends on miscibility of two blending polymers. As an example, Saito and Inoue reported limited combinations of polymers as shown in Table 1.5.[12]

Table 1.5 Birefringence-free polymer blends

Polymer pair (negative Δn / positive Δn)	Composition (weight ratio)	Stretching Temperature (°C)
PMMA / PVDF	80:20	90
PMMA / VDF･TrEF-58	90:10	90
PMMA / PEO	65:35	90
PS / PPO	71:29	180
S･LMI-19 / PPO	73.5:26.5	180
S･PMI-16 / PPO	74.5:25.5	180
S･CMI-17 / PPO	75.5:24.5	180
S･MAN-8 / PC	77:23	180
AS-25 / NBR-40	40:60	90

where the respective abbreviations in Table 1.5 are as follows:

PVDF : poly(vinylidene fluoride)

VDF･TrEF-58 : poly(vinylidene fluoride-cc-trifluoroethylene) (58 mol% VDF)

PEO : poly(ethylene oxide)

PPO : poly(phenylene oxide)

S･LMI-19 : poly(styrene-co-lauloyl maleimide) (19 wt% LMI)

S･PMI-16 : poly(styrene-co-phenyl maleimide) (16 wt% PMI)

S･CMI-17 : poly(styrene-co-cyclohexyl maleimide) (17 wt% CMI)

S･MAN-8 : poly(styrene-co-maleic anhydride) (8 wt% MAN)

AS-25 : poly(acrylonitrile-co-styrene) (25 wt% AN)

NBR-40 : poly(acrylonitrile-co-butadiene) (40 wt% AN)

Another method is to randomly copolymerize plural monomers with positive and negative birefringence.[18-30] In this method called “random copolymerization”, monomers with positive and negative birefringence are copolymerized in an appropriate ratio to

produce a polymer chain exhibiting almost zero birefringence even under orientation. Figure 1.7 shows a schematic diagram to illustrate the cancelation of birefringence with the random copolymerization. As anisotropy of polarizability is canceled at the polymer chain unit, a copolymer composed of the polymer chains demonstrates almost zero birefringence even when it is oriented. In addition, since the copolymer is an aggregate of polymer chains with the same monomer unit ratio and does not generate phase separation, it can acquire high transparency. Koike and his group reported copolymers, which were produced with random copolymerization and exhibited transparency, as shown in Table 1.6.[18, 19]

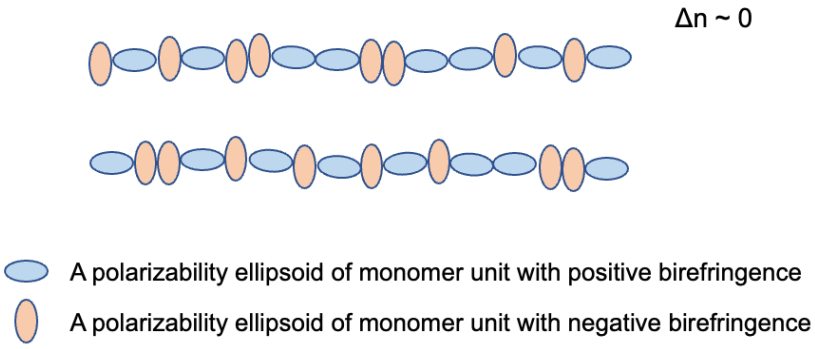

Figure 1.7 Cancelation of birefringence with the random copolymerization

Table 1.6 Birefringence-free random copolymers

Monomer pair (negative *Δn* / positive *Δn*)	Copolymerization ratio (weight ratio)
MMA / 3FMA	45:55
MMA / BzMA	82:18

where the respective abbreviations in Table 1.6 are as follows:

MMA : Methyl methacrylate

3FMA : Trifluoroethyl methacrylate

BzMA : Benzyl methacrylate

Another approach is to add anisotropic low-mass molecules[31-37] or birefringent crystals[38-43] which possess opposite birefringence to original materials. Figure 1.8 shows a schematic diagram to illustrate the compensation for birefringence by doping anisotropic molecules. This is the case of anisotropic molecules with positive birefringence appended to a polymer with negative birefringence. Anisotropic molecules have an elongated rod-like molecular shape in the same direction as their polarizability ellipsoid. When the polymer chains are oriented during molding, the anisotropic molecules are oriented along with the orientation of the polymer chains because of the rod-like molecular shape. By doping anisotropic molecules with the opposite sign to anisotropy of polarizability of the polymer chains, optical anisotropy of the polymer can be offset within a region of the molecular size level, thus canceling birefringence. The same effect on compensating for birefringence can be achieved when doping needle-shaped birefringent crystals, which possess opposite birefringence to a neat polymer, into the polymer. A unique feature of this approach is that it may be possible to achieve a material with extremely low birefringence while maintaining almost the same optical and thermal properties as the original material, because amounts of additive anisotropic molecules and birefringent crystals are relatively small.

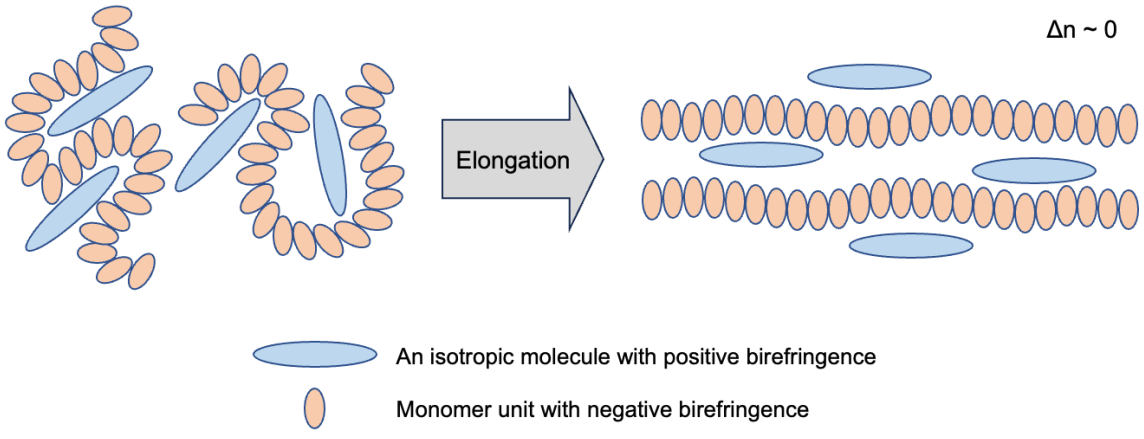

Figure 1.8 Cancelation of birefringence by doping anisotropic molecules

Some other methods have been attempted. Nishio, Teramoto, and their group reported that birefringence could be controlled by grafting different materials to original materials.[44, 45] Yamaguchi, Nobukawa, and their group showed that birefringence of cellulose esters and wavelength dispersion of its birefringence could be controlled by substitution of multiple ester groups[46-48] and formation of porous structures.[49, 50]

1.2.3 Issues in compensating for birefringence

Although various methods have been developed to compensate for birefringence of optical polymers, some issues still remain in the respective methods. The polymer blend which is produced by mixing two polymers with positive and negative birefringence generally has difficulty with the miscibility of the two different polymers, eventually causing low transparency. Therefore, the reported combinations of polymers are limited as illustrated in Table 1.5. The polymer blend which overcame the difficulty of the miscibility and the random copolymerization which is produced by copolymerizing two monomers with positive and negative birefringence can generate a new material with high transparency. However, since the attained material is produced by blending or copolymerizing raw materials with different optical properties, such as refractive indices, it shows different optical properties from original monomers or polymers. Thus, its optical and thermal properties other than the birefringence are altered from the original ones due to the polymer blend or the random copolymerization. This is not desired for currently used optical materials. In contrast, the method, in which anisotropic low-mass molecules or birefringent crystals are added to an original material, can maintain almost the same optical and thermal properties as the original material. However, this method has difficulty in raising compatibility between the original material and the additives. Because amounts of additive anisotropic molecules and birefringent crystals are relatively small. If the compatibility is low, not only appropriate compensation for birefringence will not be able to realize, but it may also worsen transparency and uniformity of the refractive index. Other methods also potentially have the same issue as the random copolymerization because their concepts are to control birefringence with appending a different material from an original material.

To compensate for birefringence of a material without changing the material's optical and thermal properties, an idea of using a bottlebrush polymer as an additive was conceived. In the following section, the details of the bottlebrush polymer are developed.

1.3 Bottlebrush polymer

1.3.1 Definition

A bottlebrush polymer (BBP) is a comb-shaped polymer with densely grafted side chains as shown in Figure 1.9. It forms a cylinder shape with the main chain elongated by excluded-volume effect of the side chains. The name “bottlebrush polymer” drives from this shape.

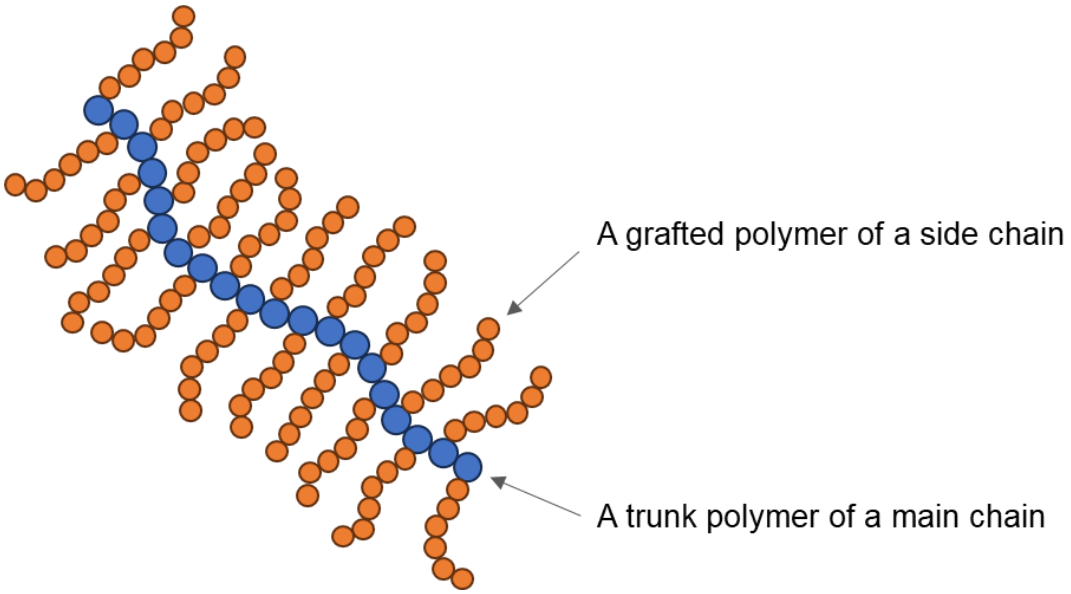

Figure 1.9 Schematic diagram of a bottlebrush polymer

1.3.2 Synthesis method

There are three main methods for synthesizing BBPs, called grafting-to, grafting-from, and grafting-through. Each method is described in detail in the following sub-sections.

1.3.2.1 Grafting-to

Grafting-to is a method of introducing side chains to a trunk polymer by polymeric reactions, a BBP is obtained by reacting the trunk polymer with side-chain polymers having reactive functional groups at the ends. Figure 1.10 shows a schematic diagram of this method.

This method is a bonding reaction between the trunk polymer and the side-chain polymers, both of which possess high molecular weight, so steric hindrance and high viscosity may be a problem. Therefore, the reaction conditions must be carefully considered to achieve both a high reaction ratio and chemoselectivity.

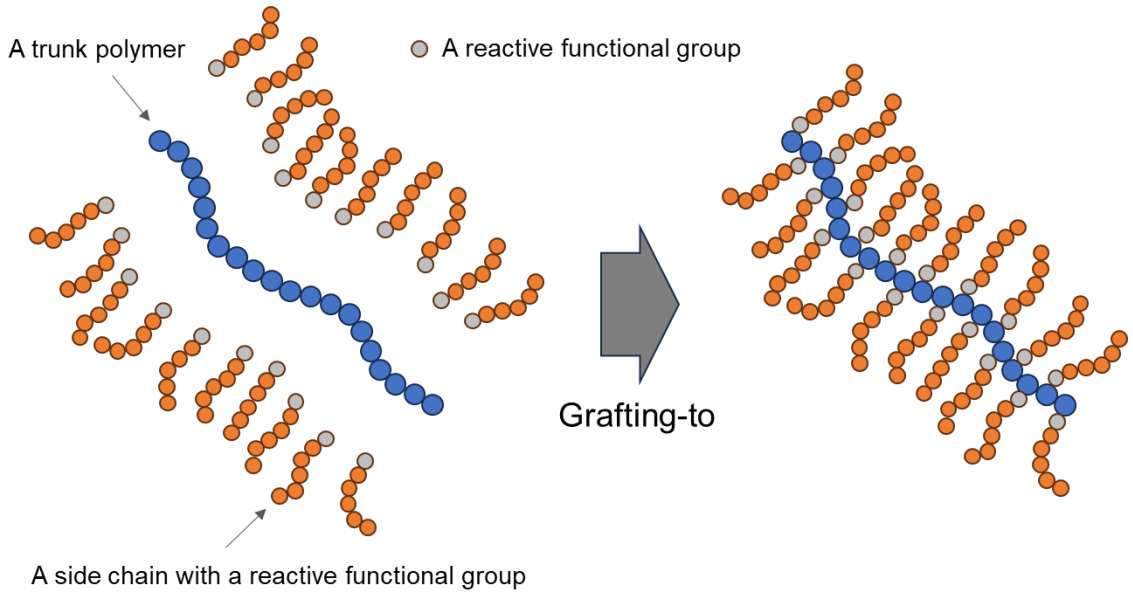

Figure 1.10 Schematic diagram of Grafting-to

1.3.2.2 Grafting-from

Grafting-from is a method of polymerizing monomers from a trunk polymer having many polymerization-active sites, a BBP is obtained by various polymerization methods using a main-chain polymer with an initiator group introduced into the repeating unit as a macroinitiator. Figure 1.11 shows a schematic diagram of this method.

It was reported that adopting living radical polymerization in the grafting-from process was very effective to synthesize BBPs, because it could generate both polymerization initiation with high efficiency and equal growth of each side-chain length, accomplishing high graft density of side chains.[51, 52] In this method, care must be taken to avoid the formation of insoluble cross-linkers and cessation of recombination that can cause polydispersion. Specifically, it should be necessary to decrease radical concentration by coordinating polymerization temperature and the catalyst's concentration. It is also effective in inhibiting cross-links of BBPs to adopt appropriate dilution condition or add initiators with low molecular weight.[51, 53]

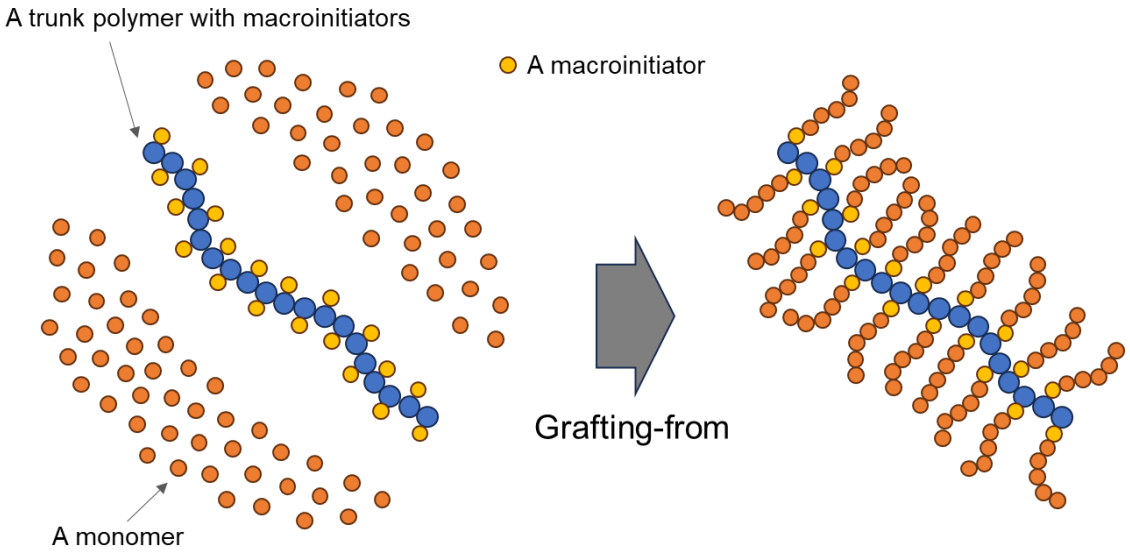

Figure 1.11 Schematic diagram of Grafting-from

1.3.2.3 Grafting-through

Grafting-through is a method of utilizing macromonomers with a polymerizable functional group at one end, a BBP is obtained by polymerizing the macromonomers. Figure 1.12 shows a schematic diagram of this method.

This method enables to synthesize ideal BBPs with one side chain per repeating unit of the main chain and with uniform length of the side chains. At the relatively early study, it was reported that BBPs could be synthesized by free radical polymerization of PS macromonomers terminated with methacrylate esters.[54] However, due to high viscosity, low concentration of terminal polymerization groups, and steric hindrance, it was difficult to increase the conversion rate of macromonomers. Afterward, it was reported that BBPs could be synthesized at high conversion rate of macromonomers by ring opening metathesis polymerization of macromonomers having norbornyl groups at the ends.[55, 56] Similar reports were also made on alternating copolymerization of macromonomers terminated with vinylbenzyl or maleimide groups.[57, 58]

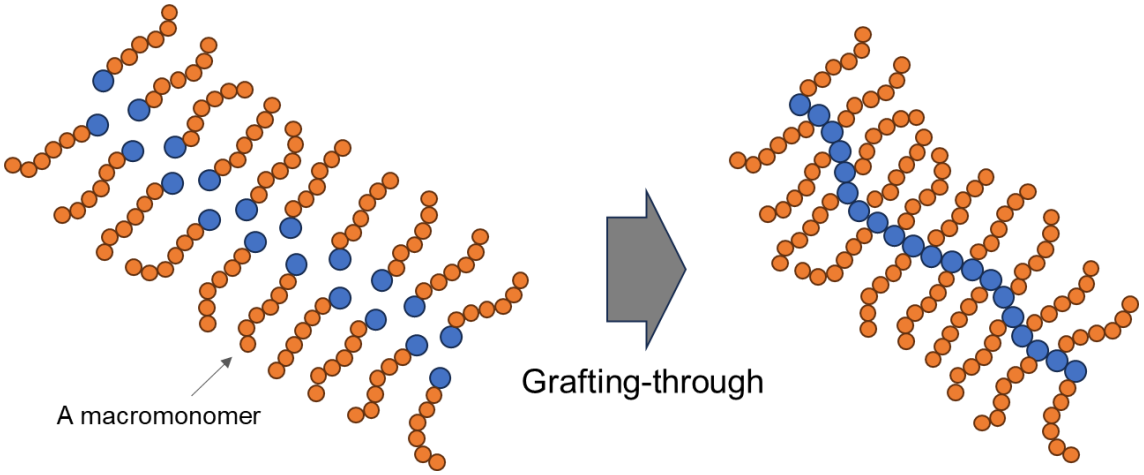

Figure 1.12 Schematic diagram of Grafting-through

1.3.3 Expected application

A BBP acts as a polymer with long persistence length since stiffness of the main chain is enhanced by excluded-volume effect of the side chains. Therefore, various applications were proposed by considering a BBP as a nano-material. M. Zhang et al. reported that BBPs with amphiphilic diblock copolymer side chains could be used as single molecular templates for the synthesis of metal, metal oxide, and metal chalcogenide nanoparticles.[59] Y. Zhang et al. demonstrated that carbon nanotubes could be functionalized with amphiphilic/Janus BBPs by uniting click chemistry with a macroinitiator approach, modifying their surfaces/substrates.[60] It was also reported that BBPs could be utilized as nano careers for bio-imaging and drug delivery, playing a role as bio-functional materials.[61] The applications of BBPs are expanding more and more, and it may be possible to create materials with excellent properties by compounding BBPs with gels and resins.

1.3.4 Application of BBPs to compensation for orientation birefringence

As a result of focusing on the configuration of the BBP, a new concept to compensate for birefringence of optical polymers has been devised. Figure 1.13 illustrates a conceptual diagram explaining the compensation for negative orientation birefringence of a linear polymer using BBPs. Orientation birefringence of polymers results from anisotropy of molecular polarizability, and a linear polymer possesses its anisotropy microscopically due to the molecular polarizability. However, since the molecular chains of the linear polymer are randomly oriented in the normal state, the molecular polarizability can be canceled macroscopically. Therefore, the linear polymer in the normal state exhibits no birefringence, becoming macroscopically isotropic as shown in Figure 1.13 (a).

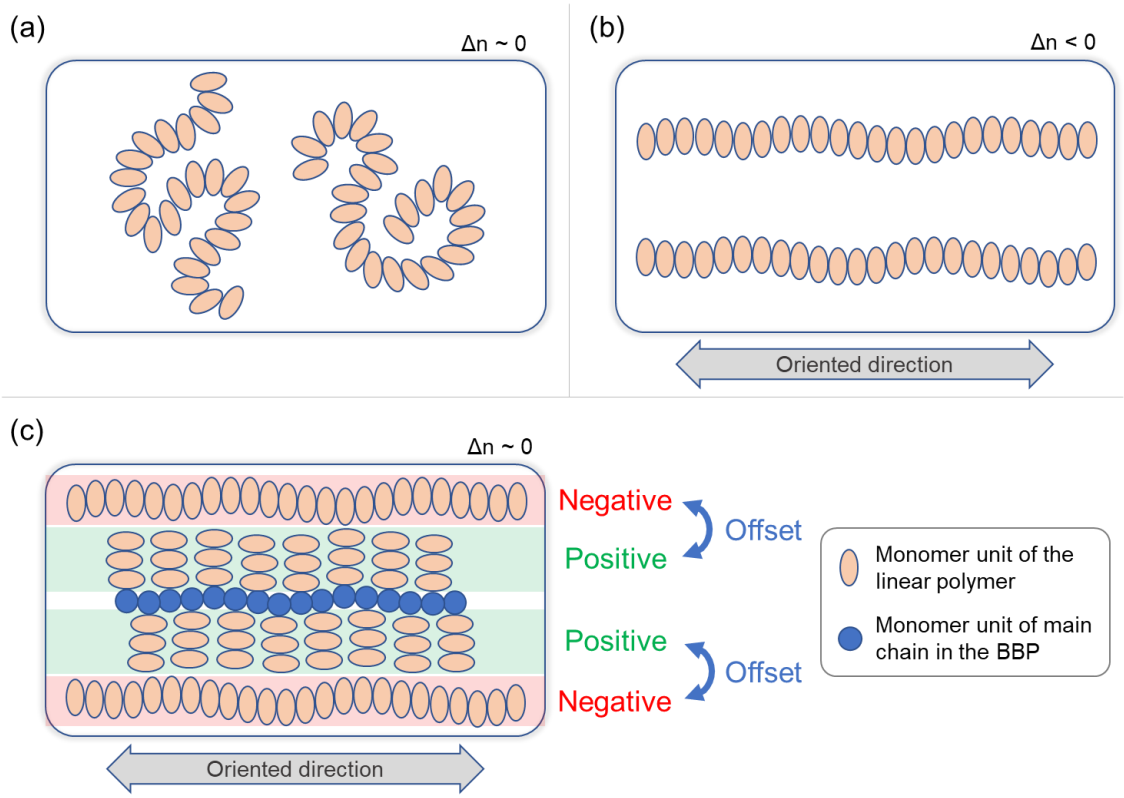

Figure 1.13 Conceptual diagram of compensation for orientation birefringence

Once the molecular chains of the linear polymer become oriented by a specific factor, the oriented polymer sample exhibits birefringence. Because the anisotropy of the molecular polarizability can no longer be mutually canceled as shown in Figure 1.13 (b). However, by mixing the linear polymer with BBPs which possess grafted side chains composed of the same polymer as the linear polymer, it is expected that the orientation birefringence can be offset.

Figure 1.13 (c) is the schematic diagram representing the oriented state of a blend-polymer sample with a BBP. When the blend sample is oriented as in Figure 1.13 (c), the molecular chains of the linear polymer are directed to the oriented direction. Simultaneously, the main chain of the BBP is also directed to the oriented direction if the length of the main chain is much longer than that of the side chain. Consequently, the grafted side chains of the BBP are directed perpendicular to the main chain (i.e., the oriented direction). In this way, it is considered that the anisotropy due to the linear polymer can be effectively cancelled by the opposite anisotropy due to the side chains of

BBPs, and when the anisotropy reaches a harmonious balance, birefringence of the blend can be completely compensated.

1.4 Objective of this study

As mentioned in the previous sections, flagship-smartphone cameras require optical polymers with extremely low birefringence to produce high-resolution images. Although some proposals to decrease birefringence were made, there have not been any practical methods to compensate for birefringence of an optical polymer without changing optical and thermal properties of the original linear polymer to date. In order to overcome this issue, a new approach has been tried in this study, generating a blend polymer of a linear polymer and BBPs with grafted side chains composed of the same polymer as the linear polymer. Therefore, the objective of this study is to compensate for orientation birefringence of optical polymers using BBPs and to verify advantages of the developed polymers when applied to actual optical design.

In Chapter 1, the background and the development of optical polymers are described, an issue of them is raised. Details of the issue and a new approach to overcome it are then introduced, and the objective of this study is clarified.

In Chapter 2, the new approach is verified through controlling orientation birefringence of PMMA by mixing linear PMMA and BBPs composed of PMMA side chains with high graft density, and the optical and thermal properties of the PMMA blends are investigated. In addition, the details of compensation for orientation birefringence are considered.

In Chapter 3, the approach is adapted to PS with a high chromatic dispersion, conducting to compensate for orientation birefringence of PS by mixing linear PS and BBPs composed of PS side chains with high graft density. Furthermore, the optical and thermal properties of the PS blends are evaluated, and the characteristics are considered.

In Chapter 4, in order to clarify effectiveness of the PS blend with the lowest birefringence, orientation birefringence of the PS blend is compared with that of the commercial optical polymers which are most commonly used in lens systems of smartphone cameras. Furthermore, the advantage of utilizing the PS blend in an optical lens system as a lens material is verified through computational evaluation of the resolution performance of the lens system designed on optical design software.

In Chapter 5, all the results acquired in this study are summarized.

Chapter 2

Control of orientation birefringence of PMMA by blending bottlebrush polymers

2.1 Background and purpose

The usage of optical polymers, especially for lenses of smartphone cameras, has been boosted because smartphones equipped with cameras have been widely spread and used all over the world.[62, 63] Recently, the imaging performance of smartphone cameras has made remarkable progress by development of complementary metal-oxide semiconductor (CMOS) image sensors with a high pixel-number. Accordingly, configurations of lens systems in smartphone cameras were optimized, image quality of some flagship smartphone cameras has even surpassed that of most compact digital still cameras. Despite such developments, birefringence of optical polymers, which can cause degradation of image quality of the flagship smartphone cameras, is one of the remaining major issues.

The birefringence of optical polymers generally results from orientation of the polymer chains (orientation birefringence) and photoelasticity (photoelastic birefringence), inducing optical anisotropy of a material with different refractive indices depending on the polarization directions of light. Since the anisotropy in optical polymers can produce unclear images with low resolution, the lens material in flagship smartphone cameras is required to possess extremely low birefringence. In fact, photoelastic birefringence can be adequately reduced by undergoing an additional annealing process for manufactured lenses, and thus, it is very important to decrease the orientation birefringence induced during the manufacturing process such as injection molding for optical polymers.

Some methods have been previously proposed to compensate orientation

birefringence. Especially, random copolymerization of plural monomers with positive and negative birefringence has been utilized for practical optical materials generating high-quality images in flagship smartphone cameras.[2, 3] However, their optical and thermal properties other than the birefringence can be altered from original properties due to the random copolymerization, which is not desired for currently used optical materials.

In order to resolve this problem, a new method is tried to control orientation birefringence of a targeted optical polymer by using bottlebrush polymers with high graft density. In this chapter, poly(methyl methacrylate) (PMMA) is selected as a targeted polymer because it is the most widely used as a typical optical polymer. As a specific procedure, hydroxyl-terminated PMMA (PMMA-OH) is first synthesized by atom transfer radical polymerization (ATRP), and norbornene-terminated PMMA (NB-PMMA) macromonomers are then prepared via condensation PMMA-OH and *exo*-5-norbornenecarboxylic acid. Thereafter, bottlebrush polymers with well-controlled PMMA side-chain length (PMMA-BBP) are produced by ring opening metathesis polymerization (ROMP) of NB-PMMA macromonomers, trying to control orientation birefringence of PMMA by blending linear PMMA with PMMA-BBP. In addition, optical and thermal properties of the blends are evaluated by comparing those of linear PMMA.

2.2 Experimental section

2.2.1 Materials

Methyl methacrylate (MMA) monomers were purchased from FUJIFILM Wako Pure Chemical Corporation and purified by vacuum distillation before use. PMMA with an average M_w of ~120,000 determined by Gel Permeation Chromatography (GPC) was purchased from Sigma-Aldrich Co. LLC as linear PMMA. Copper(I) bromide (CuBr), exo-5-norbornenecarboxylic acid, and the third-generation Grubbs catalyst (G3, $C_{38}H_{40}Br_2Cl_2N_4Ru$) were purchased from Sigma-Aldrich Co. LLC. *N*,*N*,*N*',*N*'',*N*''-pentamethyldiethylenetriamine (PMDETA), hexane, triethylamine, and methanol were purchased from FUJIFILM Wako Pure Chemical Corporation. 2-hydroxyethyl 2-bromo-2-methylpropanoate (HEBiB), oxalyl chloride, and ethyl vinyl ether were purchased from Tokyo Chemical Industry Co., Ltd. Deoxidized toluene, deoxidized tetrahydrofuran (THF), and dichloromethane (DCM) were purchased and used without any purification.

2.2.2 Synthesis of norbornene-terminated PMMA macromonomers

At first, synthesis of PMMA-OH with low molecular weight was conducted. Purified MMA (15 g, 150 mmol) and deoxidized toluene (15 mL) were put into a 150 mL pressure vessel in a glove box under an argon atmosphere. Next, CuBr (0.22 g, 1.5 mmol) and PMDETA (0.31 mL, 1.5 mmol) were added into the vessel and dissolved by stirring. HEBiB (1.09 mL, 7.5 mmol) was then added to the solution as an initiator of ATRP. After the vessel was quickly sealed with an exclusive cap, the vessel was withdrawn from the glove box and stirred for 2 h at 70°C in an oil bath. After that, the reaction mixture was cooled in ice water and exposed to air to finish ATRP, which was diluted twice with acetone. The solution was passed through an alumina column to remove copper complex. Thereafter, the solution was concentrated by an evaporator, and the sample was precipitated in hexane (1000 mL) at room temperature and dried in a vacuum oven for 72 h at 50°C.

Synthesis of NB-PMMA macromonomers followed as the next step. *Exo*-5-norbornenecarboxylic acid (2.16 g, 15.7 mmol) was put into a 250 mL two-necked round-

bottom flask and dissolved in deoxidized toluene (10.9 mL) under an argon atmosphere. Oxalyl chloride (1.34 mL, 15.7 mmol) was added to the solution and the mixture was stirred for 30 min at room temperature. The extra pressure in the flask was released by opening the plug for a moment, and the mixture was stirred again for 1 h at 60°C, before stirring for another 1 h at 70°C in an oil bath. The reaction mixture was then cooled down to room temperature and residual oxalyl chloride was removed under vacuum. Meanwhile, PMMA-OH (6.0 g, 3.0 mmol) and triethylamine (2.24 mL, 16.0 mmol) were put into another 250 mL two-necked round-bottom flask and dissolved in deoxidized toluene (27.2 mL) under an argon atmosphere. The mixture was stirred for 30 min at 60°C in an oil bath to obtain a homogeneous solution, and additionally degassed in three consecutive freeze-pump-thaw cycles. Finally, the solution was added to the original flask with cannulation and the mixture was stirred for 12 h at 100°C in an oil bath. This procedure was mainly conducted as described in the previous study.[64] The sample was extracted by precipitating into cold methanol (~-70°C, 1000 mL) and dried in a vacuum oven for 72 h at 50°C.

2.2.3 Synthesis of PMMA-BBP by ROMP of NB-PMMA macromonomers

NB-PMMA (2.0 g) was added to a 250 mL two-necked round-bottom flask and dissolved in deoxidized THF (30 mL). After the flask was sealed with a plug and a rubber cap, the solution was additionally degassed in three consecutive freeze-pump-thaw cycles, the flask was then filled with argon gas. The NB-PMMA solution was brought into a glove box under an argon atmosphere. G3 (1.47 mg) dissolved in THF was prepared in a scintillation vial and the solution was added quickly to the NB-PMMA solution to synthesize bottlebrush polymers. The mixture was stirred for 21 h while shutting out light, and the reaction was terminated by adding ethyl vinyl ether (2.0 mL). A synthesis with ROMP using G3 often finishes in a short time (~10 min).[56, 64] However, since the main-chain length of the bottlebrush polymers in this study was comparatively long, the reaction was conducted for 21 h to complete the bottlebrush polymer synthesis. The sample was precipitated in methanol (1000 mL) and dried in a vacuum oven for 72 h at 50°C. All processes except for drying were conducted at room temperature.

2.2.4 Blending linear PMMA with PMMA-BBP

Linear PMMA and PMMA-BBP were added to 200 mL round-bottom flasks with magnetic stirrers in the several blending ratios of 100:0, 90:10, 80:20, 73:27, and 60:40. Each sample was adjusted to be 2.0 g in total weight and DCM (38 g) was added to each flask as solvent. The mixtures were stirred for 1 h at room temperature, before each blend sample was precipitated in methanol (800 mL) and dried in a vacuum oven for 72 h at 50°C to obtain white powder samples.

2.2.5 Fabrication of blend films by compression molding

Film samples were prepared from the blends of linear PMMA and PMMA-BBP by compression molding. A blend sample of ~0.6 g was sandwiched between two PET films at the pressure of 8 MPa and at 180°C for 5 min,[65] where the gap between the two PET films was kept at ~0.3 mm. After that, the sample was taken out and cooled to room temperature. The film samples with ~0.3 mm thickness were eventually obtained. Each blend film was then cut into a rectangular shape of ~ 5 mm in width and >15 mm in length.

2.2.6 Chemical structure analyses

Proton nuclear magnetic resonance (^{1}H NMR) spectra were recorded by the 400 MHz NMR spectrometer (JNM-ECZ400S, JEOL Ltd.) to confirm the degree of polymerization and the composition of NB-PMMA samples. The degree of polymerization of synthesized polymers was estimated by comparing integral values of the peaks derived from initiator, functional-groups, and monomer units. The number of scans was 32 and the relaxation time was 5 sec. Each ~20 mg sample was dissolved in $CDCl_3$ (0.8 mL) and used for measurements. GPC analysis was performed using high-performance liquid chromatography (HPLC) (Prominence, Shimadzu Corporation) to confirm molecular-weight distributions of each sample using $CHCl_3$ eluent at a flow rate of 1.0 mL/min at 25°C. Polystyrene standards (Shodex STANDARD SM-105, Showa Denko K.K.) were used as calibration samples. Each ~10 mg sample dissolved in $CHCl_3$ (1 mL) was used for the measurement.

2.2.7 Thermal property

Glass transition temperature of each sample was measured using DSC (DSC25, TA Instruments). The measurement was conducted for each ~10 mg sample which was put and sealed in an aluminum pan under a nitrogen atmosphere. All measurements were conducted at the heating rate of 10°C/min, and the temperature range was between 0°C and 200°C.

2.2.8 Characterization of birefringence

Birefringence of each sample was recorded as average retardation using the 2-D Birefringence Measurement System (WPA-100, Photonic Lattice, Inc.). The apparatus could easily measure 2-D birefringence including information about the amount and the direction of retardation, indicating optical path difference between the directions perpendicular and parallel to stretching. In this study, the sign of birefringence was defined as plus if the refractive index ($n_{//}$) parallel to the stretching direction of a film sample was larger than the refractive index ($n_{\perp}$) perpendicular to the stretching direction.

2.2.9 Characterization of optical property

Light transmittance of each sample was measured using spectrophotometer (UH4150, Hitachi High-Tech Corporation) to evaluate transparency. The measurements were performed in the wavelength range of 400 - 800 nm measuring each 1 nm. Refractive indices of each sample were measured at 25°C using a multi-wavelength Abbe refractometer (DR-M2, Atago Co., Ltd.). The measurements of the refractive indices were conducted at the wavelengths of 486 nm (hydrogen F-line), 588 nm (helium d-line), and 656 nm (hydrogen C-line), and the Abbe numbers expressing information about chromatic dispersion of the materials were calculated from the refractive indices.

2.3 Results and discussion

2.3.1 Synthesis of PMMA-BBP and blending linear PMMA with PMMA-BBP

The synthetic scheme of PMMA-BBP is demonstrated in Figure 2.1. First, hydroxyl-terminated PMMA-OH monomers with the controlled molecular-chain length and molecular-weight distribution were synthesized by ATRP. ATRP is an effective living radical polymerization method to produce a polymer with a uniform chain length.[66, 67] Previously it was reported that chain-length controlled PMMA by ATRP was successfully synthesized using a CuBr catalyst and a PMDETA ligand,[68-70] therefore, they were also utilized to synthesize PMMA-OH in this study. As an initiator for ATRP, HEBiB including hydroxy groups was utilized considering the following synthetic process. The degree of polymerization (*DP*) of PMMA in PMMA-OH was measured as ~26 by ^{1}H NMR spectra analysis as shown in Figure 2.2. Since a target value of *DP* was set at ~30 in this synthesis, the result was quite appropriate. Then, the PMMA-OH were converted into norbornene-terminated NB-PMMA macromonomers through condensation with *exo*-5-norbornenecarboxylic acid chloride, and PMMA-BBP with high graft density were synthesized by ROMP of the NB-PMMA macromonomers using G3. Since this grafting-through method was very useful to produce bottlebrush polymers with a high conversion ratio of macromonomers,[55, 56, 64] it was employed to synthesize PMMA-BBP in this study.

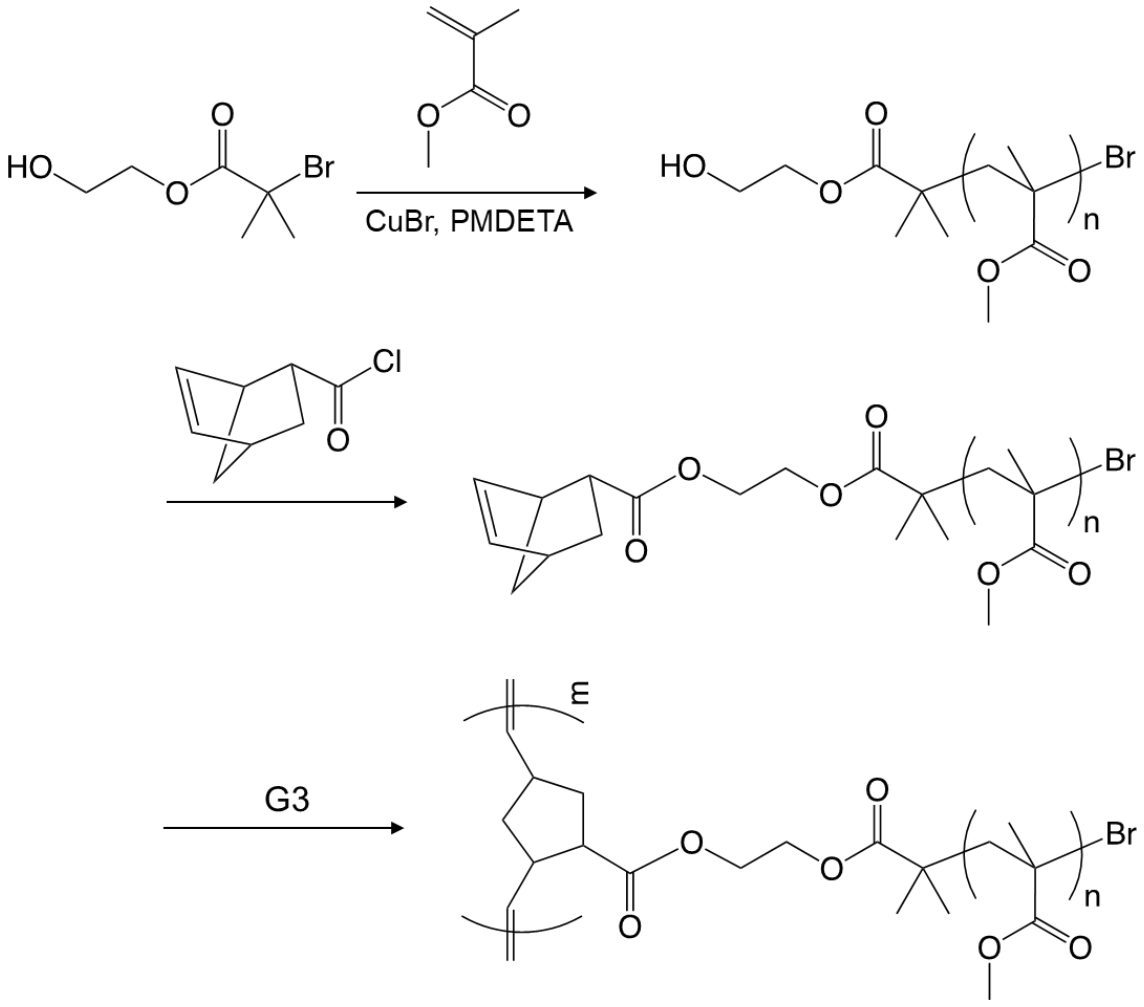

Figure 2.1 Synthetic scheme of PMMA-BBP

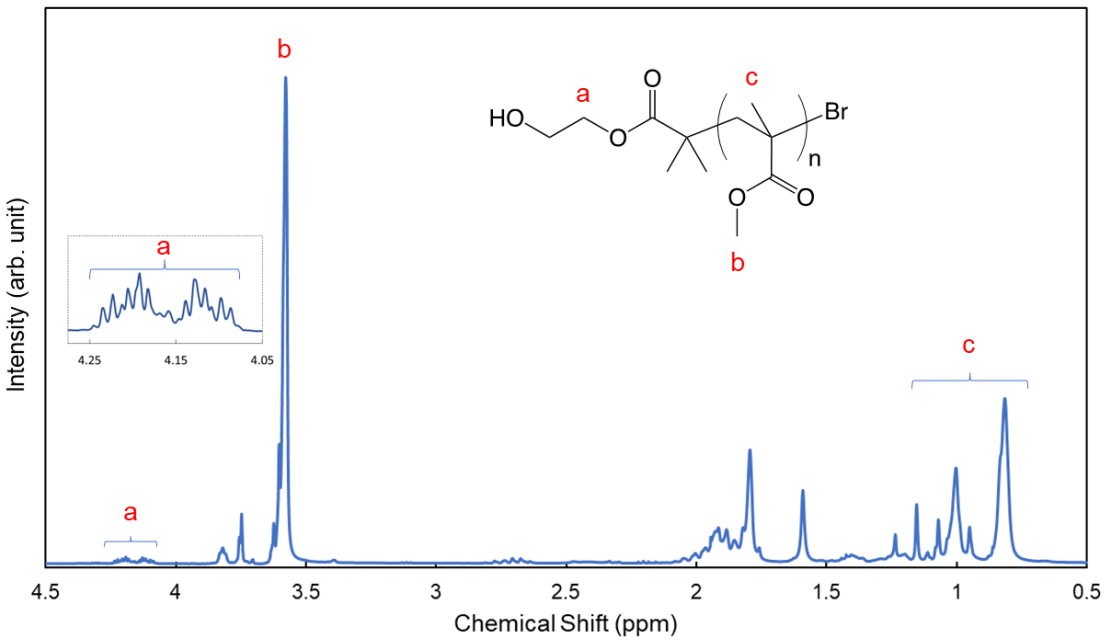

Figure 2.2 ^{1}H NMR spectrum of synthesized PMMA-OH

The *DP* of PMMA in NB-PMMA macromonomers (DP_s) was measured as ~29 by ^{1}H NMR spectra analysis before ROMP as shown in Figure 2.3. The *DP* of norbornene main chains (DP_m) was set at 600, and accordingly the synthesized bottlebrush polymer had a configuration of DP_m ~600 of norbornene main chains with DP_s ~29 of PMMA side chains. The conversion ratio from NB-PMMA macromonomers to PMMA-BBP was estimated to be over 82% by GPC analysis as shown in Figure 2.4. The results indicated that the desired bottlebrush polymers were successfully produced through the synthesis of NB-PMMA macromonomers. Chemical structures including molecular weights, polydispersity, and DP_s of each sample were analyzed by GPC, which are summarized in Table 2.1.

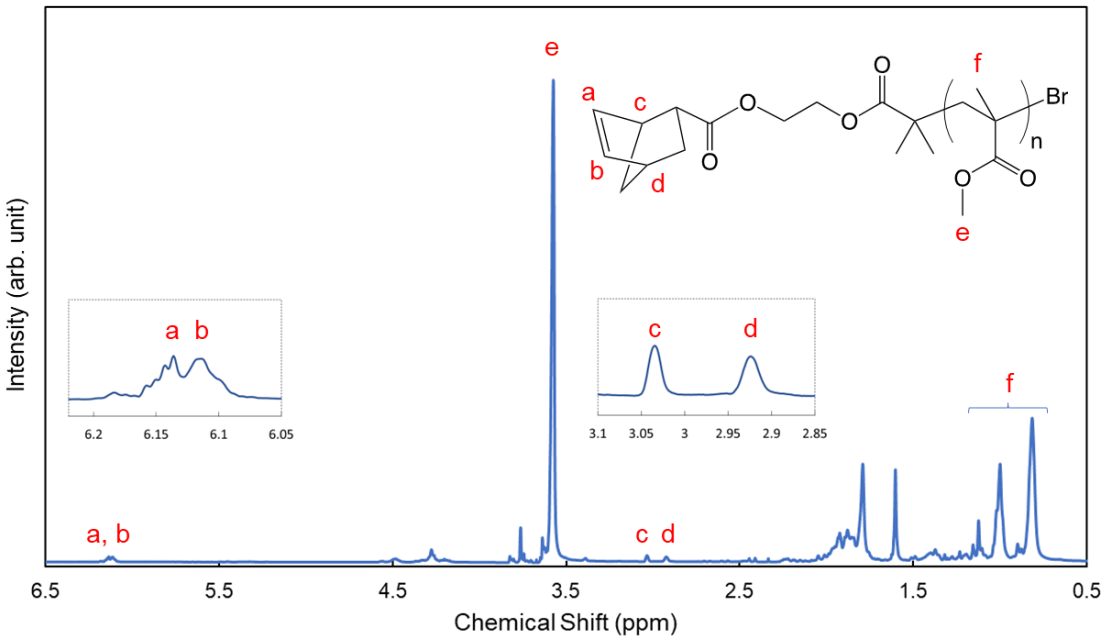

Figure 2.3 ^{1}H NMR spectrum of synthesized NB-PMMA macromonomer

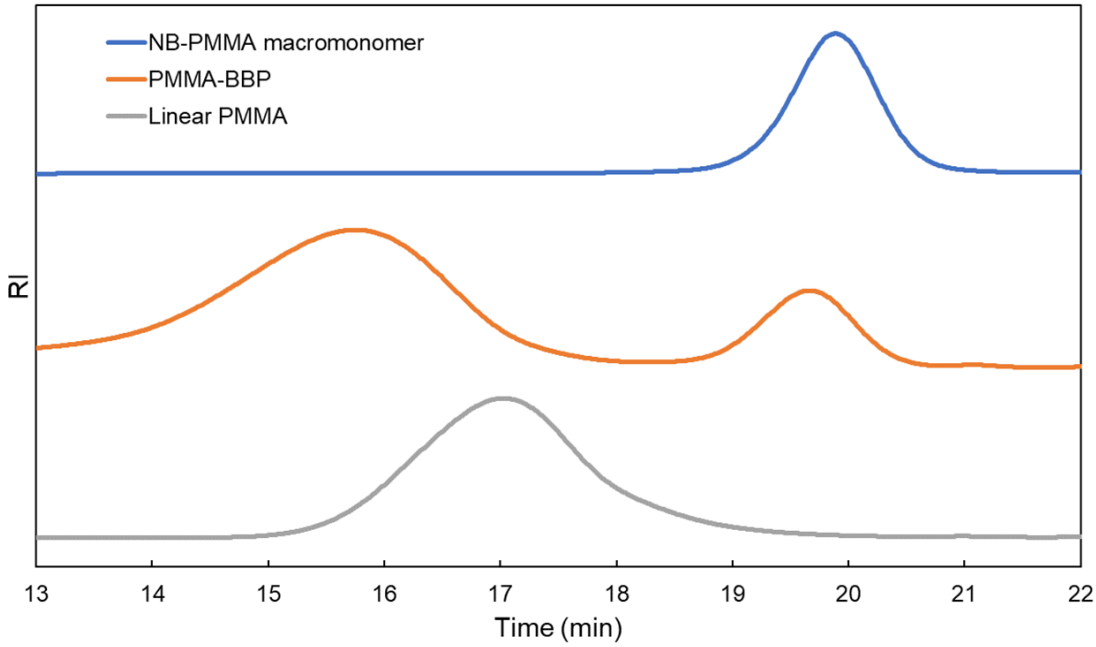

Figure 2.4 GPC traces of NB-PMMA macromonomer, PMMA-BBP, and Linear PMMA

Table 2.1 Characteristics of the synthesized samples and the prepared samples

Sample	M_n[a]	M_w[a]	M_w/M_n[a]	DP_s [b]
NB-PMMA macromonomer	3,100	3,800	1.23	29
PMMA-BBP	230,000	1,700,000	7.66	-
Linear PMMA	41,000	89,000	2.19	-

[a] Determined by GPC, [b] Determined by ^{1}H NMR

Next, blend samples (PMMA/PMMA-BBP) were prepared by mixing PMMA-BBP with linear PMMA. To determine the optimized blending ratio of PMMA to PMMA-BBP, at which the orientation birefringence would be most effectively offset, PMMA/PMMA-BBP were prepared in various ratios from 100:0 (linear PMMA) to 60:40. In detail, after careful selection, the blending ratios of 100:0, 90:10, 80:20, 73:27, and 60:40 were chosen.

2.3.2 Thermal properties

The glass transition temperature (T_g) was determined from the second heating scan of DSC curves. Figure 2.5 shows the DSC results of linear PMMA, PMMA-BBP, and PMMA/PMMA-BBP with different blending ratios of linear PMMA to PMMA-BBP. Triangles in Figure 2.5 indicate the T_g positions. It was found that T_g of each sample were clearly detected around 110°C. Through the DSC analysis, T_g of linear PMMA was recognized to be 111.5°C and T_gs of the blend samples with the ratios of 90:10, 80:20, 73:27, and 60:40 were detected at 108.3°C, 106.4°C, 106.1°C, and 105.0°C, respectively. T_g slightly decreased as the blending ratio of PMMA-BBP increased, because T_g of PMMA-BBP was estimated to be 102.0°C. This may be due to the fact that norbornene, which compose the main chain of PMMA-BBP, possessed the lower T_g than linear PMMA. Actually, the decrease was almost negligible, and it was considered that the blending of PMMA-BBP had little effect on the thermal property of PMMA.

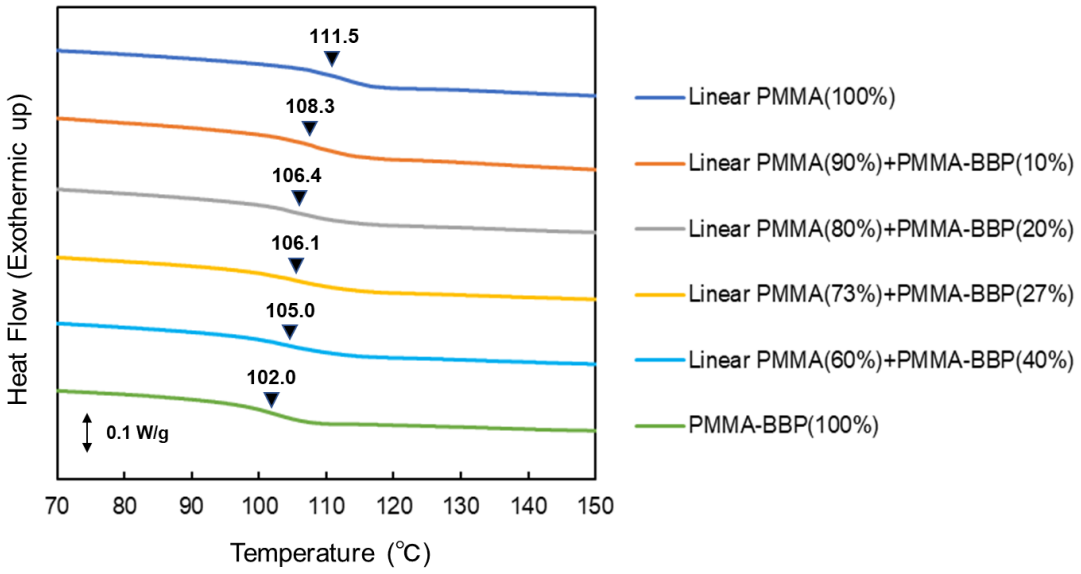

Figure 2.5 DSC traces of linear PMMA, PMMA-BBP, and PMMA/PMMA-BBP with various blending ratios

2.3.3 Orientation birefringence

Blend-film samples with ~0.3 mm thickness were prepared by a compression molding, and the blend films were cut into rectangular shapes with ~5 mm in width and >15 mm in length. All rectangle samples were then uniaxially elongated with a dynamic mechanical analyzer (RSA-3, TA Instruments) to the desired strain (ε). The elongation process was conducted for the part of ~5 mm in length of each sample at 115°C with the extension rate of 0.1 mm/s. After stretching, each sample was rapidly cooled to room temperature with a cooling system by liquid nitrogen. Thereafter, the samples were observed with the 2-D birefringence measurement system (WPA-100, Photonic Lattice, Inc.) to confirm their birefringence ($\Delta n = n_{//} - n_{\perp}$). WPA-100 is composed of a polarized image sensor that can simply measure birefringence with high precision and get useful information about the amount and the direction of birefringence, which cannot be measured with the polarization microscopes that have been used to measure birefringence. It can also directly detect the data of retardation ($\Delta\lambda$) corresponding to birefringence, where the relationship between Δn and $\Delta\lambda$ can be represented as $\Delta n = \Delta\lambda / d$, where d is

the thickness of film samples.

Figure 2.6 shows the data of birefringence for the film samples with different blending ratios against strains. It is already known that linear PMMA denotes negative birefringence,[71] which was also confirmed for linear PMMA in this study. Moreover, it was clearly observed that the absolute value of birefringence linearly increased as the strain increased. This should be due to the fact that molecular orientation was promoted with the increase in the strain of the samples. Regarding the blend samples, birefringence increased at each strain as PMMA-BBP content increased, and birefringence of PMMA/PMMA-BBP with the blending ratio of 60:40 was found to be positive at all strains. Therefore, it was confirmed that oriented bottlebrush polymers could generate positive birefringence that could effectively cancel the opposite negative birefringence of oriented linear PMMA. Moreover, birefringence of PMMA/PMMA-BBP with the blending ratio of 73:27 became almost zero at all strains, indicating that the 73:27 sample was indeed the most effective content at which birefringence could be entirely removed.

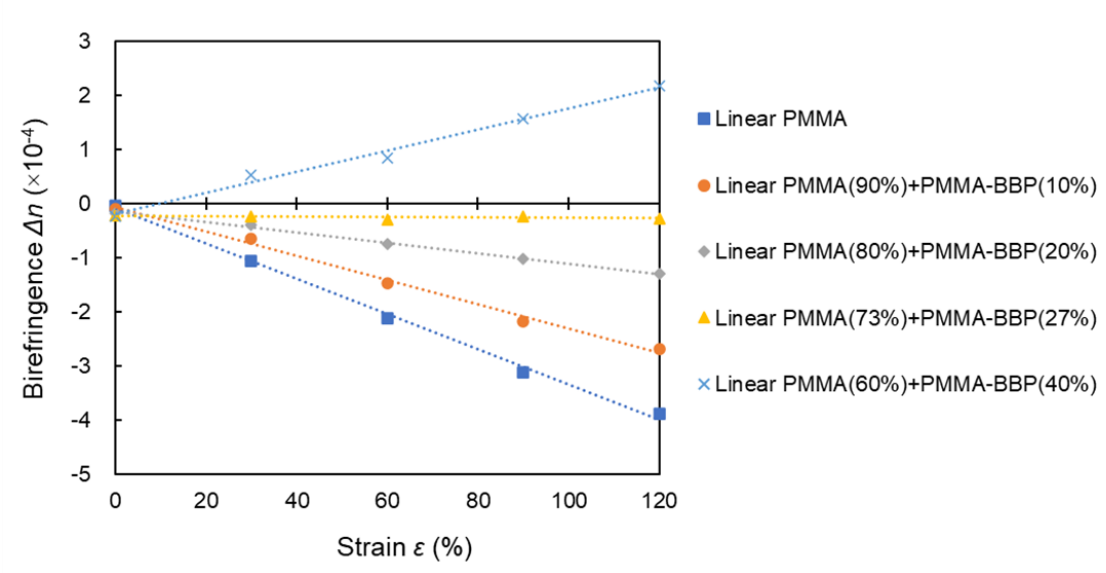

Figure 2.6 Birefringence vs. strain on film samples of linear PMMA and PMMA/PMMA-BBP with various blending ratios

Figure 2.7 shows the representative retardation data measured with WPA-100 on the samples stretched at 90% of strain. The colors in the data represent the amount of retardation and the arrows indicate the direction of the delayed axis which presents the direction with a higher refractive index. The data visually illustrate that the degree of retardation dramatically changed as the blending ratio of PMMA-BBP increased, and the direction of the delayed axis rotated about 90 degrees for the sample with the blending ratio of 60:40. The results revealed that orientation birefringence could be adequately removed by blending linear PMMA and PMMA-BBP at a fixed ratio.

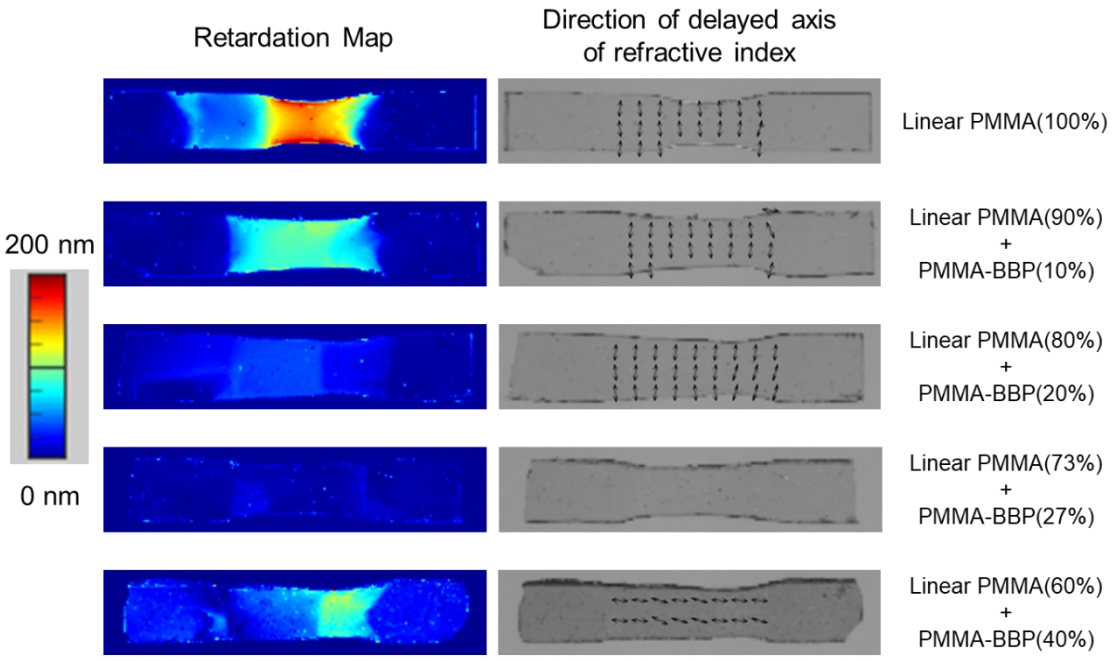

Figure 2.7 Retardation data on film samples of linear PMMA and PMMA/PMMA-BBP with various blending ratios

According to the previous study on zero-birefringence optical polymers,[72] it is considered that orientation birefringence of the blend sample applies to the following formula:

$$\Delta n = \Delta n_{\mathrm{PMMA}} \times \frac{\alpha}{100} + \Delta n_{\mathrm{Bottlebrush}} \times \frac{100 - \alpha}{100} \qquad (2.1)$$

where, Δn, Δn_{PMMA}, and $\Delta n_{\mathrm{Bottlebrush}}$ are orientation birefringence of the blend sample, linear PMMA, and PMMA-BBP, respectively. α (wt%) and 100-α (wt%) are the weight ratios of linear PMMA and PMMA-BBP. As orientation birefringence can be derived from anisotropy of molecular polarizability, Δn_{PMMA} depends on anisotropy of polarizability of MMA monomers. $\Delta n_{\mathrm{Bottlebrush}}$ also depends mainly on anisotropy of polarizability of MMA monomers, because PMMA-BBP are mainly composed of PMMA brunches. In addition, since the MMA monomers in PMMA-BBP are grafted perpendicularly to the main-chain polymers of PMMA-BBP, the MMA monomers become perpendicular to those of linear PMMA, and thus the positive/negative signs of $\Delta n_{\mathrm{Bottlebrush}}$ and Δn_{PMMA} become opposite. Therefore, the birefringence of linear PMMA can be canceled by the birefringence of PMMA-BBP. Additionally, birefringence of PMMA-BBP can also be derived from norbornenes and ATRP initiators as well as the major components of the bottlebrush polymers. In practice, however, birefringence created by norbornenes and ATRP initiators should be lower than that by PMMA brunches of PMMA-BBP, and no change in the opposite signs of $\Delta n_{\mathrm{Bottlebrush}}$ and Δn_{PMMA} occurs.

Following Equation 2.1, if the effect of birefringence of norbornenes and ATRP initiators is completely negligible, the theoretical blending ratio of linear PMMA to PMMA-BBP for the complete compensation for birefringence of PMMA should be 50:50. However, in the actual experiment, when the blending ratio of linear PMMA to PMMA-BBP was 73:27, Δn became almost zero. It is considered that this may highly be due to positive birefringence of norbornenes and ATRP initiators, which may also make some compensation for birefringence caused by linear PMMA. In fact, in the previous study by Ban et al.,[73] it was reported that polynorbornene indeed possessed positive intrinsic

birefringence. Therefore, it would be necessary to consider the effect of birefringence created by norbornenes and ATRP initiators in order to accomplish complete compensation for orientation birefringence.

2.3.4 Refractive indices

Table 2.2 shows refractive indices (n_F, n_d, and n_C) at the wavelengths of hydrogen F (486 nm), helium d (588 nm), and hydrogen C (656 nm) lines, respectively, on film samples of linear PMMA and PMMA/PMMA-BBP with different blending ratios of linear PMMA to PMMA-BBP, and also Abbe numbers (v_d). v_d is widely used in optics as the value showing chromatic dispersion property, calculated by the following equation.[4]

$$v_d = \frac{n_d - 1}{n_F - n_C} \tag{2.2}$$

Therefore, low chromatic dispersion corresponds to a large v_d, while high chromatic dispersion corresponds to a small v_d. Linear PMMA indicated n_d = 1.493 and v_d = 60.9. Moreover, all PMMA/PMMA-BBP also showed almost similar values, which were n_d = 1.493 and v_d = 60.9 - 62.4. It is considered that PMMA/PMMA-BBP maintain almost the same n_d and v_d as the linear PMMA. The results suggest that compensation for birefringence with PMMA-BBP does not affect n_d and v_d of linear PMMA.

Table 2.2 Refractive indices and Abbe numbers of linear PMMA and blends with various PMMA/PMMA-BBP blending ratios

Sample	n_F	n_d	n_C	ν_d
Linear PMMA (100%)	1.498	1.493	1.490	60.9
Linear PMMA (90%) + PMMA-BBP (10%)	1.499	1.493	1.491	62.4
Linear PMMA (80%) + PMMA-BBP (10%)	1.498	1.493	1.490	61.6
Linear PMMA (73%) + PMMA-BBP (27%)	1.498	1.493	1.490	60.9
Linear PMMA (60%) + PMMA-BBP (40%)	1.498	1.493	1.491	62.4

2.3.5 Light transmittance

Figure 2.8 shows light transmittance on film samples of linear PMMA and PMMA/PMMA-BBP with different blending ratios of linear PMMA to PMMA-BBP. While linear PMMA demonstrated high transmittance beyond 90% in the wavelength range of 400 - 800 nm, PMMA/PMMA-BBP indicated lower transmittance at short wavelength than linear PMMA. It was also observed that transmittance decreased more as the content ratio of PMMA-BBP in PMMA/PMMA-BBP increased more.

Initially, it was expected that PMMA/PMMA-BBP would show as high transmittance as linear PMMA, because they were mostly composed of PMMA side chains. However, the lower transmittance emerged at short wavelength on actual samples. Regarding the results, it is assumed that bromine (Br) contained in ATRP initiators may have caused the decrease of transmittance. As shown in Figure 2.1, Br existed at an end group in NB-PMMA macromonomer. Some parts of Br could be free in synthesizing NB-PMMA macromonomers, and the bromines, which were continuously left in PMMA-BBP, may have induced the decrease of transmittance. Actually, it was also observed that blend film samples with a higher content ratio of PMMA-BBP appeared more yellowish.

PMMA/PMMA-BBP with the blending ratio of 73:27, which demonstrates almost zero birefringence at any strains, had less than 70% transmittance at 420 nm and the transmittance in the wavelength range of 450 - 475 nm was less than 80%. For optical polymers to utilize as optical lenses and films, it is generally required to possess higher transmittance than 75% at 420 nm and 80% in the range of 450 - 650 nm. Therefore, in order to utilize PMMA/PMMA-BBP with the blending ratio of 73:27 as an optical material for optical lenses and films, it would be necessary to further improve light transmittance at short wavelength by optimizing the synthetic process.

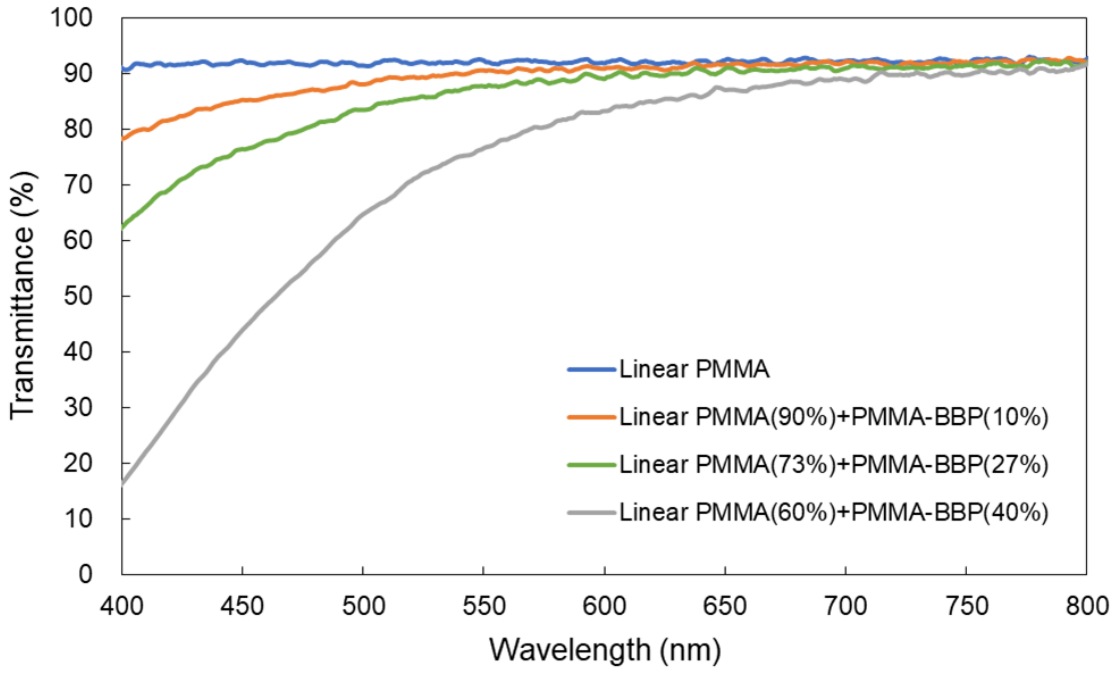

Figure 2.8 Light transmittance on film samples of linear PMMA and PMMA/PMMA-BBP with various blending ratios

2.4 Summary of this chapter

In this chapter, a new method was introduced to control orientation birefringence of PMMA by mixing linear PMMA and PMMA-BBP with high graft density, and the optical and thermal properties of the blends were examined. In addition, the mechanism of compensation for orientation birefringence was considered. The achievements were listed as follows:

i. PMMA bottlebrush polymers with well-controlled side-chain length could be successfully produced by ROMP of NB-PMMA macromonomers prepared via condensation of PMMA-OH synthesized by ATRP and *exo*-5-norbornenecarboxylic acid, indicating that PMMA-BBP had an optimized high aspect ratio of the main chain to the side chain.

ii. Orientation birefringence of PMMA could be controlled by mixing linear PMMA and PMMA-BBP. This was because negative birefringence of elongated linear PMMA could be offset by positive birefringence of elongated PMMA-BBP. Especially, when a blending ratio of linear PMMA to PMMA-BBP was 73:27, the sample demonstrated complete compensation for orientation birefringence against any strains.

iii. The principle of controlling orientation birefringence using bottlebrush polymers was considered from anisotropy of molecular polarizability. On the blend samples, it was illustrated that while negative birefringence was produced by MMA monomers in linear PMMA oriented parallel to the stretching direction, positive birefringence was generated by MMA monomers in side chains of PMMA-BBP oriented perpendicular to the stretching direction. In addition, it was suggested that it would be necessary to consider the effect of birefringence created by norbornenes in main chains and ATRP initiators in order to completely compensate orientation birefringence.

iv. The glass transition temperatures of linear PMMA, PMMA-BBP, and PMMA/PMMA-BBP were examined through DSC analysis. The glass transition

points of all samples were detected at ~110°C, with no significant differences, and thus it was considered that the blending of PMMA-BBP had little effect on the thermal property of PMMA.

v. Refractive indices and Abbe numbers of linear PMMA and PMMA/PMMA-BBP were measured with the abbe refractometer, all PMMA/PMMA-BBP indicated almost the same n_d and ν_d as linear PMMA. It suggested that compensation for birefringence with PMMA-BBP did not affect n_d and ν_d of linear PMMA.

vi. Light transmittances on film samples of linear PMMA and PMMA/PMMA-BBP were measured with the spectrophotometer. While linear PMMA showed high transmittance beyond 90% through the range of visible wavelength, PMMA/PMMA-BBP exhibited decrease of transmittance at shorter wavelength than 550 nm. In addition, as the content ratio of PMMA-BBP in PMMA/PMMA-BBP increased more, transmittance of the sample decreased more. Since it was assumed that Br contained in ATRP initiators might have caused the decrease of transmittance, further improvement of the synthetic process would be required in order to utilize PMMA/PMMA-BBP as an optical polymer with high transparency.

Chapter 3

Compensation for orientation birefringence of polystyrene by blending bottlebrush polymers

3.1 Background and purpose

Optical polymers have been widely used in various optical applications, the usage of optical polymers has been increasing, especially in lenses for smartphone cameras.[62, 63] Because optical polymers are lightweight, low cost, and suitable for mass production of lenses with aspherical surfaces and free-form surfaces. Recently, optical polymers are also attracting attention as optical materials used in head-mounted devices for virtual reality (VR) and augmented reality (AR). With the enhanced image quality of some flagship smartphone cameras, and with increasing focus on VR and AR, an optical polymer producing clearer and higher-resolution images by eliminating birefringence is eagerly awaited. Such birefringence generally results from the orientation of polymer chains (orientation birefringence) and photoelasticity (photoelastic birefringence), causing optical anisotropy, where the refractive index varies depending on the polarization direction of light. While photoelastic birefringence can be sufficiently reduced by annealing manufactured lenses made of optical polymers, reducing orientation birefringence produced during manufacturing processes such as injection molding has been challenging.

In the previous chapter, it was reported that the orientation birefringence of poly(methyl methacrylate) (PMMA), which was a targeted optical polymer, could be effectively controlled and reduced by mixing PMMA bottlebrush polymers (PMMA-BBP) with side chains composed of the same polymer as the targeted polymer. As a first step to validate this new approach, PMMA was selected in the first stage because it is the most widely utilized as a typical optical polymer. However, since linear PMMA is

originally known as an optical polymer with relatively low orientation birefringence, it is used as it is in optical applications requiring optical materials with low orientation birefringence. The truth is, for enhancing resolution of optical lens systems, it is necessary to reduce orientation birefringence of optical polymers which is different from PMMA. In order to understand the fact, chromatic aberration is discussed below.

The chromatic dispersion is another problematic phenomenon, in which the refractive index depends on wavelengths: the refractive index of a long wavelength is smaller than that of a short wavelength, causing chromatic aberration. In lens systems of flagship smartphone cameras and head-mounted devices, it is necessary to adequately compensate for such chromatic aberration as well as birefringence. To compensate for chromatic aberration of lens systems, mixing several optical materials with high and low chromatic dispersion are indispensable.[4, 74, 75] Also, it is known that PMMA, cyclo-olefin polymers (COP), and cyclo-olefin copolymers (COC) with low chromatic dispersion denote relatively low birefringence, while polystyrene (PS) and polycarbonate (PC) with high chromatic dispersion possess considerably high birefringence.[8, 76-78] The optical properties of these typical optical polymers are summarized in Table 3.1.[3] Therefore, to realize complete compensation for both birefringence and chromatic aberration of lens systems, it should be extremely important to utilize PS and PC with high chromatic dispersion, at the same time, canceling orientation birefringence of the polymers. Especially, PS is used as an effective polymer for various applications, but the usage of PS as an optical polymer has been limited due to its high optical anisotropy. Thus, reducing orientation birefringence of PS has considerable potential benefits in the optical fields.

Table 3.1 Optical properties of the typical optical polymers

Item	PMMA	COP	COC	PC	PS
Refractive index (n_d)	1.49	1.53	1.54	1.58	1.59
Abbe number (ν_d)	58	56	56	30	31
Birefringence (Δn)	Low	Middle	Low	High	High

In this chapter, the compensation for orientation birefringence of PS with high chromatic dispersion is implemented by mixing bottlebrush polymers with PS side chains. Norbornene-terminated PS (NB-PS) macromonomers are prepared by atom transfer radical polymerization (ATRP) using ATRP initiator including norbornene units. PS bottlebrush polymers (PS-BBP) are then synthesized by ring-opening metathesis polymerization (ROMP) of the NB-PS macromonomers, attempting to compensate for orientation birefringence of PS by blending linear PS with the PS-BBP. In addition, photoelastic birefringence and other optical properties of the PS blends are investigated.

3.2 Experimental section

3.2.1 Materials

Styrene monomers were purchased from FUJIFILM Wako Pure Chemical Corporation and purified by vacuum distillation before use. Polystyrene with an average M_w of ~192,000 and poly(methyl methacrylate) with an average M_w of ~120,000 determined by Gel Permeation Chromatography (GPC) were purchased from Sigma-Aldrich Co. LLC as linear PS and linear PMMA. Copper(I) bromide (CuBr), *exo*-5-norbornenecarboxylic acid, and the third-generation Grubbs catalyst (G3, $C_{38}H_{40}Br_2Cl_2N_4Ru$) were purchased from Sigma-Aldrich Co. LLC. *N*,*N*,*N*',*N*'',*N*''-pentamethyldiethylenetriamine (PMDETA), triethylamine, and methanol were purchased from FUJIFILM Wako Pure Chemical Corporation. 2-Hydroxyethyl 2-bromo-2-methylpropanoate (HEBiB), 1-ethyl-3-(3-dimethylaminopropyl)carbodiimide hydrochloride (WSCI), 4-dimethylaminopyridine (DMAP), and ethyl vinyl ether were purchased from Tokyo Chemical Industry Co., Ltd., and used as received. Deoxidized *N*,*N*-dimethylformamide (DMF), deoxidized tetrahydrofuran (THF), and dichloromethane (DCM) were purchased and used without any purification. Typical PC (AD-5503, Teijin Limited) and special PC (EP-5000, Mitsubishi Gas Chemical Company, Inc.) were provided by their respective manufacturers for this study, and used as received.

3.2.2 Synthesis of norbornene-terminated PS macromonomers

First, the ATRP initiator with norbornene units was synthesized by condensation of *exo*-5-norbornenecarboxylic acid and HEBiB. *exo*-5-Norbornenecarboxylic acid (3.44 g, 24.9 mmol), HEBiB (5.0 g, 23.7 mmol), WSCI (4.77 g, 24.9 mmol), and DMAP (0.58 g, 4.74 mmol) were dissolved in DCM (130 mL), and the mixture solution was stirred for 24 h at room temperature. After the reaction, the solution was extracted with saturated $NaHCO_3$ (aq), pure water, and brine. Then, the organic layer was dried over $MgSO_4$, filtered, and concentrated by using an evaporator. The product was purified by silica column chromatography using $CHCl_3$ as an eluent and subsequent vacuum distillation. The product was obtained as a colorless and transparent liquid (5.65 g, 72%). Thereafter,

purified styrene monomers (40 g, 385 mmol) and DMF (156 mL) were put into a 350 mL pressure vessel in a glove box under an argon atmosphere. Next, CuBr (0.57 g, 4.0 mmol) and PMDETA (0.84 mL, 4.0 mmol) were added into the vessel and dissolved by stirring. The synthesized ATRP initiator with norbornene units (1.32 g, 4.0 mmol) was then added to the solution. After the vessel was quickly sealed with an exclusive cap, the vessel was withdrawn from the glove box and stirred for 24 h at 70°C in an oil bath. After that, the reaction mixture was cooled in ice water, exposed to air to finish ATRP, and diluted with acetone. The solution was passed through an alumina column to remove the copper complex. Finally, the solution was concentrated by an evaporator, and the sample was precipitated in cold methanol and dried in a vacuum oven for 168 h at room temperature.

3.2.3 Synthesis of bottlebrush polymer by ROMP of NB-PS macromonomers

NB-PS macromonomers (4.0 g) were added to a 150 mL pressure vessel and dissolved in deoxidized THF (75.0 mL) in a glove box under an argon atmosphere. G3 (3.69 mg) dissolved in THF was prepared in a scintillation vial, and the solution was appended quickly to the NB-PS solution to synthesize PS-BBP. The mixture was stirred for 30 min by shutting out light, and the reaction was terminated by adding ethyl vinyl ether (4.0 mL). The sample was isolated three times by precipitating in methanol (800 mL) and dried in a vacuum oven for 168 h. All processes were conducted at room temperature.

3.2.4 Blending linear PS with PS bottlebrush polymers

Linear PS and PS-BBP were added to 200 mL round-bottom flasks with magnetic stirrers in several blending ratios of 100:0, 75:25, 50:50, and 30:70. Each sample was adjusted to be 2.0 g in total weight, and DCM (38 g) was added to each flask as solvent. The mixtures were stirred for 1h at room temperature, before each blend sample was precipitated in methanol (800 mL) and dried in a vacuum oven for 168 h at room temperature to acquire white powder samples.

3.2.5 Fabrication of films by compression molding

Film samples were prepared from linear PS, blends of linear PS and PS-BBP, and linear PMMA by compression molding. A sample of ~0.6 g was sandwiched between two PET films at a pressure of 8 MPa and at 180°C for 5 min.[65] After that, the sample was taken out and cooled to room temperature. In the process, the thickness of the film samples was adjusted to be ~0.1 mm. Each blend film was then cut into a rectangular shape of ~5 mm in width and ~25 mm in length.

Film samples of commercial optical polymers were also prepared from AD-5503 and EP-5000 by compression molding. A sample of ~0.6 g was sandwiched between two polyimide films for 5 min at the pressure of 8 MPa and at the glass transition temperature of each polymer plus 70°C, which was 215°C for AD-5503 and EP-5000, where the gap between the two polyimide films was kept at ~0.15 mm. After that, the sample was taken out and cooled to room temperature. The film samples with ~0.15 mm thickness were eventually obtained. Each blend film was then cut into a rectangular shape of ~5 mm in width and ~25 mm in length.

3.2.6 Chemical structure analyses

^{1}H NMR spectra were measured by a 400 MHz NMR spectrometer (JNM-ECZ400S, JEOL Ltd.) to confirm the degree of polymerization and composition of the NB-PS samples. The degree of polymerization of the synthesized polymers was estimated by comparing the integral values of the peaks derived from initiator, functional-groups, and monomer units. The number of scans was 32, and the relaxation time was 5 sec. Each ~20 mg sample was dissolved in $CDCl_3$ (0.8 mL) and used for the measurements. GPC analysis was conducted using high-performance liquid chromatography (HPLC) (Prominence, Shimadzu Corporation) to confirm molecular-weight distributions of each sample using $CHCl_3$ eluent at the flow rate of 1.0 mL/min at 25°C. Polystyrene standards (Shodex STANDARD SM-105, Showa Denko K.K.) were used as calibration samples. Each ~10 mg sample dissolved in $CHCl_3$ (1 mL) was applied for the measurement.

3.2.7 Thermal property

Glass transition temperature of each sample was measured by using DSC (DSC25, TA Instruments). The measurements were conducted for each ~10 mg sample which was placed and sealed in an aluminum pan under a nitrogen atmosphere. All measurements were conducted at the heating rate of 10°C/min, and the temperature range was set between 0°C and 200°C.

3.2.8 Characterization of birefringence

Birefringence of each sample was recorded as the average retardation using the Birefringence Measurement System (WPA-100, Photonic Lattice, Inc.). The apparatus could readily measure 2-D birefringence including information about the amount and the direction of retardation, indicating an optical-path difference between the two directions perpendicular and parallel to the stretching. In this study, the sign of birefringence was defined as plus if the refractive index ($n_{//}$) parallel to the stretching direction of a film sample was larger than the refractive index ($n_{\perp}$) perpendicular to the stretching direction. This definition of the sign is generally used in the field of optics.

3.2.9 Characterization of optical properties

Light transmittance of each sample was measured using a spectrophotometer (UH4150, Hitachi High-Tech Corporation) to evaluate transparency. The measurements were performed in the wavelength range of 400 - 800 nm, measuring each 1 nm. The refractive indices of each sample were measured using a multi-wavelength Abbe refractometer (DR-M2, Atago Co., Ltd.). The measurements of the refractive indices were conducted at wavelengths of 486 nm (hydrogen F-line), 588 nm (helium d-line), and 656 nm (hydrogen C-line), and the Abbe numbers expressing information about the chromatic dispersion of the materials were calculated from the refractive indices.

3.3 Results and discussion

3.3.1 Synthesis of PS-BBP and blending linear PS with PS-BBP

The synthetic scheme of PS-BBP is demonstrated in Figure 3.1. First, an ATRP initiator with norbornene units was prepared through condensation of *exo*-5-norbornenecarboxylic acid and HEBiB. The ^{1}H NMR spectrum of the synthesized ATRP initiator is presented in Figure 3.2. Then, NB-PS macromonomers with a well-controlled molecular-chain length and molecular-weight distribution were synthesized by ATRP using the synthesized ATRP initiator. ATRP is one of effective living radical polymerization methods to produce polymers with a uniform chain length,[66, 67] and thus, it was also utilized to produce NB-PS macromonomers in this study. In addition, it was previously reported that PS with well-controlled chain lengths was successfully synthesized by ATRP using a CuBr catalyst and a PMDETA ligand,[79-81] which were also applied to our synthesis of NB-PS macromonomers. Next, PS-BBP with high graft density were synthesized by ROMP of the NB-PS macromonomers.[82] Namely, the grafting-through method was used to produce bottlebrush polymers with a high conversion ratio of macromonomers. The degree of polymerization of PS in the NB-PS macromonomers (DP_s) before synthesizing PS-BBP was estimated as ~18 by ^{1}H NMR as shown in Figure 3.3. The degree of polymerization of norbornene main chains (DP_m) in PS-BBP was set at 600, indicating that the synthesized PS-BBP had a configuration of DP_m ~600 of norbornene main chains and DP_s ~18 of PS side chains. The conversion ratio from NB-PS macromonomers to PS-BBP was estimated to be over 98% by GPC analysis, exhibiting a higher conversion ratio than that from NB-PMMA macromonomers to PMMA-BBP demonstrated in Chapter 2. This may have resulted from employment of the process in which ATRP initiator with norbornene units were synthesized in advance. These results indicated that the desired PS-BBP were successfully synthesized through ROMP of NB-PS macromonomers. The chemical structures including molecular weights and polydispersity of each sample were analyzed by GPC as shown in Figure 3.4, and the results are summarized with DP_s estimated by ^{1}H NMR in Table 3.2.

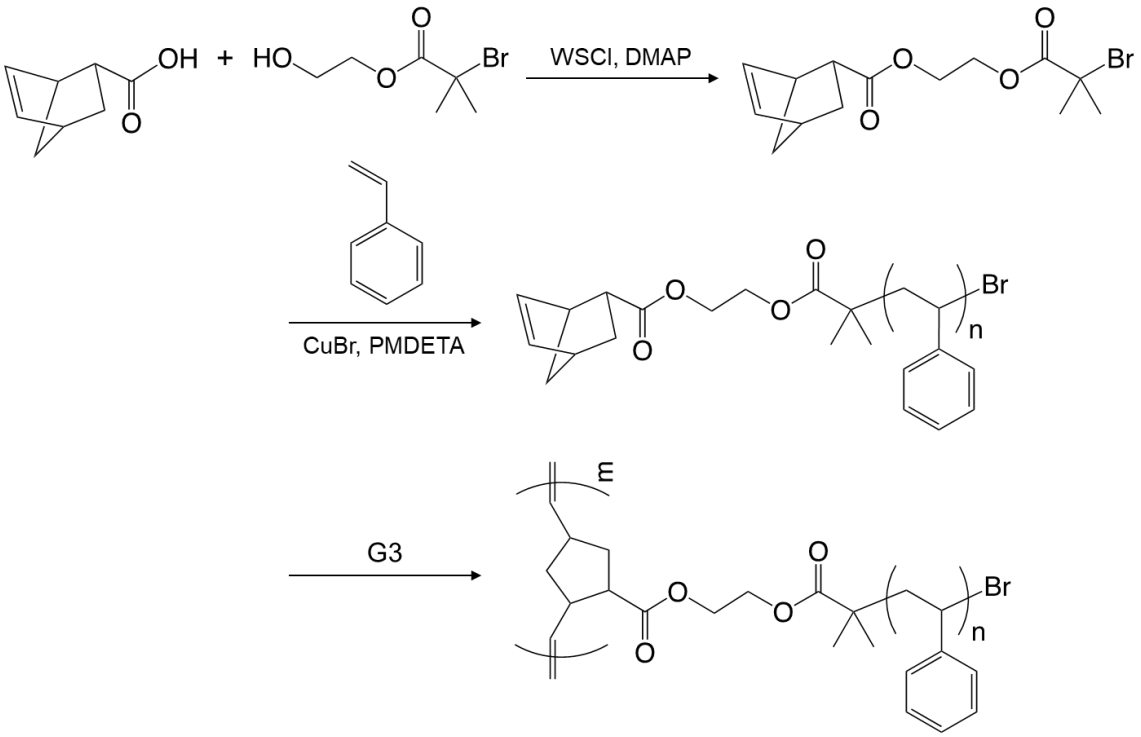

Figure 3.1 Synthetic scheme of PS-BBP

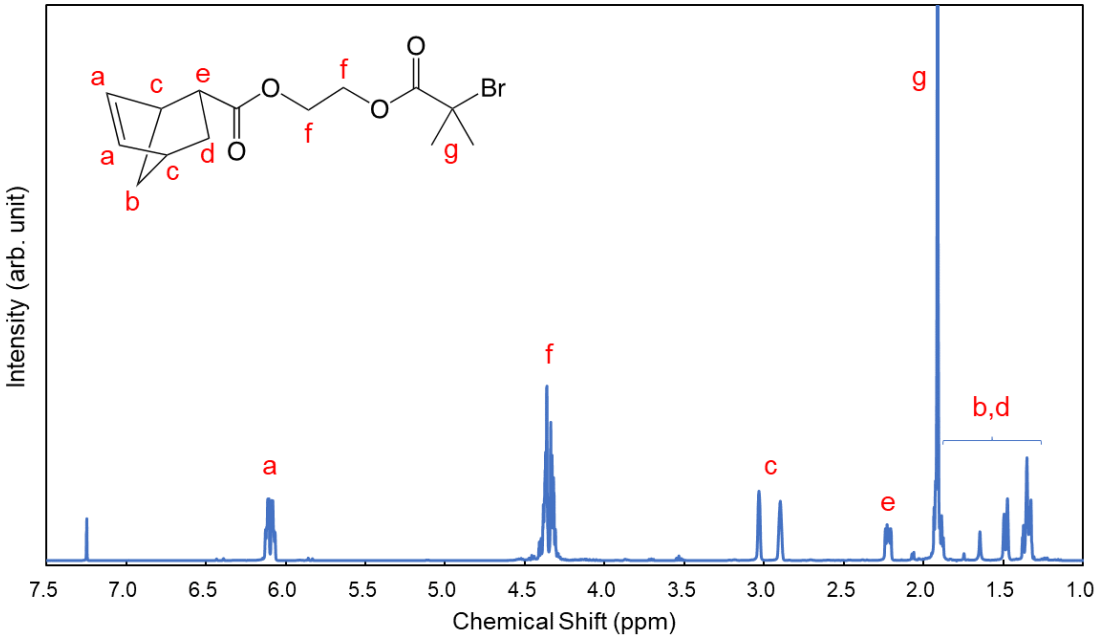

Figure 3.2 ^{1}H NMR spectrum of synthesized ATRP initiator with norbornene units

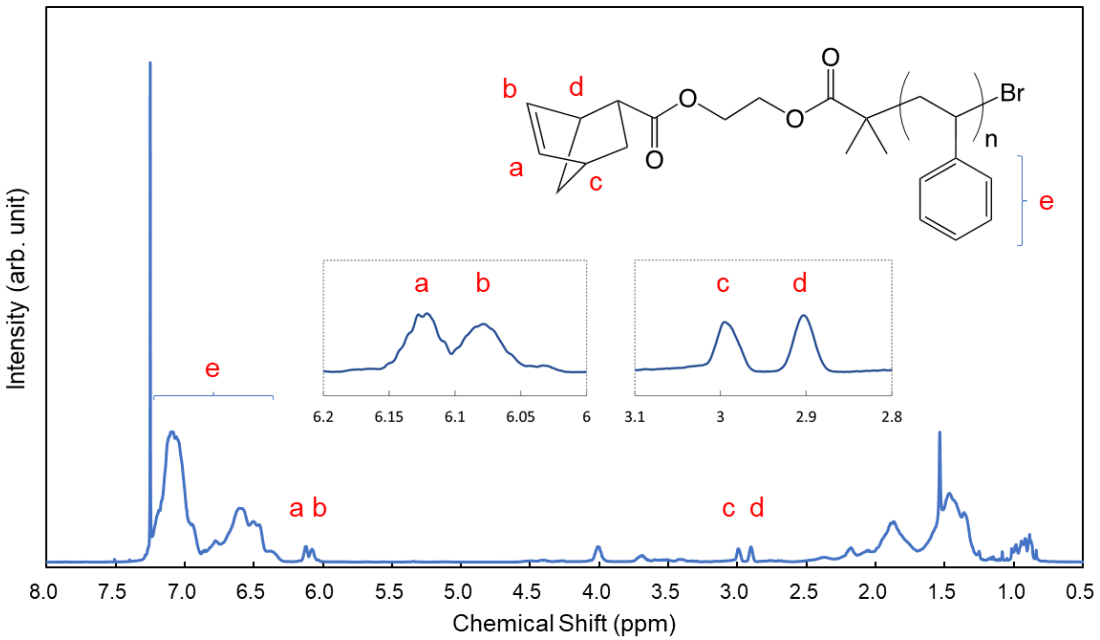

Figure 3.3 ^{1}H NMR spectrum of synthesized NB-PS macromonomer

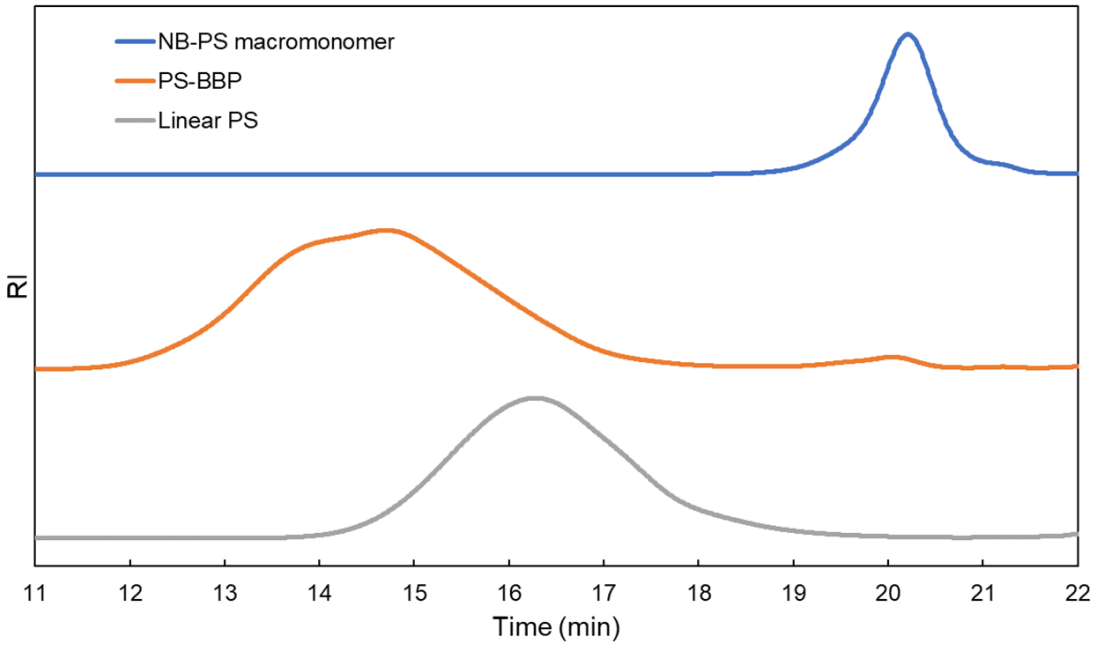

Figure 3.4 GPC traces of NB-PS macromonomer, PS-BBP, and Linear PS

Table 3.2 Characteristics of the synthesized samples and the prepared samples

Sample	M_n[a]	M_w[a]	M_w/M_n[a]	DP_s[b]
NB-PS macromonomer	2,200	2,800	1.27	18
PS-BBP	470,000	1,800,000	3.83	-
Linear PS	75,000	220,000	2.93	-

[a] Determined by GPC, [b] Determined by ^{1}H NMR

Then, blend samples of linear PS and PS-BBP (PS/PS-BBP) were prepared. To determine the optimized blending ratio of linear PS to PS-BBP, at which the orientation birefringence could be effectively compensated, the blending ratios were changed as100:0 (linear PS), 75:25, 50:50, and 30:70. All samples were produced in the same fashion.

3.3.2 Thermal properties

The glass transition temperature (T_g) of each sample was estimated from the second heating scan of DSC results. Figure 3.5 shows the DSC results of linear PS, PS-BBP, and the blend samples with different blending ratios of linear PS and PS-BBP. Triangles in Figure 3.5 indicate the T_g positions. Through the DSC analysis, while linear PS and PS-BBP exhibited only one T_g each at 103.9°C and 88.8°C, respectively, both T_g at ~103°C and ~90°C were observed for the blend samples, which were likely derived from linear PS and PS-BBP, respectively. The results indicated that phase separation could occur between linear PS and PS-BBP. In this study, the side-chain length of PS-BBP could be much shorter than the chain length of linear PS. Considering the previous reports concluding that the large difference in entropy between long and short chains caused phase separation,[83-90] the similar phase separation can occur between linear PS and PS-BBP in the blend samples. Practically, such phase separation is not desirable, since it would narrow the temperature range of compression molding and heat pressing for the production of optical elements. However, since the difference of T_g between linear PS and PS-BBP was only about 15°C, the blend samples could be utilized as an optical polymer by choosing appropriate thermal condition in the manufacturing process.

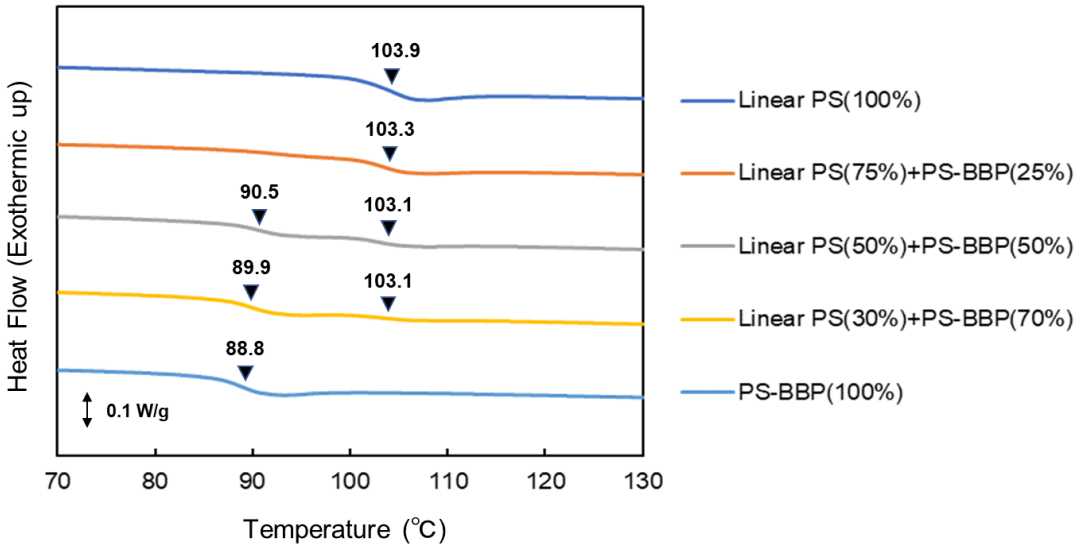

Figure 3.5 DSC traces of linear PS, PS-BBP, and PS/PS-BBP with various blending ratios

3.3.3 Orientation birefringence

Film samples of linear PS and PS/PS-BBP with ~0.1 mm thickness were prepared by compression molding, cut into a rectangular shape of ~5 mm in width and ~25 mm in length. All the samples were then heated and uniaxially elongated on a dynamic mechanical analyzer (RSA-3, TA Instruments) to a designated strain (ε). The elongation process was actually applied to the part of ~5 mm in length of each sample at 101°C with the extension rate of 0.1 mm/s. After stretching, each sample was rapidly cooled to room temperature by liquid nitrogen. Thereafter, retardations of the samples were observed with a 2-D birefringence measurement system (WPA-100, Photonic Lattice, Inc.) to measure their birefringence ($\Delta n = n_{//} - n_{\perp}$). WPA-100 possesses a polarized image sensor that can accurately measure birefringence with useful information about the amount and the direction of birefringence. It can directly detect the data of retardation ($\Delta\lambda$) corresponding to birefringence that can be translated by $\Delta n = \Delta\lambda / d$, where d is the thickness of film samples.

Figure 3.6 shows the representative retardation data measured by WPA-100 on linear PS, PS/PS-BBP with different blending ratios, and linear PMMA film samples

stretched at 120% of strain. The linear PMMA samples were prepared to compare the birefringence data with those of PS/PS-BBP samples. The colors show the amount of retardation, and the monochrome figures represent the directions of delayed axes described by arrows, presenting the direction of higher refractive indices. The data visually demonstrate that the amount of retardation sharply decreased as the ratio of PS-BBP increased, while the direction of the delayed axis of refractive index showed the same for each sample. It indicates that orientation birefringence of PS could be effectively compensated at the blending ratio of 30:70 without causing overcompensation that may change the direction of the delayed axis of the refractive index. Moreover, considering the fact that orientation birefringence of the PS blend with the blending ratio of 30:70 was almost the same as that of PMMA, the PS blend could also become a promising optical polymer comparable to PMMA with low birefringence. In addition, a comparison with the retardation of a film sample with a blending ratio of 0:100 (PS-BBP only) would also have been desirable, however, the strength of this sample was too brittle to be processed into the desired sample, so preparation of the film sample was abandoned.

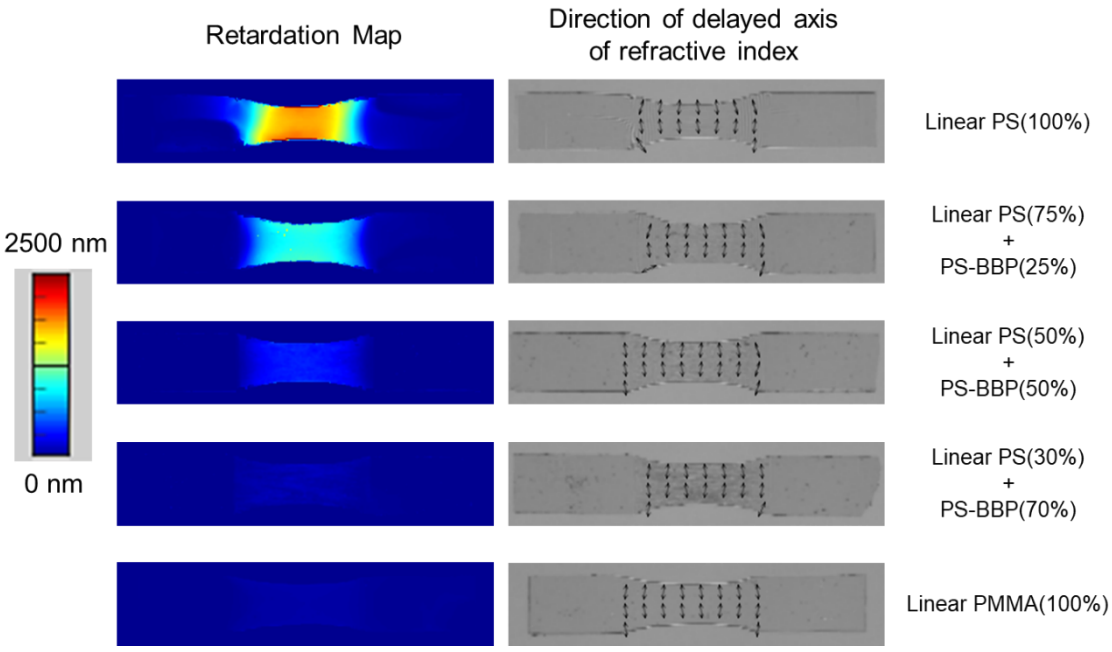

Figure 3.6 Retardation data on film samples of linear PS, PS/PS-BBP with various blending ratios, and linear PMMA

Figure 3.7 shows birefringence data against strain of linear PS, PS/PS-BBP with different blending ratios, and linear PMMA. Linear PS indeed exhibited negative birefringence at each strain and, furthermore, it was found that the absolute values were much larger than the ones of linear PMMA.[76, 91-93] Also, Figure 3.7 shows that the absolute value of the birefringence linearly increased as the strain increased. It indicates that molecular orientation was induced by the increase in the strain of the samples. As for the blend samples, birefringence went up at each strain as the PS-BBP content increased. The results revealed that oriented PS-BBP produced positive birefringence, relieving the negative birefringence caused by the oriented linear PS. Eventually, the birefringence value of the sample at the blending ratio of 30:70 was found to be almost the same as that of linear PMMA at each strain as presented in Figure 3.8.

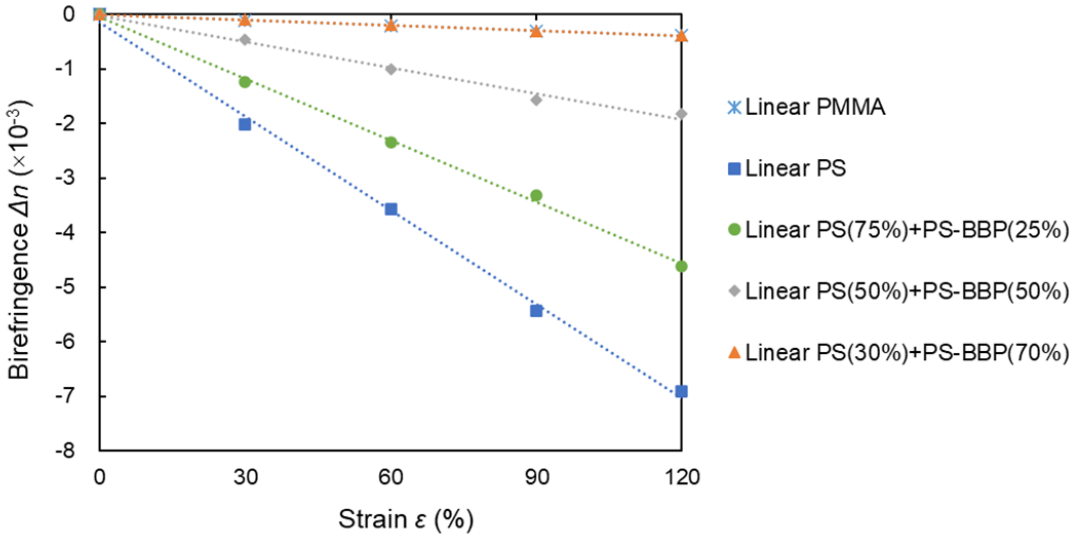

Figure 3.7 Birefringence vs. strain on film samples of linear PS, PS/PS-BBP with various blending ratios, and linear PMMA

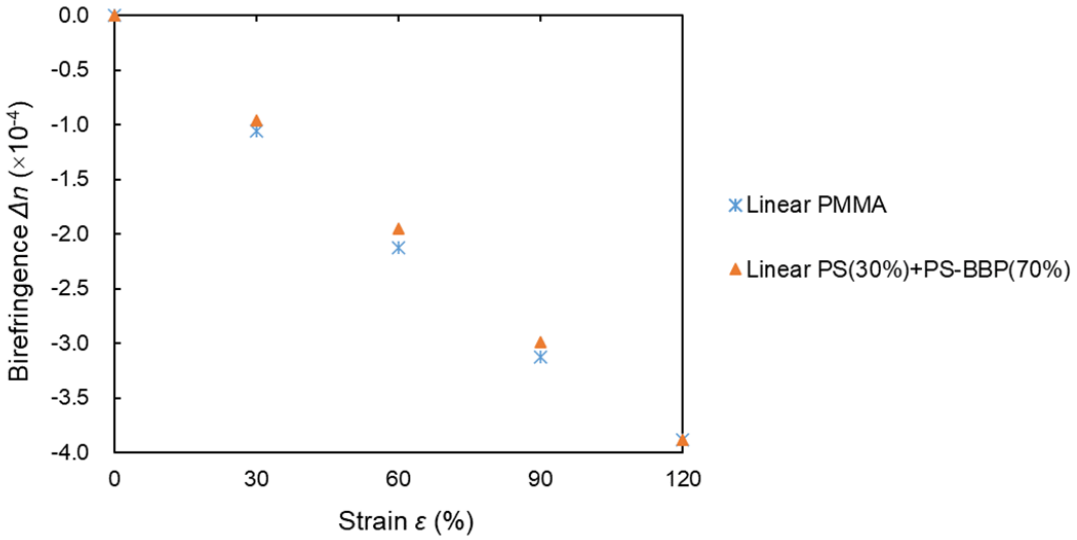

Figure 3.8 Enlarged plots of birefringence vs. strain on film samples of linear PMMA and PS/PS-BBP at the blending ratio of 30:70

According to the previous study on zero-birefringence optical polymers,[72] it is considered that the orientation birefringence of PS blend samples conforms to the following formula:

$$\Delta n_{\mathrm{PS/PS-BBP}} = \Delta n_{\mathrm{PS}} \times \frac{\alpha}{100} + \Delta n_{\mathrm{PS-BBP}} \times \frac{100-\alpha}{100} \qquad (3.1)$$

where, $\Delta n_{\mathrm{PS/PS\text{-}BBP}}$, Δn_{PS}, and $\Delta n_{\mathrm{PS\text{-}BBP}}$ are the orientation birefringence of the PS blend samples, linear PS, and PS-BBP, respectively. α (wt%) and 100- α (wt%) are the weight ratios of linear PS and PS-BBP. As orientation birefringence of polymers is generally caused by anisotropy of molecular polarizability, Δn_{PS} should depend on anisotropy of polarizability of styrene monomers in linear PS. $\Delta n_{\mathrm{PS\text{-}BBP}}$ is also highly dependent on anisotropy of polarizability of styrene monomers in PS-BBP, because many parts of PS-BBP are composed of styrene monomers in the side chains. When PS blend samples are uniaxially elongated, the molecular chains of linear PS can be oriented along the stretching direction. Then the main chains of the PS-BBP can also be oriented along the

stretching direction, but by simultaneously orienting the densely grafted side chains perpendicular to the main chains. This is because styrene monomers of PS-BBP are grafted perpendicular to the main chain of PS-BBP, thus making the positive/negative signs of $\Delta n_{\text{PS-BBP}}$ and Δn_{PS} opposite. As mentioned in Chapter 2, it should be necessary to consider the effect of birefringence created by norbornenes in main chains and ATRP initiators in order to completely compensate for orientation birefringence. The effect may be considered negligible in this case, though. This is because PS-BBP are mostly composed of PS side chains and the anisotropy of the styrene monomers is comparatively large. In the study on PMMA, it was considered that norbornenes and ATRP initiators generated a certain contribution to the orientation birefringence of PMMA. However, since intrinsic birefringence of PS is more than 20 times higher than that of PMMA,[8] the contribution of norbornenes and ATRP initiators could be negligible in the system of linear PS and PS-BBP. Therefore, it was first expected that the absolute values of $\Delta n_{\text{PS-BBP}}$ and Δn_{PS} should be almost the same and that the proper ratio of linear PS to PS-BBP in PS/PS-BBP to compensate for orientation birefringence should be around 50:50. However, even PS/PS-BBP with the ratio of 50:50 demonstrated much residual orientation birefringence, whereas PS/PS-BBP with the ratio of 30:70 possessed little residual orientation birefringence. This may be due to the difference in T_g between linear PS and PS-BBP in PS/PS-BBP, causing phase separation. In such phase separation, the PS-BBP region could relax relatively fast after stretching due to the lack of molecular entanglement. It is, therefore, considered that the molecular chains of linear PS could be readily oriented along the stretching direction, while the main chains in PS-BBP could not be completely oriented along the stretching direction due to the fast relaxation. The incomplete orientations of main-chain PS-BBP resulted in the incomplete molecular orientations of the side-chain PS-BBP, which were perpendicular to the molecular chains of linear PS in the film samples cooled to room temperature after stretching. It indicates that the birefringence value of PS-BBP with a positive sign may have shifted to a smaller value and that 50:50 for the blending ratio was insufficient to cancel the birefringence. Actually, the birefringence could only be canceled with a larger amount of PS-BBP, which was found to be around 30:70 to adequately compensate for the birefringence.

Based on the results of compensation for orientation birefringence by PMMA-BBP in the previous chapter and PS-BBP in this section, the concept of molecular design of desirable BBP is summarized in Figure 3.9. It indicates the four important factors a) – d) in designing BBP blended with a linear polymer to effectively control orientation birefringence of the linear polymer. The most important thing is to select the same monomer unit as that composing of the linear polymer for side chains in the BBP. This is an absolute requirement to control birefringence of the linear polymer by the BBP. Next, it is essential to control the length of side chains in the BBP. To realize the main chain elongated by excluded-volume effect of the side chains, the side chains in BBP should require a certain length. On the other hand, if the length of the side chains is so long that interaction between side chains occurs, the elongation of the main chain in the BBP may be impaired. In addition, high polydispersity of side chains may affect rigidity of the main chain. Therefore, it is important to select appropriate side-chain length and polydispersity of the BBP. Then, it is also necessary to select a proper monomer unit for the main chain in BBP. It is desirable to select the monomer unit possessing not only low intrinsic birefringence but also the same optical, mechanical and thermal properties as the monomer unit of side chains in BBP (i.e. the monomer unit of the linear polymer). It can be also important that the main chain is easy to synthesize and its degree of polymerization is easy to control. In this study, the norbornene was selected as the monomer unit of the main chain. This is not only because the norbornene is easy to control the degree of polymerization by Grubbs catalyst, but also because there is optical reason that the norbornene is the monomer unit constituting the main chain in COP and COC, which are optical polymers utilized in imaging lens systems requiring high resolution. Finally, it is crucial to control the main-chain length of the BBP. To appropriately compensate for orientation birefringence of the elongated linear polymer, the main chain in the BBP must be oriented to the same direction as the oriented linear polymer. Therefore, it is required that the length of the main chain is much longer than that of the side chains. It is expected that the molecular design of BBP described above can properly compensate for orientation birefringence.

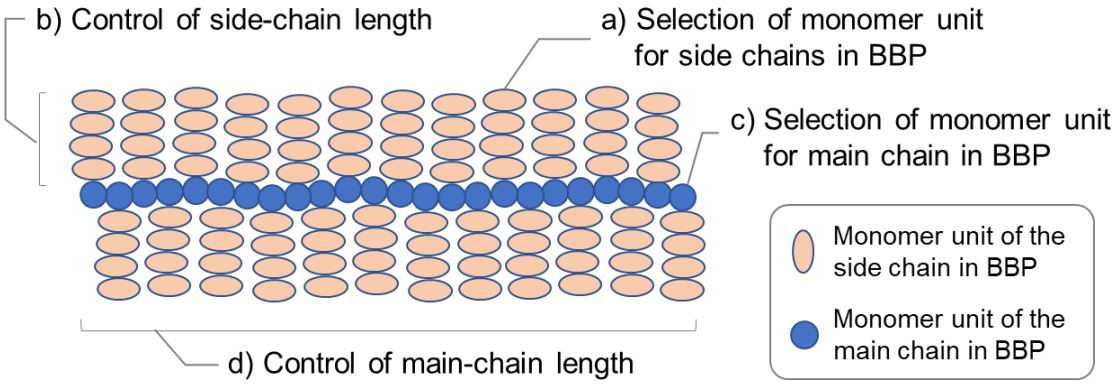

Figure 3.9 Concept of molecular design of desirable BBP

To evaluate the birefringence of PS/PS-BBP with the blending ratio of 30:70, the birefringence results were compared with those of commercial optical polymers currently used in the lens applications. Figure 3.10 shows the representative retardation data measured by WPA-100 on typical PC (AD-5503, Teijin Limited), special PC (EP-5000, Mitsubishi Gas Chemical Company, Inc.), PS/PS-BBP with the blending ratio of 30:70, and linear PS samples stretched at 120% of strain. The colors show the amount of retardation, and the monochrome figures represent the directions of delayed axes described by arrows, presenting the direction of higher refractive indices. Since PS was an optical polymer with high chromatic dispersion, two representative PC materials with high chromatic dispersion in commercial optical polymers were selected for comparison. The visual data illustrated that PS/PS-BBP with the blending ratio of 30:70 possessed much less retardation than typical PC and linear PS, which also exhibited low retardation close to special PC. Figure 3.11 shows birefringence data against strain for typical PC, special PC, PS/PS-BBP with the blending ratio of 30:70, and linear PS. Among the samples, it was found that typical PC and linear PS possessed very large birefringence. Due to the large birefringence, the two materials cannot be utilized as lens materials for flagship smartphone cameras and head-mounted devices that require lower birefringence to attain high resolution. Special PC, such as EP-5000 on the other hand, exhibited much less birefringence than typical PC and PS, which may contribute to the enhancement of the performance of flagship smartphone cameras and head-mounted devices. PS/PS-BBP with the blending ratio of 30:70 also presented very small birefringence, though not small

enough as compared with special PC (Figure 3.12). Nevertheless, as mentioned above, PS/PS-BBP exhibited almost the same level of birefringence as linear low-birefringence PMMA that is widely utilized as optical polymers. Hence, it is considered that PS/PS-BBP could be a promising candidate for an optical polymer with high chromatic dispersion and low birefringence.

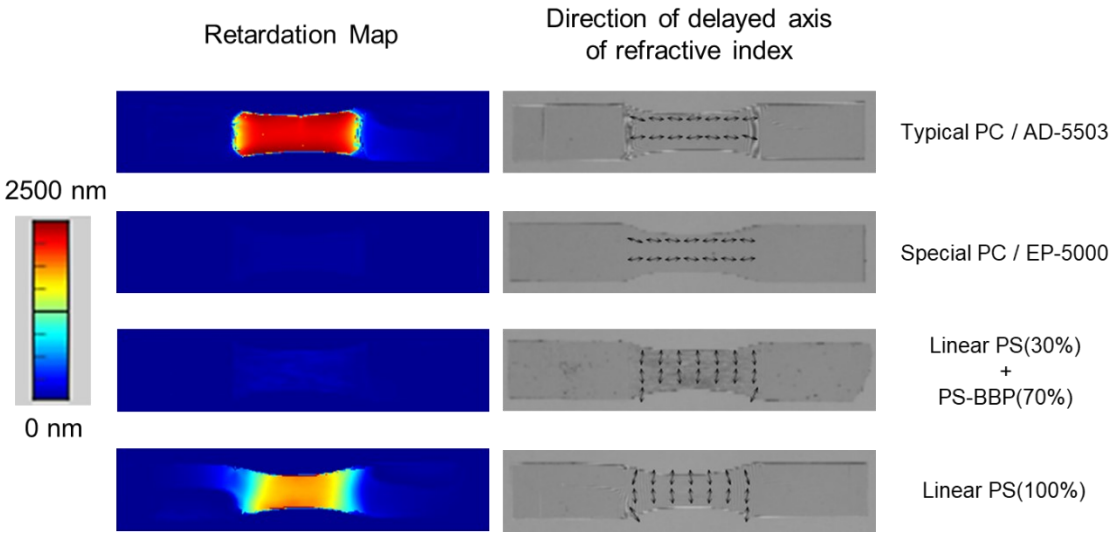

Figure 3.10 Retardation data on film samples of typical PC, special PC, PS/PS-BBP at the blending ratio of 30:70, and linear PS

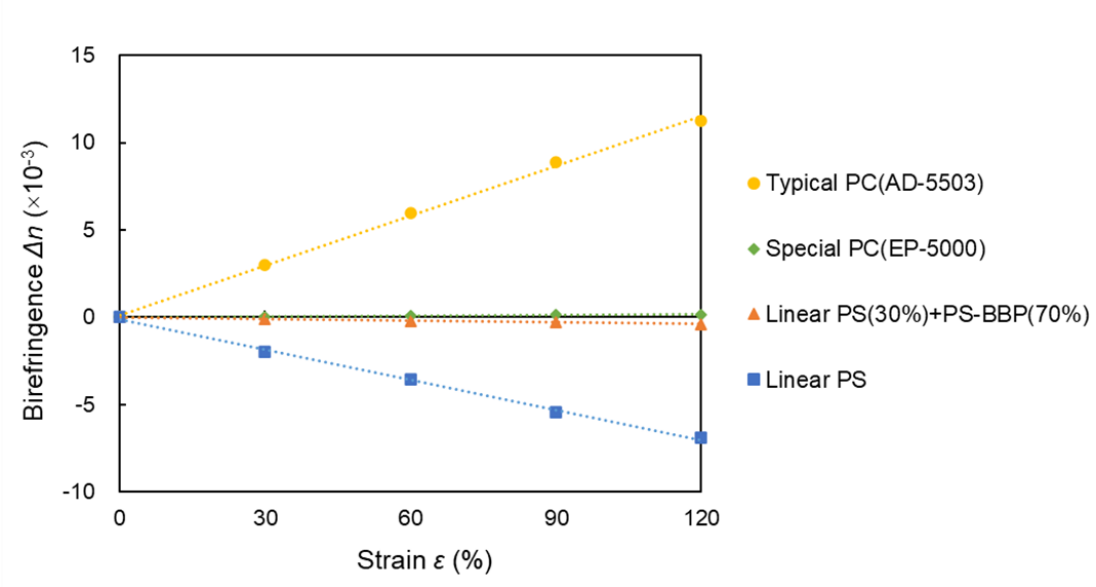

Figure 3.11 Birefringence vs. strain on film samples of typical PC, special PC, PS/PS-BBP at the blending ratio of 30:70, and linear PS

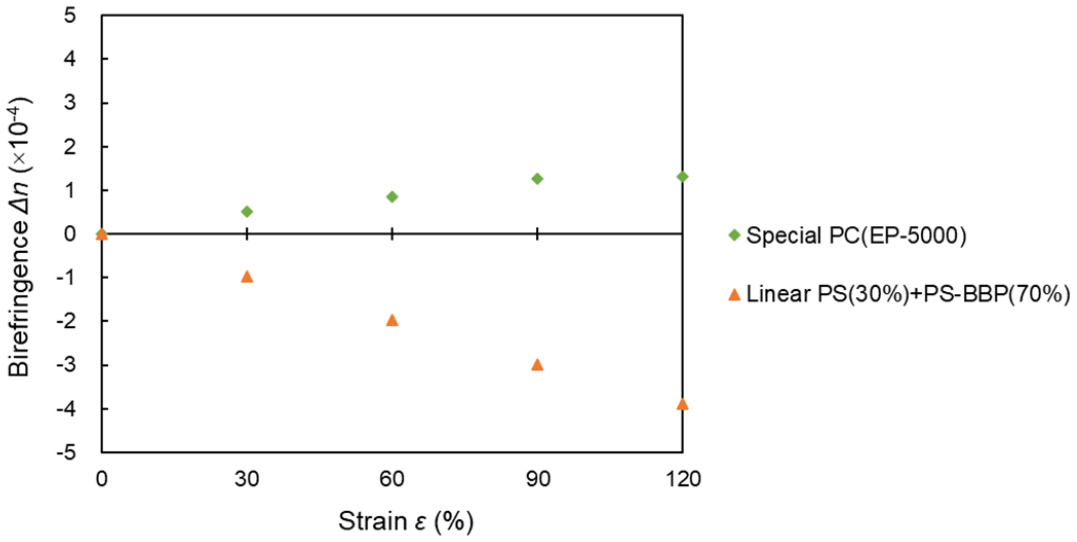

Figure 3.12 Enlarged plots of birefringence vs. strain on film samples of special PC and PS/PS-BBP at the blending ratio of 30:70

3.3.4 Photoelastic birefringence

In addition to orientation birefringence, photoelastic birefringence of linear PS and PS/PS-BBP with different blending ratios was evaluated. Film samples were fabricated following the same procedure as that mentioned in the previous section. All rectangle samples were uniaxially elongated with a handmade device that could hold both sides of the samples before applying designated strain (ε). Elongation was applied to the part of ~5 mm in length of each sample at room temperature. The retardation data were employed to calculate birefringence using the formula described in the previous section.

Figure 3.13 shows the representative retardation data measured by WPA-100 on linear PS and PS/PS-BBP with different blending ratios stretched at 0.16% strain within the range of elastic deformation at room temperature. The colors indicate the amount of retardation, and the arrows in the monochrome figures represent the directions of delayed axes, presenting the direction of higher refractive indices. Dashed orange lines indicate approximate outlines of the samples. The photoelastic birefringence of PS is known to differ from the orientation birefringence by showing the positive birefringence to the stretching direction,[9, 94] and the direction of the delayed axis of the refractive index is parallel to the stretching direction. In this study, the delayed axes of all samples in Figure 3.13 were also found to be in the same direction as the stretching direction. Moreover, the amount of retardation increased as the ratio of PS-BBP increased, unlike the compensation for orientation birefringence. Figure 3.14 shows the data of photoelastic birefringence against strain for linear PS and PS/PS-BBP with different blending ratios. The results indicate that the values of positive birefringence linearly increased as the strain increased on all samples. In the previous study on methacrylates by Shafiee et al,[9, 30] it was demonstrated that some groups in the side chains of polymers were mainly oriented, while main chains were hardly oriented during the generation of photoelastic birefringence, and thus a phenyl ring had a positive contribution to photoelastic birefringence. It is, therefore, considered that phenyl groups in linear PS and PS-BBP of this study were also mainly oriented, while main chains of linear PS and PS-BBP were not oriented during the elastic deformation. As a result, positive birefringence appeared on the photoelastic birefringence in this study. As for the blend samples, positive

birefringence at each strain increased as the PS-BBP content increased. The results suggest that the phenyl groups in PS-BBP orient more strongly than the phenyl groups in linear PS. It is surmised that the small molecular-weight part of PS in the side chain of PS-BBP, which could move slightly during the elastic deformation of the blend film, facilitated the molecular motion and the configuration changes, contributing to relatively strong orientation of phenyl groups compared to those in the linear PS molecular chains, leading to the increase in positive birefringence. PS-BBP exhibited lower T_g than linear PS as presented in Figure 3.5. This result indicated that PS brushes of PS-BBP relaxed more quickly than PS matrix, thus moving more easily than linear PS. In addition, below the T_g with possible intermolecular interactions such as $\pi\pi$ stacking between phenyl groups, phenyl groups on the side chains of PS brushes can be readily oriented in the stretching direction due to the ease of movement as drawn in Figure 3.15, resulting in the increase of positive signs of photoelastic birefringence. Thus, it is considered that blending PS-BBP with linear PS produced a negative impact on the compensation for photoelastic birefringence. However, as the amount of the photoelastic birefringence was less than 1.0×10^{-4} for each sample, which is much smaller than the amount of the orientation birefringence, the impact of the photoelastic birefringence increase by PS-BBP should be negligible.

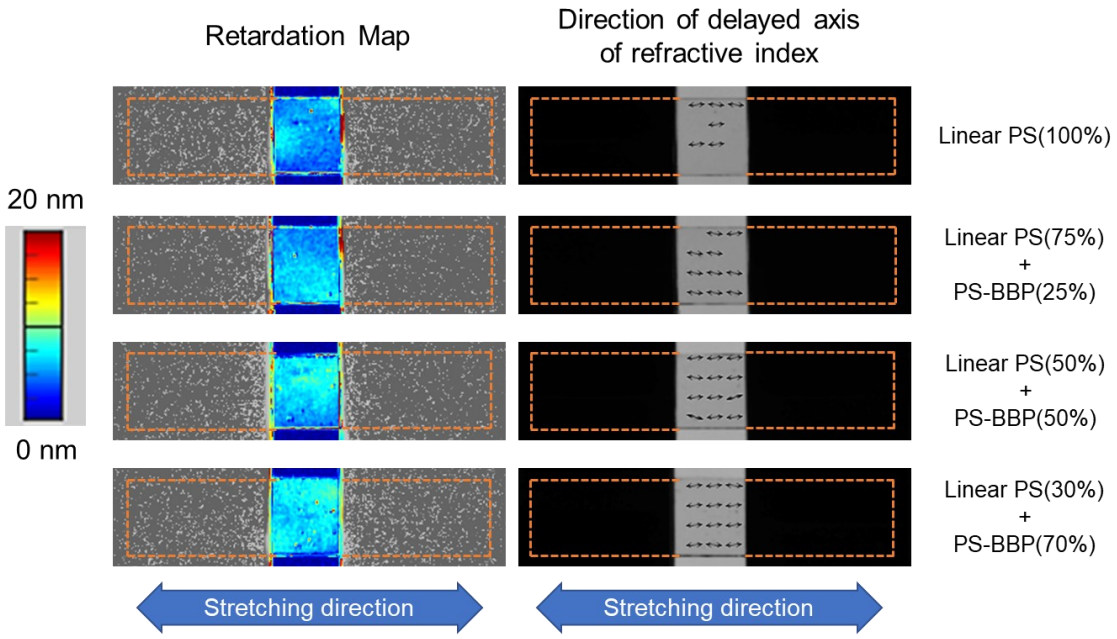

Figure 3.13 Retardation data on film samples of linear PS and PS/PS-BBP with the blending ratios of 75:25, 50:50, and 30:70, under elastic deformation

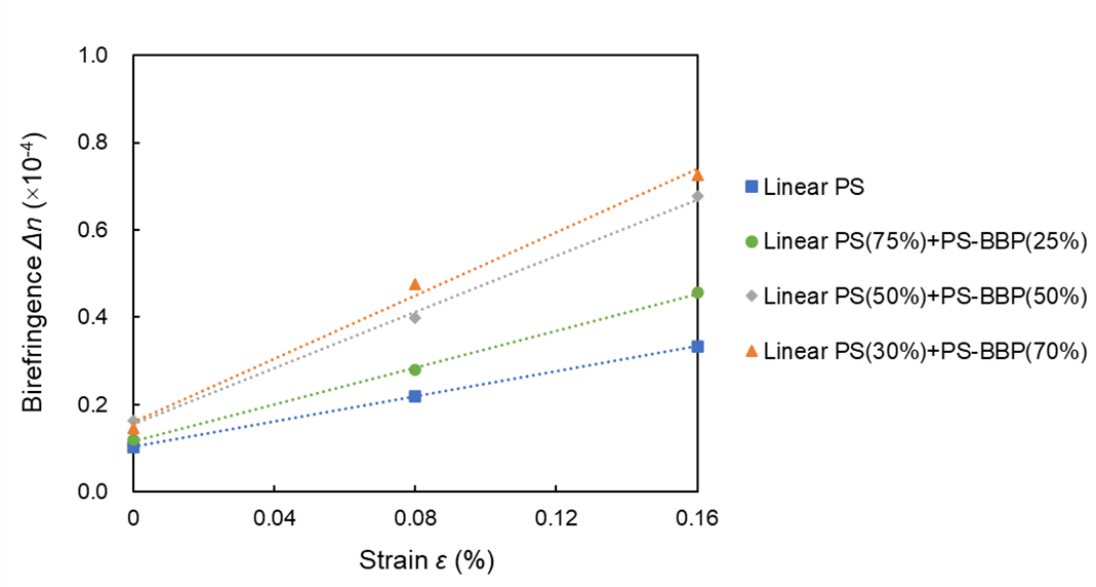

Figure 3.14 Birefringence vs. strain on film samples of linear PS and PS/PS-BBP with the blending ratio of 75:25, 50:50, and 30:70

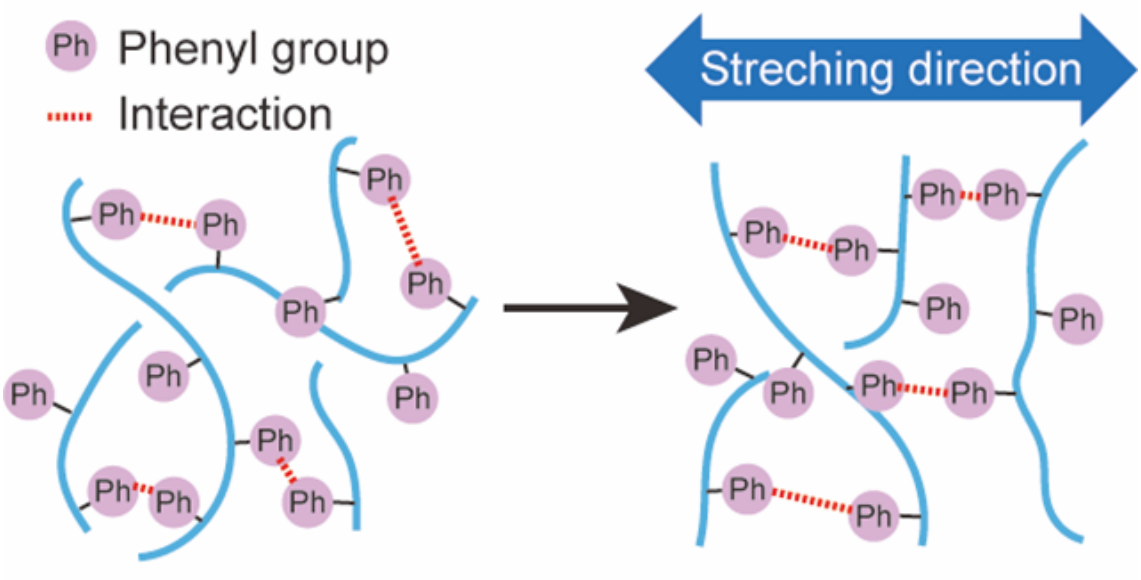

Figure 3.15 Contribution of PS brushes in PS-BBP to photoelastic birefringence

3.3.5 Refractive indices

Table 3.3 shows refractive indices (n_F, n_d, and n_C) at the wavelengths of hydrogen F (486 nm), helium d (588 nm), and hydrogen C (656 nm) lines, respectively, on film samples of linear PS and PS/PS-BBP with different blending ratios, and also the Abbe numbers (v_d) indicating chromatic dispersion property. v_d is calculated by the following equation.[4]

$$v_d = \frac{n_d - 1}{n_F - n_C} \tag{3.2}$$

Namely, low chromatic dispersion corresponds to a large v_d, while high chromatic dispersion corresponds to a small v_d. Linear PS indicated n_d = 1.590 and v_d = 31.5. All PS/PS-BBP denoted almost similar values of n_d = 1.587 - 1.590 and v_d = 31.4 - 31.5, and only very slight decrease in the refractive index was observed on PS/PS-BBP with the blending ratios of 50:50 and 30:70. It is, therefore, concluded that PS/PS-BBP can maintain almost the same refractive index and Abbe number as linear PS, and that PS blends may be a promising optical polymer with high chromatic dispersion (the low Abbe number).

Table 3.3 also includes n_d and v_d of AD-5503 (typical PC) and EP-5000 (special PC). As presented in the previous section, EP-5000 demonstrated pretty low birefringence compared to AD-5503. It is known that since EP-5000 are synthesized by random copolymerization of two different monomers with positive and negative birefringence,[2, 3] the optical properties of the resulting polymers change from the original material. In fact, n_d and v_d of EP-5000 were completely different from those of AD-5503, indicating that special PC acquired its low birefringence by changing its original optical properties. In contrast, the compensation for orientation birefringence with the bottlebrush polymers did not affect optical properties such as n_d and v_d, indicating the advantage of the unique bottlebrush-polymer blend system, minimizing birefringence by simultaneously maintaining its original optical properties.

Table 3.3 Refractive indices (n_F, n_d, and n_C) and the Abbe numbers (v_d) of linear PS, PS/PS-BBP with different blending ratios, typical PC, and special PC

Sample	n_F	n_d	n_C	v_d
Linear PS (100%)	1.603	1.590	1.585	31.5
Linear PS (75%) + PS-BBP (25%)	1.603	1.590	1.585	31.4
Linear PS (50%) + PS-BBP (50%)	1.602	1.589	1.583	31.5
Linear PS (30%) + PS-BBP (70%)	1.601	1.587	1.582	31.4
Typical PC (AD-5503)	1.596	1.583	1.577	30.2
Special PC (EP-5000)	1.654	1.635	1.627	24.0

3.3.6 Light transmittance

Figure 3.16 shows the light transmittance of a linear PS film and PS/PS-BBP films with different blending ratios of linear PS to PS-BBP. The transmittances of linear PMMA and PMMA bottlebrush mixed polymers (PMMA/PMMA-BBP) films were also presented for comparison, which were the same samples demonstrated in Chapter 2. Linear PS demonstrated high transmittance beyond 85% in the wavelength range of 400 - 800 nm, while PS/PS-BBP indicated slightly lower transmittance at a short wavelength than linear PS. The results were similar to those of PMMA/PMMA-BPP. In fact, the lowering of the transmittance was considerably suppressed compared to PMMA/PMMA-BBP, even the blend film samples with a higher content ratio of PS-BBP appeared only slightly yellowish, similar to the special PC used as a lens material for smartphone-camera lenses. The improvement may be due to the developed synthetic processes of PS-BBP: improved synthesis and purification methods that could avoid the desorption of bromine (Br) as also mentioned in 3.2 Experimental section. The methods were not employed for the synthesis of PMMA-BBP in the previous study mentioned in Chapter 2, and thus PMMA/PMMA-BBP samples looked more yellowish especially at the blending ratio of 60:40 than the PS blend samples. It was considered that the slight decrease in transmittance of PS/PS-BBP at short wavelength was due to the oxidation of norbornenes constituting the main chains of PS-BBP. Since PS/PS-BBP were thermally compressed at 180°C for 5 min, the double bonds of norbornenes may have been partly oxidized at such high temperature. Nevertheless, the mixed sample with the blending ratio of 30:70 still had over 77% of light transmittance at 420 nm, while the transmittance at 450 - 650 nm also remained more than 82%, indicating the possibility of the PS/PS-BBP sample with the blending ratio of 30:70 to be utilized as an optical material for optical lenses and films.

Generally, a blend material with phase separation should have an issue of compatibility, occasionally resulting in low transparency. PS/PS-BBP samples in this study, however, demonstrated high transparency, although they may experience phase separation. This is because PS-BBP were mainly composed of the same styrene monomers as those in linear PS, and thus, regardless of the blending ratios, PS/PS-BBP

could possess almost the same refractive index as that of linear PS as mentioned in the previous section. Because of this similarity in the refractive index, PS/PS-BBP could maintain the transparency required for optical polymers even under phase separation.

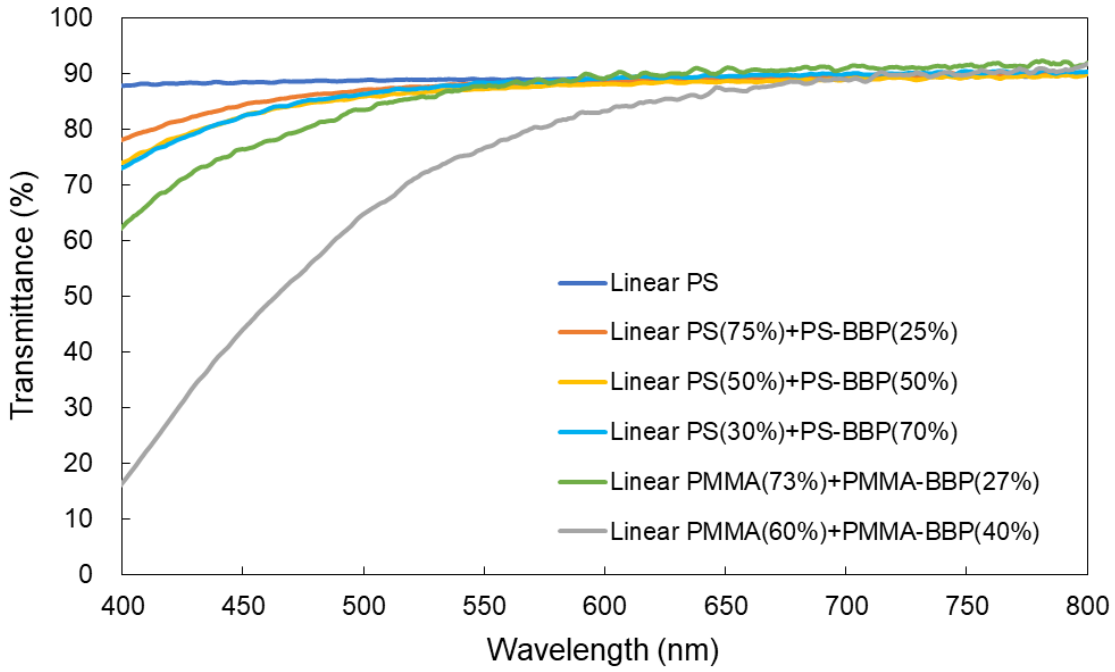

Figure 3.16 Light transmittance on films of linear PS, PS/PS-BBP with various blending ratios and PMMA/PMMA-BBP with the blending ratios of 73:27 and 60:40

3.4 Summary of this chapter

In this chapter, a trial was conducted to compensate for orientation birefringence of PS with a high chromatic dispersion by mixing linear PS and PS-BBP with high graft density. The optical and thermal properties of the PS blends were evaluated, and the characteristics were considered. The achievements were listed as follows:

i. PS bottlebrush polymers with well-controlled side-chain length could be successfully produced by ROMP of NB-PS macromonomers prepared by ATRP using ATRP initiator with norbornene units, indicating that PS-BBP had an optimized high aspect ratio of the main chain to the side chain.

ii. Orientation birefringence of PS could be compensated for by mixing linear PS and PS-BBP. This was because negative birefringence of elongated linear PS could be cancelled by positive birefringence of elongated PS-BBP, as well as the control of orientation birefringence for PMMA mentioned in Chapter 2. Especially, when a blending ratio of linear PS to PS-BBP was 30:70, the sample demonstrated extremely low orientation birefringence of $|\Delta n| \sim 3.9 \times 10^{-4}$ even under 120% of strain. It was almost the same amount of orientation birefringence as linear PMMA which is the most widely used as an optical polymer with low birefringence. It indicated that PS/PS-BBP with the blending ratio of 30:70 could be a promising candidate for an optical polymer with a high chromatic dispersion and low birefringence.

iii. Photoelastic birefringence of linear PS and PS/PS-BBP was examined as well. Photoelastic birefringence of linear PS showed positive values to stretching direction, which were different from negative values of orientation birefringence. Photoelastic birefringence of PS/PS-BBP also represented positive values, moreover, the amount of birefringence increased at each strain as the content ratio of PS-BBP increased. It indicated that blending PS-BBP with linear PS produced a negative impact on the compensation for photoelastic birefringence. However, since the amount of the photoelastic birefringence was much smaller than that of orientation birefringence for

each sample, the impact of the increase in photoelastic birefringence by PS-BBP could be negligible.

iv. The glass transition temperatures of linear PS, PS-BBP, and PS/PS-BBP were examined through DSC analysis. While linear PS and PS-BBP exhibited only one T_g at ~104°C and ~89°C, respectively, PS/PS-BBP had both T_g at ~103°C and ~90°C, which were likely derived from linear PS and PS-BBP, respectively. The results suggested that phase separation could occur between linear PS and PS-BBP. Such phase separation was not suitable for narrowing the temperature range of manufacturing process on an optical polymer. However, since the difference of T_g between linear PS and PS-BBP was only about 15°C, PS/PS-BBP could be utilized as an optical polymer by choosing appropriate thermal condition in the manufacturing process.

v. Refractive indices and Abbe numbers of linear PS and PS/PS-BBP were measured with the abbe refractometer, all PS/PS-BBP indicated almost the same n_d and ν_d as linear PS. It was considered that compensation for birefringence with PS-BBP did not affect n_d and ν_d of linear PS, as well as the results of PMMA/PMMA-BBP demonstrated in Chapter 2.

vi. Light transmittances on film samples of linear PS and PS/PS-BBP were evaluated with the spectrophotometer, and were also compared with those of PMMA/PMMA-BBP illustrated in Chapter 2. While linear PS showed high transmittance beyond 85% through the range of visible wavelength, PS/PS-BBP exhibited slightly lower transmittance at short wavelength than linear PS. However, the lowering of the transmittance was considerably improved compared to PMMA/PMMA-BBP. This might be because revised synthesis and purification methods that could avoid the desorption of Br were introduced on the synthetic process of PS-BBP. The PS/PS-BBP with the blending ratio of 30:70 still demonstrated over 77% of light transmittance at 420 nm, and the transmittance at 450 - 650 nm also remained more

than 82%, indicating that the PS/PS-BBP sample could be utilized as an optical material for optical lenses and films.

Chapter 4

Application of low-birefringence polystyrene to imaging lens systems requiring high resolution

4.1 Background and purpose

In recent years, optical polymers have been used in many optical devices because of lightweight and low cost. Especially, with the global proliferation of camera-equipped smartphones, optical polymers have been greatly applied to plastic lenses for smartphone cameras.[62, 63] Plastic lenses utilized in lens systems of imaging devices enabled mass production of lenses with aspherical surfaces and free-form surfaces, realizing precise compensation for spherical aberration, coma aberration and distortion even in small-size lens systems.[95, 96] In order to acquire high image-quality on such lens systems, it is also necessary to appropriately compensate for chromatic aberration. Then, multiple optical materials with high and low Abbe numbers are indispensable.[4, 74, 75] The Abbe number (ν_d) is the value showing chromatic dispersion property of the material, calculated by the following equation.

$$\nu_d = \frac{n_d - 1}{n_F - n_C} \tag{4.1}$$

where n_F, n_d, and n_C are refractive indices of the material at the wavelengths of hydrogen F (486 nm), helium d (588 nm), and hydrogen C (656 nm) lines, respectively. Since various optical polymers have been recently developed,[97-104] it has become possible to effectively reduce the chromatic aberration even in imaging lens systems composed solely

of multiple plastic lenses. In addition, studies on improvement of transparency,[105, 106] prediction of the refractive index,[107-109] and correlations of the refractive index and the Abbe number to the degree of polymerization[110, 111] have been proceeded in optical polymers as well as development of polymers with high refractive indices.[112] Despite these developments, birefringence of optical polymers has still remained an issue causing degradation in image quality.

Regarding birefringence of practical optical polymers, it is known that poly(methyl methacrylate) (PMMA), cyclo-olefin polymer (COP), and cyclo-olefin copolymer (COC) with large ν_d possess relatively low birefringence, while normal polystyrene (PS) and polycarbonate (PC) with small ν_d possess considerably high birefringence.[8, 76-78] Consequently, COP and COC with large ν_d can be used for imaging lens systems requiring high resolution, while normal PS and PC with small ν_d cannot be employed. Therefore, it is very important to reduce birefringence of materials with small ν_d. Some special PCs and fluorene polyesters with small ν_d and low birefringence were developed to date.[2, 3, 104] However, they are such high-cost optical materials produced by copolymerization of several expensive monomers that it is difficult to realize low-cost mass production using lens systems including these materials. In contrast, inexpensive normal PS and PC have been widely used in various applications. Especially, the cost of PS can be lower than PMMA, which is known as the low-cost optical polymer, when used in mass-produced lenses. These facts indicate that both high-resolution imaging and low-cost mass productions can be achieved by using PS with small ν_d and low birefringence together with COP and COC.

In Chapter 3, novel PS with ν_d of 31.5 was developed, which exhibited extremely low birefringence (LB-PS). Its low birefringence was accomplished by mixing linear PS and bottlebrush polymers with well-controlled PS side chains (PS-BBP) in the ratio of 30:70. In addition, LB-PS indicated high transparency with the same refractive index and the Abbe number as those of linear PS. Thus, it was expected that LB-PS could be a promising optical material for imaging lens systems with low birefringence and high resolution. However, the birefringence of LB-PS has not been yet compared with COP and COC, which are indispensable for compensating for chromatic aberration of lens

systems and are utilized together with small v_d materials such as LB-PS. Above all, it has not been clearly demonstrated that LB-PS is useful in increasing practical resolution of specific lens systems.

In this chapter, the birefringence of the developed LB-PS is compared with that of the representative COP and COC, which are most commonly utilized in imaging lens systems requiring high resolution, confirming if LB-PS possesses low-birefringence property required for imaging lens systems with high resolution. Then, with a lens system designed based on the data of an imaging lens system disclosed in a patent, it is calculated how many advantages the use of PS with v_d of 31.5 as an optical material has in optical design. Moreover, considering the respective birefringence of COP, linear PS and LB-PS, practical resolution performance of each lens system is estimated, and specific effects of birefringence on resolution are evaluated with modulation transfer function (MTF) and image simulation in computational studies.

4.2 Experimental section

4.2.1 Materials

Polystyrene (PS) with the average M_w of ~192,000 determined by Gel Permeation Chromatography was purchased from Sigma-Aldrich Co. LLC as linear PS. LB-PS was prepared by mixing linear PS and PS-BBP in the ratio of 30:70, PS-BBP were synthesized by ring-opening metathesis polymerization of norbornene-terminated PS macromonomers produced via atom transfer radical polymerization. COP (ZEONEX-K26R, Zeon Corporation) and COC (APL-5014CL, Mitsui Chemicals, Inc.) were provided by their respective manufacturers for this study, and used as received.

4.2.2 Fabrication of films by compression molding

Film samples of PS were prepared from linear PS and LB-PS by compression molding. LB-PS was identical to the sample which was mentioned as the blend of linear PS and PS-BBP with the blending ratio of 30:70 in Chapter 3. Each sample of ~0.6 g was sandwiched between two PET films at the pressure of 8 MPa and at 180°C for 5 min.[65] Thereafter, the samples were taken out and cooled to room temperature. In the process, thickness of the film samples was adjusted to be ~0.1 mm. Each film was then cut into a rectangular shape of ~5 mm in width and ~25 mm in length.

Film samples of commercial optical polymers were also prepared from ZEONEX-K26R and APL-5014CL by compression molding. Each sample of ~0.6 g was sandwiched between two polyimide films at the pressure of 8 MPa and at the glass transition temperatures of each polymer plus 70°C, which were 213°C for ZEONEX-K26R and 205°C for APL-5014CL. The specimens were thermally pressed for 5 min, where the gap between the two polyimide films was kept at ~0.15 mm. After that, the samples were taken out and cooled to room temperature. Consequently, film samples with ~0.15 mm thickness were obtained. Each film was then cut into a rectangular shape of ~5 mm in width and ~25 mm in length.

4.2.3 Evaluation of birefringence

All the rectangular samples were heated to their glass transition temperatures and uniaxially elongated on a dynamic mechanical analyzer (RSA-3, TA Instruments) to the designated strain (ε). The elongation process was conducted to the section of ~5 mm in length of each sample at the extension rate of 0.1 mm/s. After stretching, each sample was rapidly cooled to room temperature with a cooling system using liquid nitrogen. Thereafter, retardations of the samples were observed with a 2-D birefringence measurement system (WPA-100, Photonic Lattice, Inc.) to measure their birefringence ($\Delta n = n_{//} - n_{\perp}$). It can directly detect the data of retardation ($\Delta\lambda$) corresponding to birefringence by $\Delta n = \Delta\lambda / d$, where d is the thickness of film samples. The birefringence of each sample was evaluated by comparing these data.

4.2.4 Optical design of a high-resolution imaging lens system using ideal PS

In order to demonstrate effectiveness of employing PS as a lens material in imaging lens systems, optical design of a high-resolution imaging lens system using ideal PS, which was assumed to be zero birefringence, was conducted. In detail, a lens system, in which PS was not utilized as a lens material, was selected among previously disclosed numerical data of imaging lens systems with high resolution. Then, a non-PS optical material used as a lens element in the lens system was replaced by the ideal PS, optimizing the entire lens system with the same constraints as the specifications of the original lens system. The computational evaluation was carried out to confirm the improvement of the resolution performance, the results of transverse ray-aberration and MTF were assessed on an optical design software (CODE V, Synopsys, Inc.).

4.2.5 Estimation of the resolution considering the effect of birefringence

The effect of birefringence on the resolution of images was evaluated using the optical design data. Specifically, each amount of orientation birefringence measured in this study was employed in COP and PS lenses in the computational lens systems, and the practical resolution was estimated with MTF calculated on CODE V. In addition, the

image simulation was executed to visually compare the difference in the resolution performance between linear PS and LB-PS, using the eSFR-ISO-chart provided from Imatest LLC through CODE V.

4.3 Results and discussion

4.3.1 Evaluation of birefringence

To comprehensively evaluate the birefringence of linear PS and LB-PS developed in Chapter 3, the comparison was made with the birefringence of commercial optical polymers: ZEONEX-K26R and APL-5014CL which are most commonly used in imaging lens systems of high-resolution smartphone cameras. Figure 4.1 shows the representative retardation data measured with WPA-100 on ZEONEX-K26R, APL-5014CL, LB-PS, and linear PS samples stretched at the strain of 120%. It was visually illustrated that linear PS had extremely large retardation, while LB-PS possessed smaller retardation than ZEONEX-K26R and almost the same retardation as APL-5014CL. Figure 4.2 shows the data of birefringence against strain for ZEONEX-K26R, APL-5014CL, LB-PS, and linear PS. In these samples, linear PS presented very high birefringence by its absolute value. Due to this property, linear PS has not been used as a lens material for flagship smartphone cameras producing high-resolution images. However, LB-PS exhibited much lower birefringence than linear PS, as mentioned in Chapter 3. Moreover, LB-PS demonstrated that its absolute value of birefringence was lower than that of ZEONEX-K26R and comparable to that of APL-5014CL as shown in Figure 4.3. APL-5014CL is recognized in the optical industries as an optical material with extremely low birefringence, and it is widely used as not only a material for imaging lens systems of high-resolution smartphone cameras but also a material for eyepiece lens systems in AR/VR devices, which require a material with much lower birefringence than imaging lens systems. Considering the fact that ZEONEX-K26R and APL-5014CL are major lens materials for these devices, LB-PS can be a promising candidate for a lens material of flagship smartphone cameras and AR/VR devices.

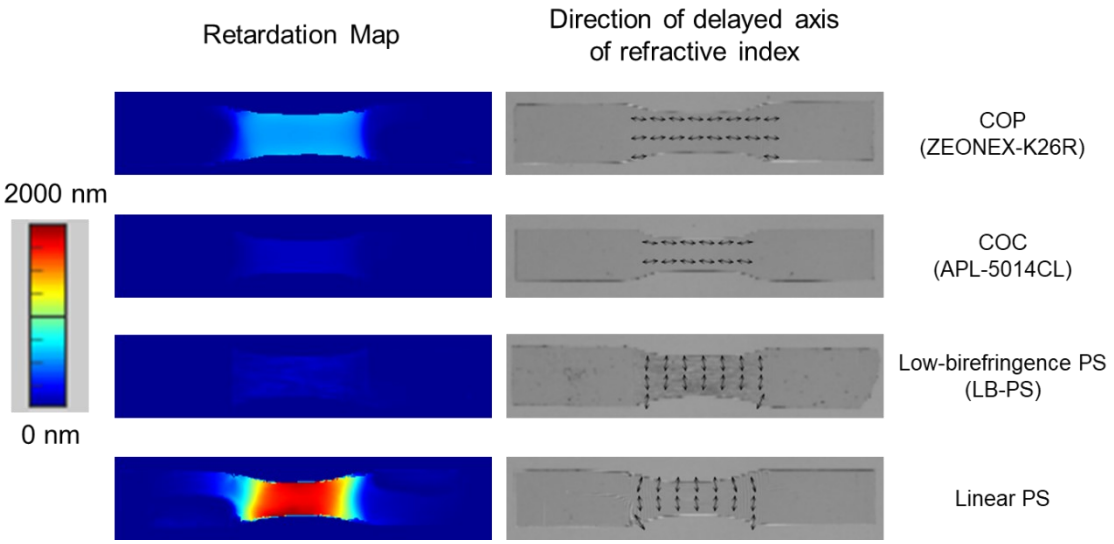

Figure 4.1 Retardation data on film samples of COP, COC, low-birefringence PS, and linear PS

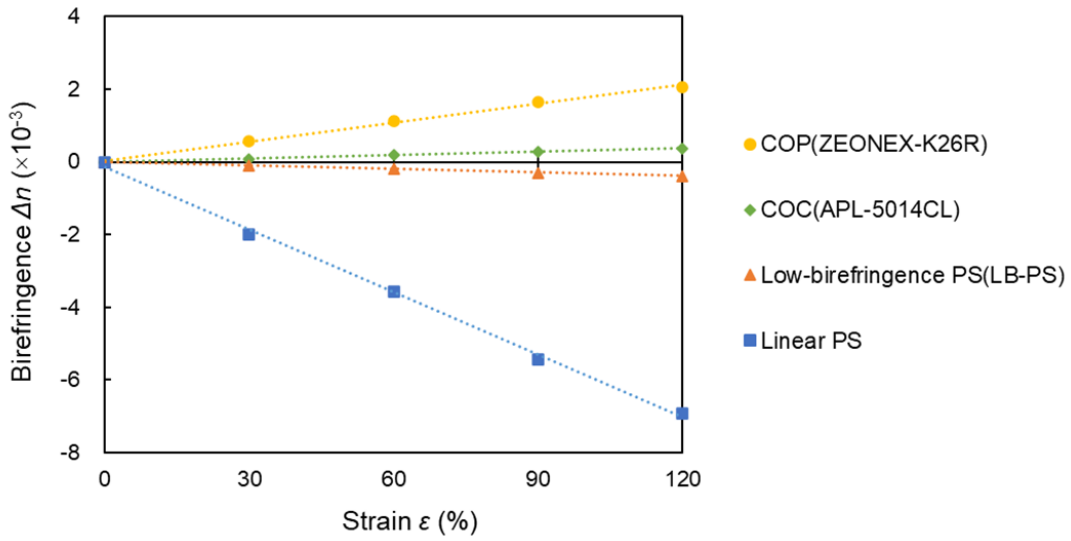

Figure 4.2 Birefringence vs. strain on film samples of COP, COC, low-birefringence PS, and linear PS

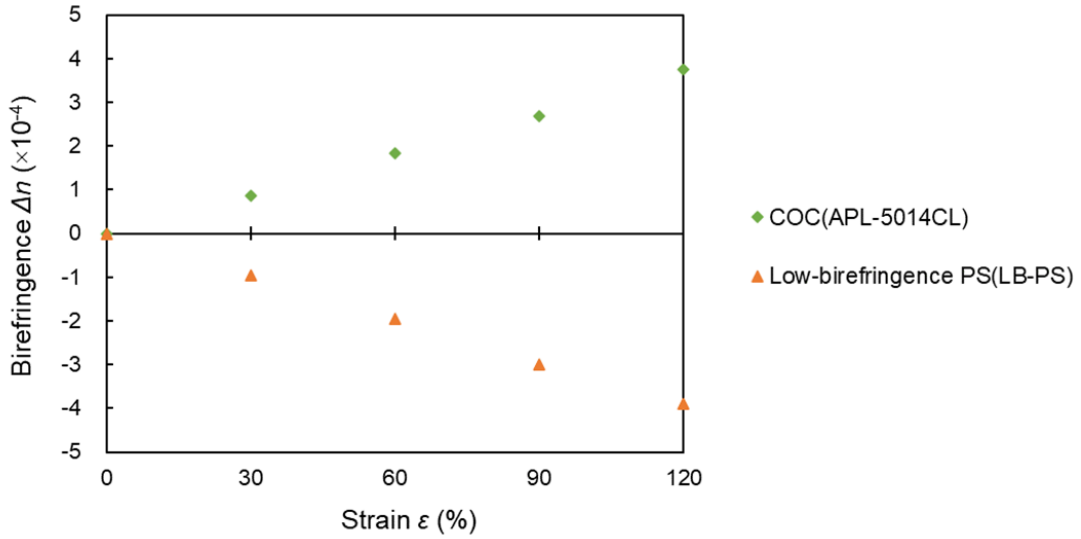

Figure 4.3 Enlarged plots of birefringence vs. strain on film samples of COC and low-birefringence PS

4.3.2 Optical design of a high-resolution imaging lens system using ideal PS

To implement optical design of a high-resolution imaging lens system using PS, the lens data of Numerical Example 1 in the patent document was adopted.[113] The data indicated that the lens system with very wide field of view was composed of 3 glass materials and 4 plastic materials without PS. The major specifications of the lens system are listed in Table 4.1. Figure 4.4 shows the cross-section of the lens system. It indicates that an object is located at infinity on the left side and an image corresponding to the object is generated through the lens system at the image plane on the right side. In Figure 4.4, each lens element in the lens system is named from L1 to L7 in order from the left side, including information of each lens material. In addition, the infrared-cut-filter (IRCF) is placed in front of the image plane to cut off unnecessary infrared light as well as protecting the image sensor. Figure 4.5 and Figure 4.6 show its transverse ray aberration curves and MTF vs. spatial frequency charts, which were evaluated at 0% (On-axis), 30%, 60%, 80%, and 100% of image height (IH). The ray traces in the cross-section

and the MTF charts at IH 0%, 30%, 60%, 80%, and 100% are presented with red, green, blue, brown, and pink lines, respectively. The transverse ray aberration curves at the wavelengths of F (486 nm), d (588 nm), and C (656 nm) lines are drawn with blue, green, and red lines, respectively. Solid lines and dotted lines in the MTF charts represent tangential and sagittal MTFs, respectively. The tangential direction of the MTF corresponds to the resolution in the radial direction from the optical axis of the lens system, while the sagittal direction of the MTF corresponds to the resolution in the rotational direction relative to the optical axis of the lens system.

Table 4.1 Major specifications of the lens system of Numerical Example 1 in the patent document

Parameter	Value
Focal length (mm)	1.45
F-number	2.85
Full field of view (degree)	150.6
Optical total track length (mm)	11.30
Chief ray angle at image plane (degree)	< 33
Projection type	2f tan (θ/2)

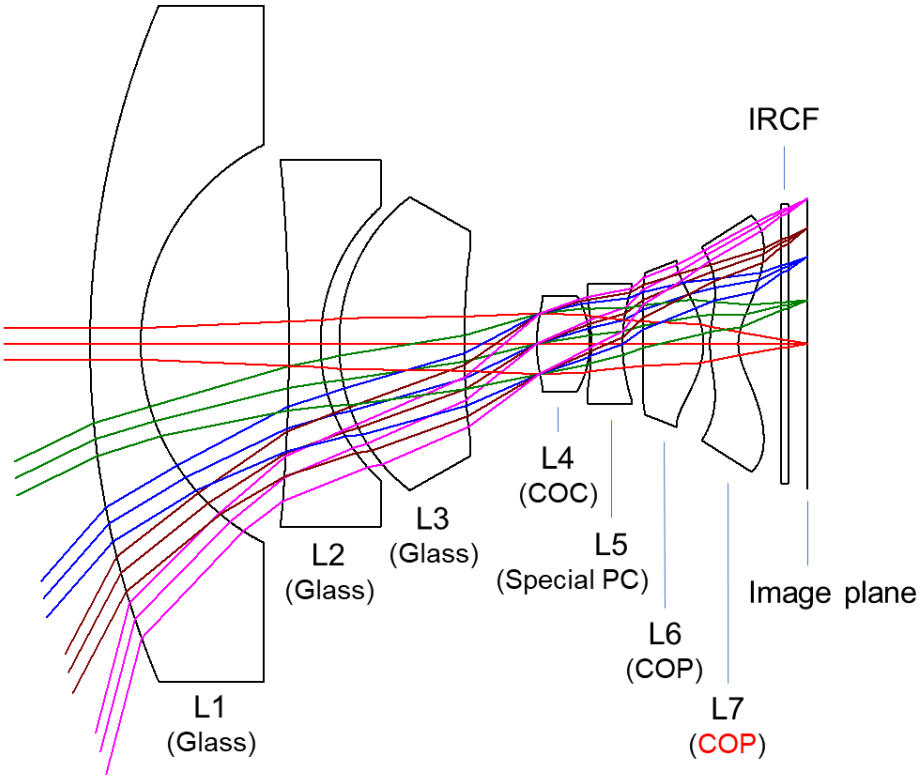

Figure 4.4 Cross-section of the lens system of Numerical Example 1 in the patent document

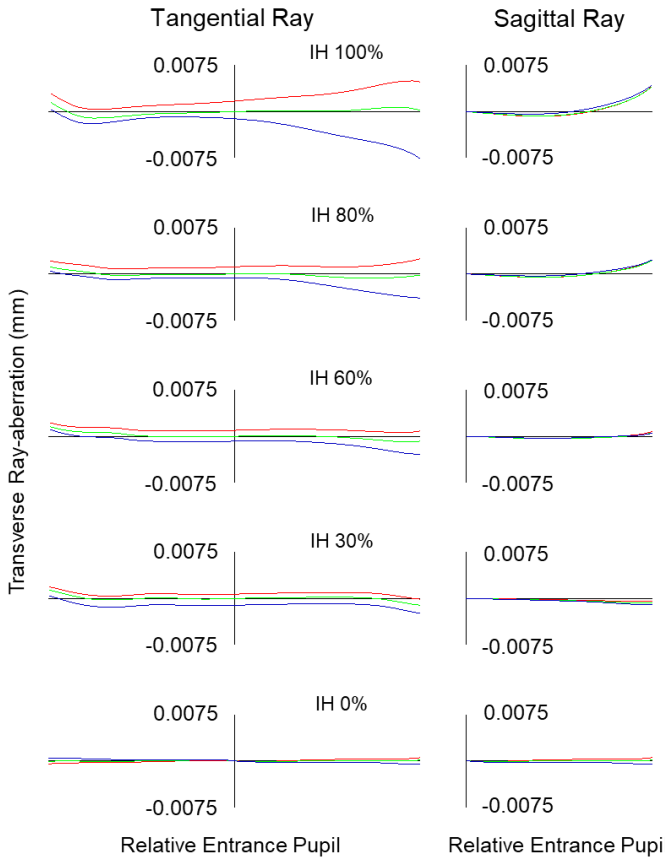

Figure 4.5 Transverse ray aberration curves of the lens system of Numerical Example 1 in the patent document

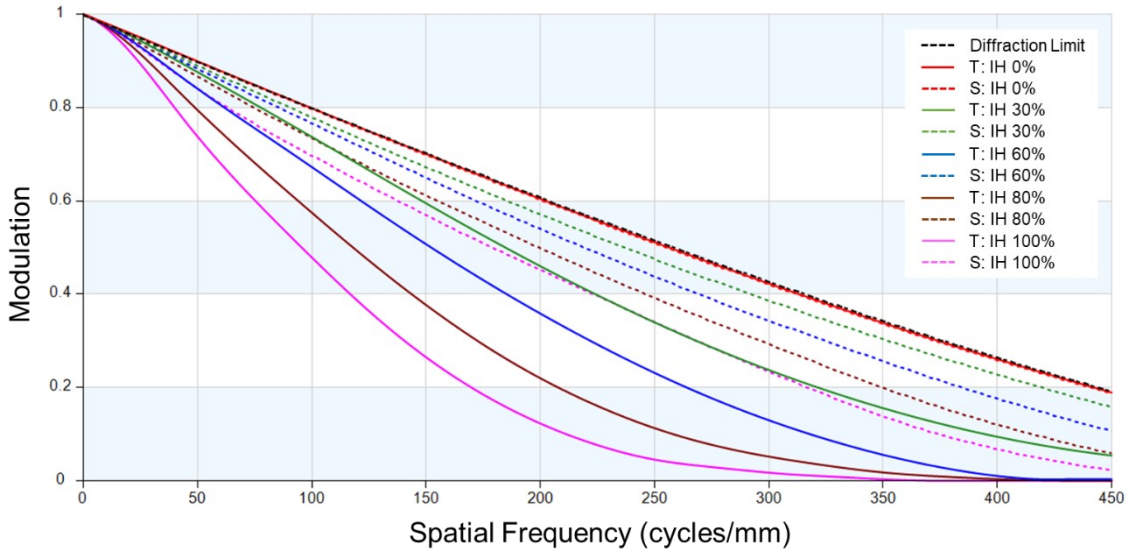

Figure 4.6 MTF vs. spatial frequency charts of the lens system of Numerical Example 1 in the patent document

In order to further enhance the resolution performance, the material of the lens element L7 closest to the image plane was changed from COP to ideal PS, which was assumed to have no birefringence. Then, the entire lens system was optimized with the same constraints as the specifications of the original lens system. Figure 4.7 shows the cross-section of the optimized lens system, and its corresponding transverse ray aberration curves and MTF vs. spatial frequency charts are shown in Figure 4.8 and Figure 4.9. Figure 4.7 - 4.9 are represented in the same conditions as Figure 4.4 - 4.6. The numerical data of the optimized lens system are listed in Table 4.2. Some lenses used in the lens system possess aspheric lens surfaces. The surface referred to as "ASP" in Table 4.2 represents an aspheric surface. The shape of the aspheric surface is defined by the following formula:

$$Z = \frac{Y^2/R}{1+\sqrt{1-(1+K)(Y/R)^2}} + \sum_{i=3}^{16} A_i Y^i \qquad (4.2)$$

where Z denotes a depth of the aspheric surface and Y denotes a height from the central axis of the aspheric surface. R denotes the paraxial radius of curvature, K denotes the conic constant, and A_3 to A_{16} denote the 3rd to the 16th order aspheric surface coefficients, respectively. Table 4.3 and Table 4.4 describe the values of aspheric surface coefficients (A_3 - A_{16}) in each aspheric surface together with the values of the conic constant K of the optimized lens system. For the computational studies in this section, all materials composing the lens systems were assumed to have no birefringence as in normal optical design.

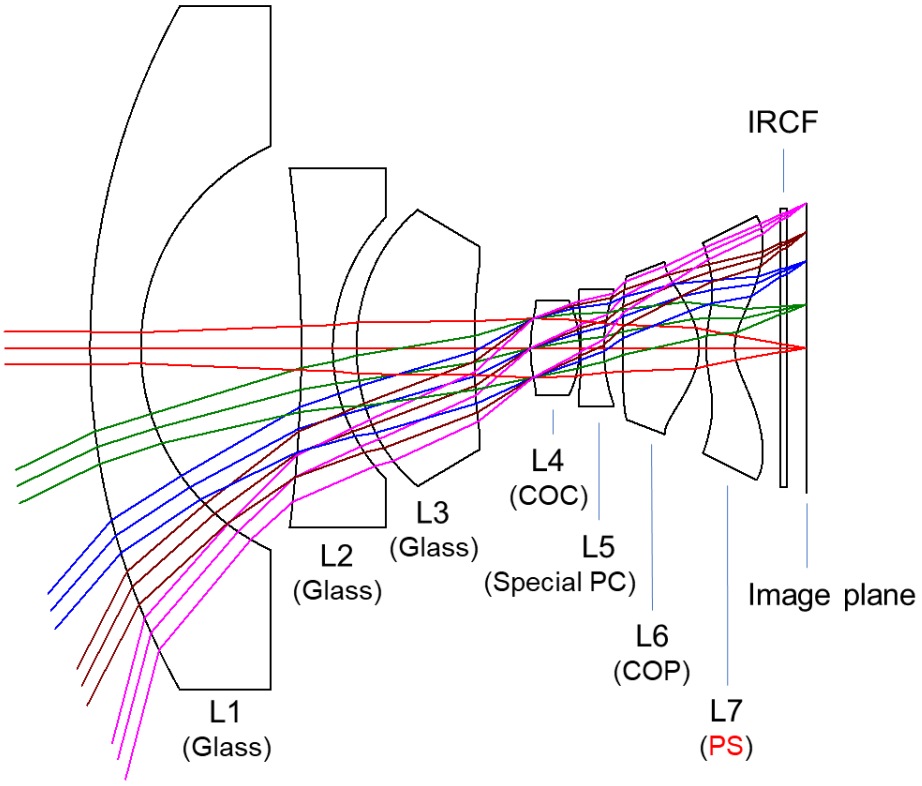

Figure 4.7 Cross-section of the lens system optimized using PS

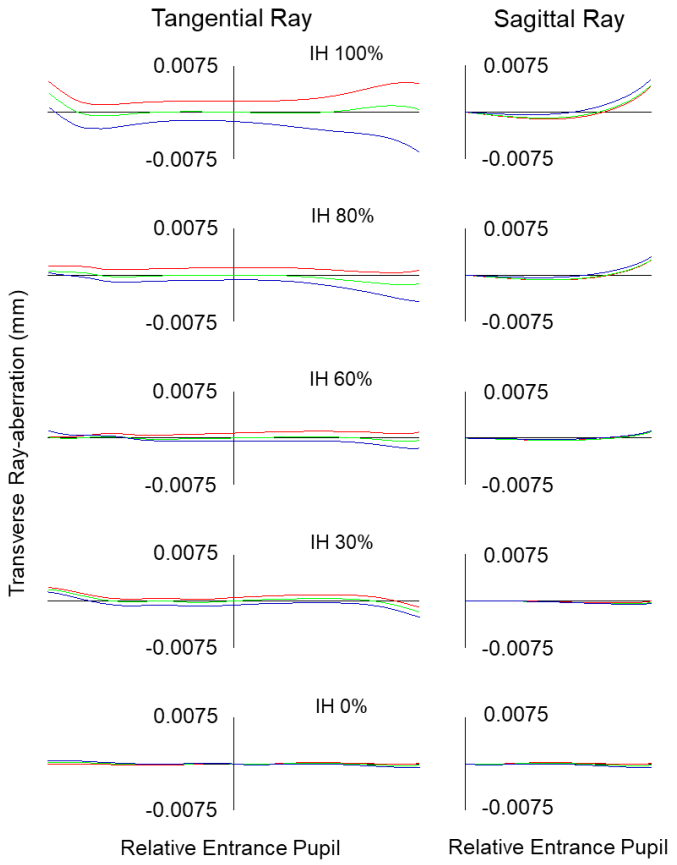

Figure 4.8 Transverse ray aberration curves of the lens system optimized using ideal PS

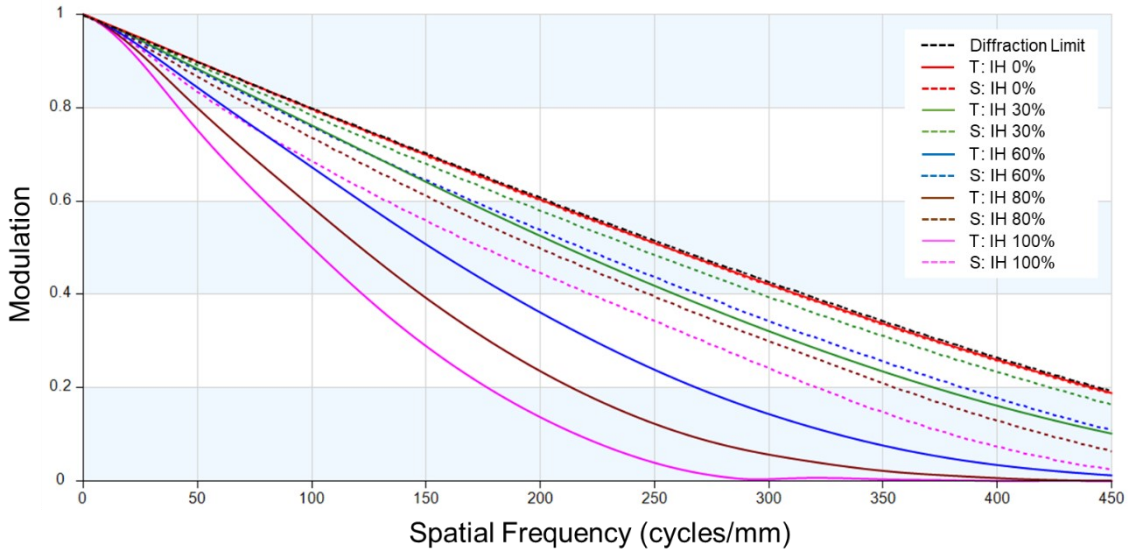

Figure 4.9 MTF vs. spatial frequency charts of the lens system optimized using ideal PS

Table 4.2 Numerical data applied to the optimized lens system

Surface	Radius (mm)	Aspheric Surface	Thickness (mm)	Refractive Index	Abbe Number	Material
1	10.976		0.80	1.835	42.7	Glass
2	3.500		2.53			
3	-22.230		0.50	1.497	81.6	Glass
4	2.968		0.37			
5	3.201	ASP	1.86	1.689	31.2	Glass
6	12.935	ASP	0.89			
Stop						
8	2.263	ASP	0.78	1.544	56.1	COC
9	-1.652	ASP	0.02			
10	-17.025	ASP	0.36	1.650	21.5	Special PC
11	2.138	ASP	0.31			
12	-21.933	ASP	1.19	1.535	56.3	COP
13	-1.007	ASP	0.11			
14	1.726	ASP	0.45	1.590	31.5	PS
15	0.736	ASP	0.72			
16	Infinity		0.11	1.517	64.2	Glass
17	Infinity		0.30			
Image						

Table 4.3 Values of the conic constant and the aspheric surface coefficients of A_3 - A_9 in each of the aspheric surfaces of the optimized lens system

Surface	K	A_3	A_4	A_5
5	0	0	3.110×10^{-3}	0
6	-9.069	0	5.327×10^{-3}	0
8	-0.840	0	-4.531×10^{-2}	0
9	1.682	0	8.129×10^{-2}	0
10	10.000	-1.919×10^{-2}	-7.616×10^{-2}	-2.629×10^{-2}
11	-9.232	-7.872×10^{-3}	-2.758×10^{-2}	6.929×10^{-2}
12	4.605	-9.656×10^{-3}	1.071×10^{-1}	-9.253×10^{-2}
13	-3.434	-4.358×10^{-2}	-2.892×10^{-2}	6.387×10^{-2}
14	-3.444	-5.405×10^{-2}	-1.690×10^{-1}	5.373×10^{-2}
15	-3.433	3.796×10^{-2}	-2.468×10^{-1}	1.691×10^{-1}
Surface	A_6	A_7	A_8	A_9
5	1.365×10^{-4}	0	-1.467×10^{-5}	0
6	-1.480×10^{-3}	0	8.782×10^{-4}	0
8	-8.525×10^{-2}	0	1.097×10^{-1}	0
9	5.194×10^{-2}	0	-8.612×10^{-2}	0
10	8.815×10^{-2}	1.045×10^{-1}	7.758×10^{-3}	-1.395×10^{-1}
11	-1.117×10^{-2}	-2.825×10^{-2}	2.499×10^{-2}	4.278×10^{-2}
12	2.632×10^{-2}	2.663×10^{-2}	9.506×10^{-3}	-3.166×10^{-2}
13	-9.523×10^{-2}	4.095×10^{-2}	1.539×10^{-2}	1.469×10^{-2}
14	1.076×10^{-2}	1.088×10^{-2}	-3.194×10^{-3}	-3.456×10^{-3}
15	-2.653×10^{-2}	-1.439×10^{-2}	4.406×10^{-3}	1.680×10^{-4}

Table 4.4 Values of the aspheric surface coefficients of A_{10} - A_{16} in each of the aspheric surfaces of the optimized lens system

Surface	A_{10}	A_{11}	A_{12}	A_{13}
5	1.302×10^{-5}	0	0	0
6	-1.431×10^{-4}	0	0	0
8	-3.102×10^{-1}	0	5.277×10^{-3}	0
9	1.017×10^{-1}	0	-1.819×10^{-2}	0
10	8.467×10^{-2}	0	0	0
11	-2.740×10^{-2}	0	0	0
12	1.317×10^{-2}	0	0	0
13	-1.130×10^{-2}	0	0	0
14	7.843×10^{-4}	4.440×10^{-4}	-2.248×10^{-4}	0
15	7.010×10^{-5}	1.674×10^{-5}	-4.243×10^{-5}	0

Surface	A_{14}	A_{15}	A_{16}
5	0	0	0
6	0	0	0
8	1.129×10^{-3}	0	0
9	6.589×10^{-3}	0	1.871×10^{-2}
10	0	0	0
11	0	0	0
12	0	0	0
13	0	0	0
14	0	0	0
15	0	0	0

In the original lens system, L7 was made of COP. As L7 had negative refractive power in the area near the optical axis, it was desirable to employ a material with smaller ν_d than COP with ν_d of ~56 in order to compensate for chromatic aberration. On the other hand, since L7 had weak but positive refractive power in the area away from the optical axis, it was also necessary to avoid making overcompensation for chromatic aberration at the peripheral area of the image, when using a material with small ν_d. In this case, by replacing it with PS which possesses ν_d of 31.5, the chromatic aberration in the area near the optical axis could be greatly improved while maintaining the resolution at the peripheral area. This can be confirmed by the results of the transverse ray-aberration curves and MTF charts. In the transverse ray-aberration curves shown in Figure 4.5 and Figure 4.8, the optimized lens system, including L7 composed of ideal PS, demonstrated a smaller color spread between C-line and F-line at IH 0%, 30%, and 60% than the original lens system, including L7 composed of COP. The optimized lens system was especially improved at IH 30%, while color spreads at any other image heights were comparable between the two lens systems. This smaller color spread indicates that chromatic aberration of the optimized lens system has been improved. Similarly, when choosing a modulation value of 20% as each evaluation frequency in the MTF charts shown in Figure 4.6 and Figure 4.9, which is commonly employed as the criterion of MTF for achieving appropriate image quality of a lens system,[114] the optimized lens system with L7 of ideal PS exhibited much higher frequency at IH 30% than the original lens system with L7 of COP, while both lens systems showed almost the same frequencies at any other image height. The frequency values of tangential MTF corresponding 20% modulation at IH 0%, 30%, 60%, 80%, and 100% are summarized in Table 4.5. As a supplement, it can be another option to replace it with a material such as special PC or fluorene polyester possessing smaller ν_d than 30 and low birefringence. It is, however, not desirable considering the high cost of the material as mentioned in the section 4.1 Background and purpose. These results indicate that employing ideal PS with no birefringence as a lens material in specific lens systems should be very effective in raising the resolution of the lens systems, where the systems have a wide field of view with compensation lenses such as L7.

Table 4.5 Frequency values of tangential MTF corresponding 20% modulation

Image height	Original lens system with L7 of COP (cycles/mm)	Optimized lens system with L7 of ideal PS (cycles/mm)
0% (On-axis)	442	442
30%	322	372
60%	264	269
80%	208	213
100%	170	177

4.3.3 Estimation of the resolution considering the effect of birefringence

The amount of actual birefringence that affected the resolution performance was estimated using the optical design data of the original lens system with L7 of COP and the optimized lens system with L7 of PS. Each amount of orientation birefringence at the strain of 120% measured for COP, linear PS and LB-PS in the previous section was assigned to L7 in each lens system on CODE V, i.e., assuming that the amount of birefringence may appear in the manufacturing process of COP and PS lenses. The situation, where strain occurs throughout the lens, would not normally occur in an actual lens sample. In the case of plastic lenses, maximum retardation can only occur near the gate of the lens. The light rays passing through the area with this retardation are affected by the birefringence, resulting in degradation of resolution. Accordingly, the resolution degradation based on this assumption can occur at certain points in the image plane. It is considered that this assumption is reasonable as a simulation to estimate the worst-case resolution performance in the image plane.

The resolution of each lens system was then evaluated by comparing each MTF. Figure 4.10 - 4.12 show MTF vs. spatial frequency charts of lens systems at IH 0%, 30%, 60%, 80%, and 100% considering birefringence of COP, linear PS and LB-PS on L7, respectively. The MTF charts with the birefringence of COP ($\Delta n = 2.1 \times 10^{-3}$) are shown in Figure 4.10, The charts with the birefringence of linear PS ($\Delta n = -6.9 \times 10^{-3}$) are shown in Figure 4.11, and the charts with the birefringence of LB-PS ($\Delta n = -3.9 \times 10^{-4}$) are shown in Figure 4.12. For the computational studies in this section, all materials except for L7

were assumed to have no birefringence in order to compare the actual effects of L7 only. In this simulation, L7 was assumed to be the material of uniaxial crystals for assigning birefringence in CODE V, and the optic axis of L7 was defined as the direction along the image height in the cross-section diagrams in Figure 4.4 and Figure 4.7. Therefore, when the birefringence value was positive, the delayed axis, which indicates the direction of higher refractive index, was defined to be along the optic axis.

In the original lens system with L7 of COP, by considering the birefringence of COP shown in Figure 4.10, MTFs demonstrated some degradations at IH 30%, 60% and 80%, compared to MTFs without considering birefringence shown in Figure 4.6. However, the degradation was not so severe that this lens system was still practical for producing resolution up to full high definition. In the optimized lens system with L7 of PS, MTFs with the birefringence of linear PS shown in Figure 4.11 severely dropped at IH 30%, 60% and 80%, compared to MTFs without considering birefringence shown in Figure 4.9. Figure 4.11 also illustrated that the MTFs at IH 60% and 80% represented spurious resolution in the region over 170 cycles/mm spatial frequency, indicating a significant degradation in resolution performance. The spurious resolution is a phenomenon in which black and white patterns are inverted, so detailed patterns, that are not originally resolved, appear to be resolved. In addition, the MTFs exhibited much lower resolution than the ones of the original lens system considering the birefringence of COP. This eventually proves that linear PS could not be utilized as an optical material for imaging lens systems requiring high resolution. In contrast, MTFs considering the birefringence of LB-PS shown in Figure 4.12 maintained almost the same values as the MTFs without considering birefringence, exhibiting higher resolution than the original lens system considering the birefringence of COP. The frequency values corresponding 20% modulation at IH 0%, 30%, 60%, 80%, and 100% are summarized in Table 4.6. The results indicate that, in manufactured practical lens systems, the birefringence of the linear PS may significantly degrade MTF, while the birefringence of the developed LB-PS demonstrated almost no degradation in MTF. Moreover, it was found that the optimized lens system with L7 of LB-PS could possess higher resolution than the original lens system with L7 of COP, in considering birefringence as well.

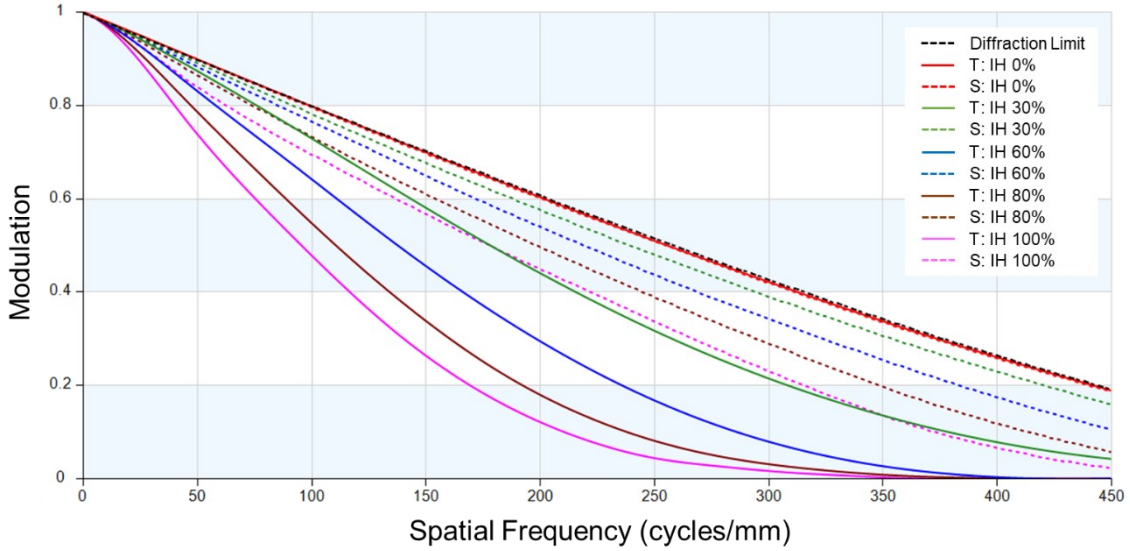

Figure 4.10 MTF vs. spatial frequency charts of the original lens system with L7 of COP including birefringence

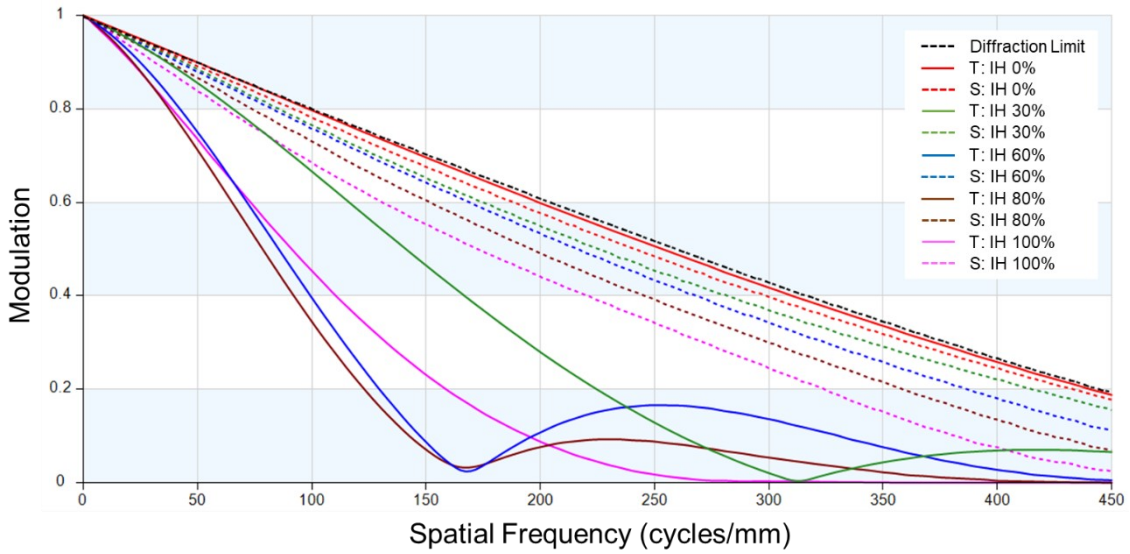

Figure 4.11 MTF vs. spatial frequency charts of the optimized lens system with L7 of linear PS including birefringence

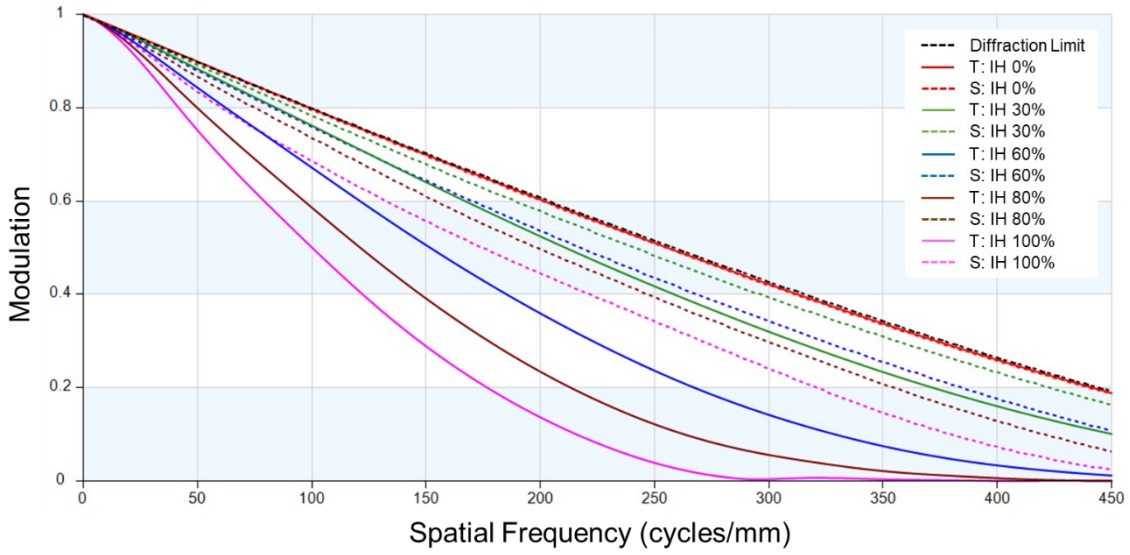

Figure 4.12 MTF vs. spatial frequency charts of the optimized lens system with L7 of LB-PS including birefringence

Table 4.6 Frequency values of tangential MTF corresponding 20% modulation for the original lens system and the optimized lens system considering birefringence of L7

Image height	COP $\Delta n = 2.1 \times 10^{-3}$ (cycles/mm)	Linear PS $\Delta n = -6.9 \times 10^{-3}$ (cycles/mm)	LB-PS $\Delta n = -3.9 \times 10^{-4}$ (cycles/mm)
0% (On-axis)	442	422	442
30%	308	226	371
60%	236	129	268
80%	192	123	213
100%	169	160	177

In order to visually compare the resolution performance between linear PS and LB-PS, image simulation was run for each lens system. Figure 4.13 shows a flow diagram of the image simulation and representative pictures on each process of the simulation. First, the enhanced eSFR-ISO-chart which was provided from Imatest LLC through CODE V was prepared as an input object. As the chart possessed a wedge pattern to evaluate resolution power up to 4000-line width per picture height (LW/PH), it was selected as the object for this simulation. Then, the raw image after passing through each

lens system including linear PS and LB-PS was simulated with CODE V. Since each raw image had a lot of distortion and darkness, post-processing to compensate for the distortion and the darkness was conducted so as not to affect the resolution to evaluate. Finally, the resolutions of the processed images were compared between the respective lens systems.

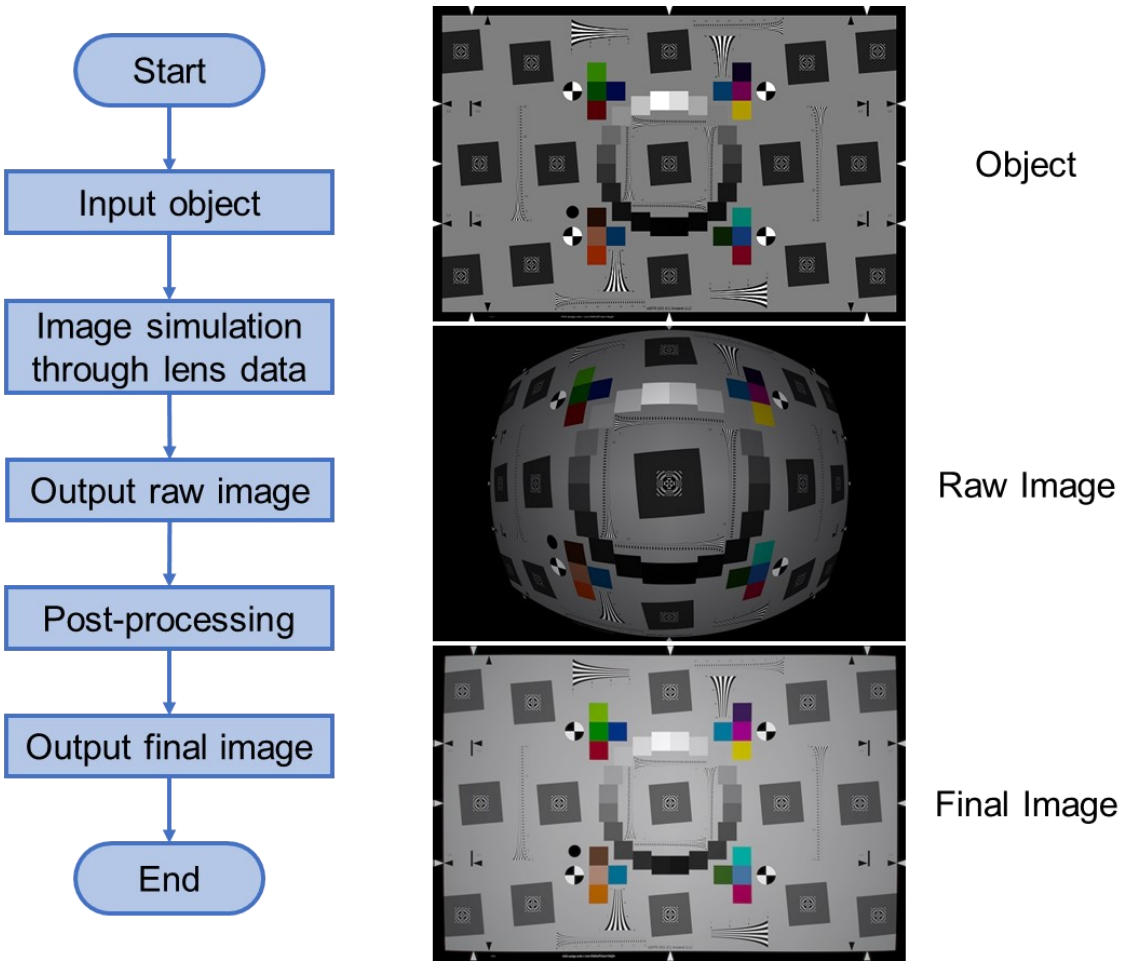

Figure 4.13 Flow diagram of the image simulation and representative pictures on each process of the simulation

Figure 4.14 is the image simulated through the lens system including linear PS, along with the enlarged diagram of a wedge pattern to estimate the resolution power in the eSFR-ISO-chart. Figure 4.15 is the one for the lens system including LB-PS. The images visually demonstrate that the lens system including the LB-PS produced the resolution beyond 1500 LW/PH, while the lens system including linear PS possessed just the resolution of ~1000 LW/PH. These results indicate that birefringence had a significant effect on the practical resolution of the lens system. It was also confirmed that LB-PS contributed greatly to generation of high-resolution images. Specifically, recent flagship smartphones are equipped with a super wide-angle camera composed of a lens system including a compensation lens such as L7 handled in this study. Also, the lens systems, which are used in recent inexpensive security cameras with a wide field of view, consist of similar configurations. Therefore, employing LB-PS as a material of the compensation lens should be very effective in raising the resolution of such lens systems with a wide field of view in smartphone cameras and security cameras.

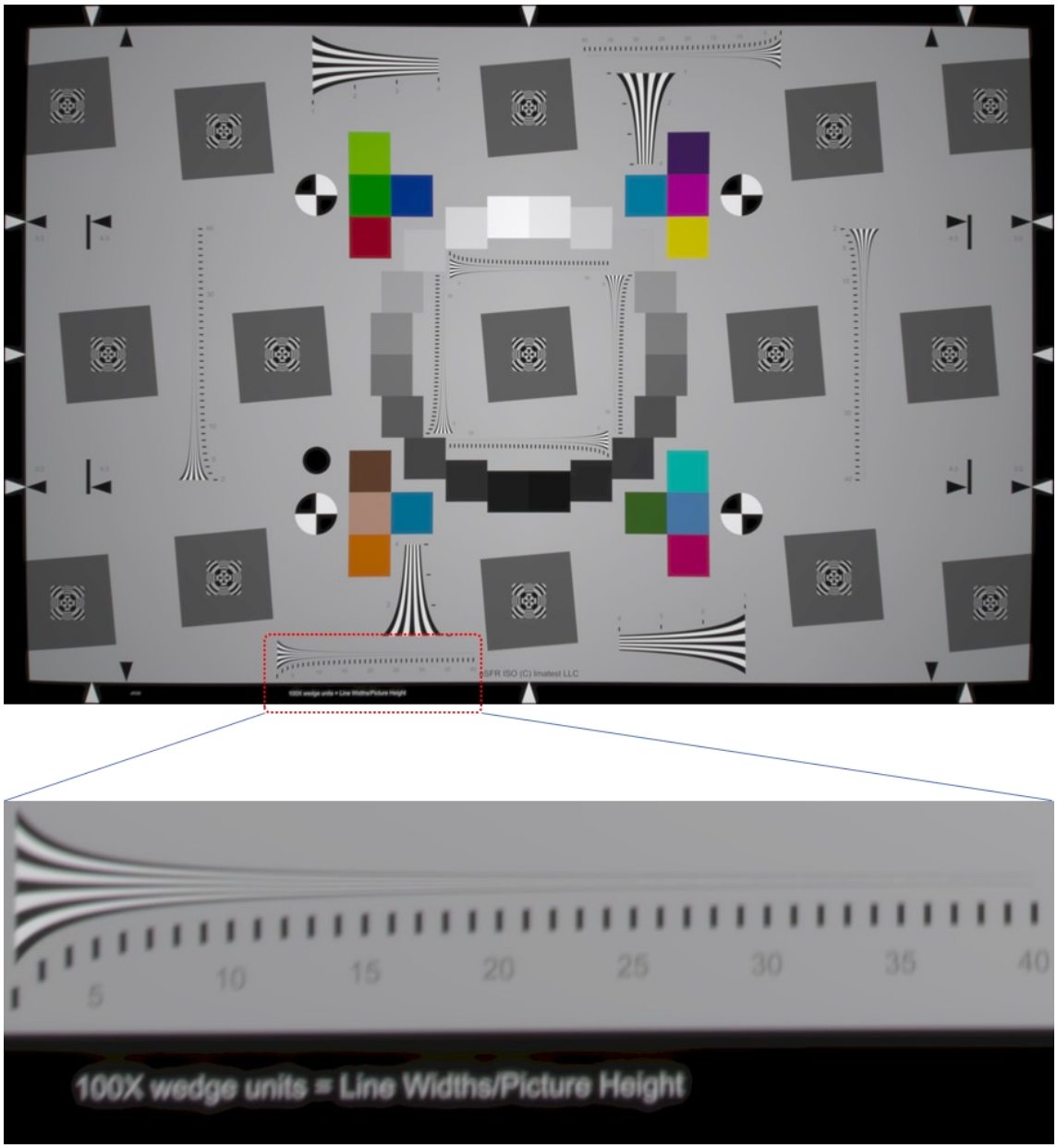

Figure 4.14 Image of the eSFR-ISO-chart simulated through the lens system including linear PS

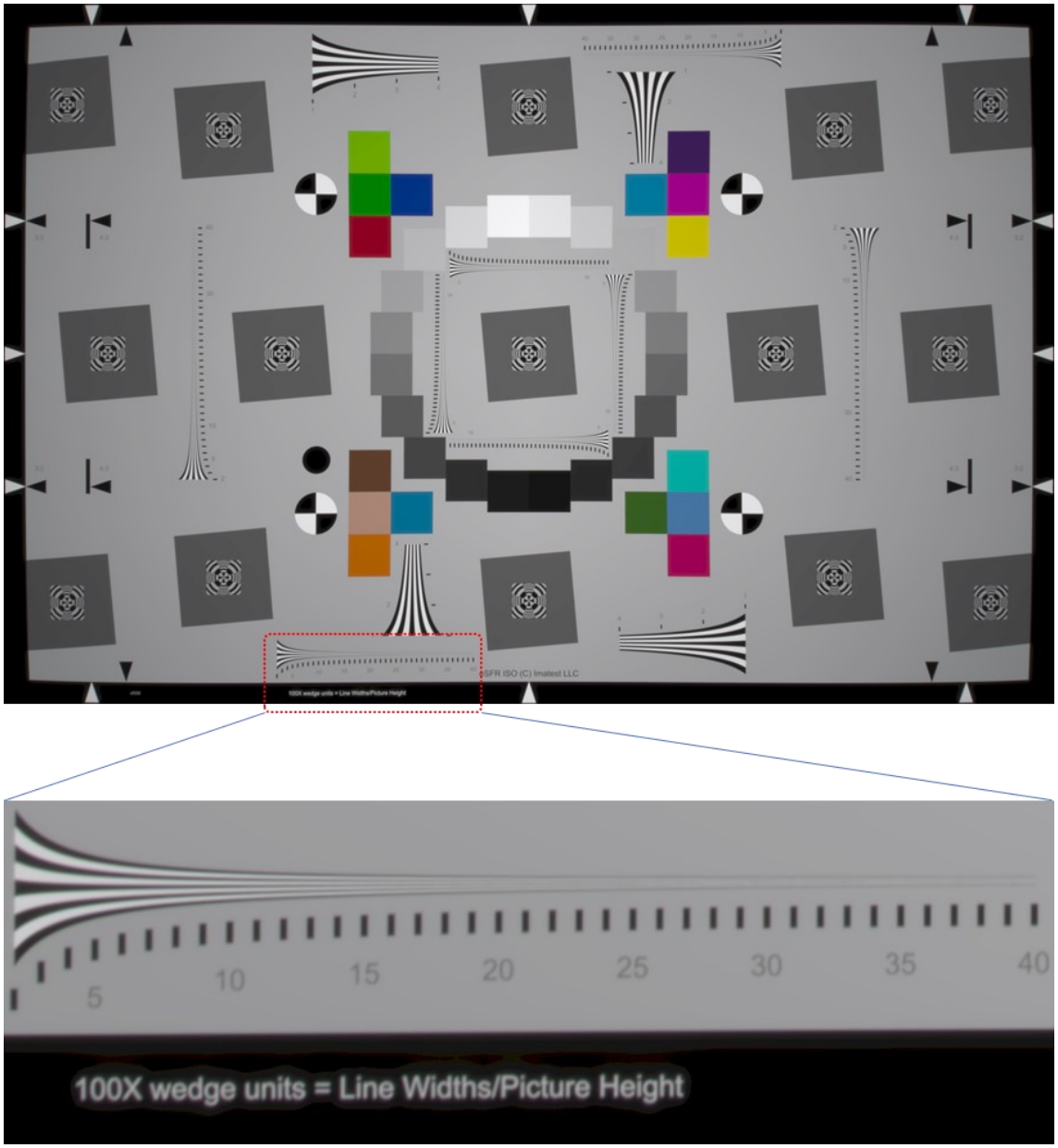

Figure 4.15 Image of the eSFR-ISO-chart simulated through the lens system including LB-PS

4.4 Summary of this chapter

In this chapter, in order to further clarify the effectiveness of LB-PS developed in Chapter 3, orientation birefringence of LB-PS was compared with that of two commercial optical polymers which are most commonly used in lens systems of smartphone cameras, and a distinct advantage of utilizing LB-PS in an optical lens system as a lens material was confirmed through resolution performance of the lens system designed on optical design software. The achievements were listed as follows:

i. Orientation birefringence of LB-PS was evaluated by comparing it with those of COP (ZEONEX-K26R) and COC (APL-5014CL) which are two commercial optical polymers most commonly used in high-resolution lens systems of flagship smartphone cameras. When estimated in terms of absolute values of birefringence, LB-PS demonstrated lower values than ZEONEX-K26R and almost the same values as APL-5014CL. It indicated that LB-PS could be a promising optical material with low birefringence for high-resolution lens systems.

ii. Optical design of a high-resolution imaging lens system using ideal PS, which was assumed to be zero birefringence, was executed on the optical design software. A lens system, in which PS was not used as a lens material, was first selected in patent data of imaging lens systems with high resolution. By replacing COP of L7 in the lens system with ideal PS and optimizing the entire lens system with the same constraints as the specifications of the original lens system, chromatic aberration and resolution performance of the lens system were improved. It illustrated that employing ideal PS with ν_d of 31.5 as a lens material was very effective in compensating for chromatic aberration in specific lens systems and raising the resolution.

iii. In order to assess the influence of birefringence to resolution of images, resolution performance was evaluated using the optical design data considering birefringence. Each measured value of orientation birefringence of COP, linear PS and LB-PS was

assigned to L7 in each lens system, the practical resolution was estimated with MTF and image simulation on the optical design software. The results illustrated that LB-PS could maintain as high resolution as the ideal PS with no birefringence while linear PS with high birefringence showed significant degradation in resolution of the lens system. Furthermore, it was also indicated that the optimized lens system with L7 of LB-PS possessed higher resolution than the original lens system with L7 of COP, even in the case of considering birefringence. These results revealed that birefringence made a serious effect on practical resolution of lens systems, and that LB-PS could be an excellent optical material to enhance the practical resolution performance while compensating for chromatic aberration of lens systems.

Chapter 5

Conclusion

In this paper, the new method to compensate for orientation birefringence was demonstrated, and the excellent polystyrene with low birefringence and high-dispersion property was developed. Moreover, practical effectiveness of the material was clarified through the design data of the specific lens system. The results were summarized as follows:

i. New bottlebrush polymers with well-controlled graft chains composed of poly(methyl methacrylate) (PMMA) were synthesized, and when they were mixed with linear PMMA appropriately, almost zero birefringence could be attained. In detail, the new PMMA bottlebrush polymers (PMMA-BBP) were synthesized by ring-opening metathesis polymerization of norbornene-terminated PMMA macromonomers prepared via atom transfer radical polymerization. Afterward, linear PMMA and PMMA-BBP were mixed to fabricate blend-film samples (PMMA/PMMA-BBP), which were uniaxially drawn to induce molecular orientations. Linear PMMA possessed a negative value for its orientation birefringence, while the value of PMMA/PMMA-BBP increased as the PMMA-BBP content increased. Finally, orientation birefringence could reach almost zero when the ratio of the linear PMMA to PMMA-BBP became 73:27 regardless of the magnitude of strain. The results revealed that orientation birefringence of PMMA could be effectively controlled and removed by blending the appropriate content of PMMA-BBP. In addition, the glass transition temperatures (T_g) of PMMA/PMMA-BBP were detected at ~110°C, indicating no significant differences in that of linear PMMA. Moreover, refractive indices (n_d) and the Abbe numbers (ν_d) of PMMA/PMMA-BBP showed almost the same n_d and ν_d as linear PMMA. These

results demonstrated that compensation for birefringence with PMMA-BBP had little effect on properties such as T_g, n_d and ν_d. On the other hand, PMMA/PMMA-BBP exhibited decrease of transmittance at shorter wavelength than 550 nm. In addition, as the content ratio of PMMA-BBP in PMMA/PMMA-BBP increased more, transmittance of the sample decreased more. As assumed that the decrease of transmittance resulted from bromine (Br) contained in ATRP initiators, it was suggested that the synthetic process should be revised to improve transparency.

ii. Outstanding polystyrene (PS) with extremely low orientation birefringence and high transparency was developed by mixing linear PS and bottlebrush polymers with well-controlled PS graft chains (PS-BBP). In detail, PS-BBP were synthesized by ring-opening metathesis polymerization of norbornene-terminated PS macromonomers produced via atom transfer radical polymerization. Blend-film samples (PS/PS-BBP) were then prepared by mixing linear PS with PS-BBP, and uniaxially drawn to introduce molecular orientations. Linear PS indicated a negative value for its orientation birefringence as well as linear PMMA, the value of PS/PS-BBP increased as the PS-BBP content increased in the same manner as PMMA/PMMA-BBP. Then, PS/PS-BBP with a specific ratio of linear PS to PS-BBP (30:70) demonstrated extremely low orientation birefringence of $|\Delta n| \sim 3.9 \times 10^{-4}$ even under 120% of strain. This result revealed that PS/PS-BBP with the blending ratio of 30:70 could be a promising material for an optical polymer with a high chromatic dispersion and low orientation birefringence. As for the T_g, while linear PS and PS-BBP exhibited only one T_g each at ~104°C and ~89°C, respectively, PS/PS-BBP showed both T_g derived from linear PS and PS-BBP. So, it was suggested that phase separation could occur between linear PS and PS-BBP. However, since the difference of T_g between linear PS and PS-BBP was only about 15°C, PS/PS-BBP could be utilized as an optical polymer by choosing appropriate thermal condition in the manufacturing process. In addition, PS/PS-BBP maintained almost the same n_d and ν_d as linear PS, as well as those of PMMA/PMMA-BBP. Furthermore, PS/PS-BBP possessed high transparency required for optical polymers across the visible-wavelength range due

to the revised synthesis process in which the adverse effects of Br were eliminated. The results indicated that the obtained PS blend could be utilized as an optical material with excellent optical properties.

iii. Practical effectiveness of the developed PS with extremely low birefringence (LB-PS) was clarified through comparison with commercial optical polymers and design data of a specific lens system. In detail, birefringence of LB-PS developed in Chapter 3 was compared with ones of COP (ZEONEX-K26R) and COC (APL-5014CL) which are most commonly utilized in imaging lens systems requiring high resolution, confirming the comparable or better birefringence-property of LB-PS. It was then illustrated that employing PS with $\nu_d = 31.5$ in design of an imaging lens system was very effective in compensating chromatic aberration and improving resolution. Furthermore, resolution performance of each lens system was estimated in consideration of birefringence of COP, linear PS and LB-PS, respectively. It was demonstrated that LB-PS could maintain high resolution while linear PS with high birefringence showed significant decrease in resolution, also indicating that LB-PS generated higher resolution than COP. These results revealed that LB-PS could be an excellent optical material to compensate for chromatic aberration of lens systems and enhance the actual resolution performance. It is highly expected that LB-PS would contribute to realizing better resolution performance of optical devices such as smartphone cameras and security cameras.

In the following, challenges to the practical application of this approach are discussed. In this study, the excellent polystyrene with low birefringence and high-chromatic-dispersion property was developed. However, several further refinements would be necessary for the practical application. They are listed as follows:

a) Improvement of mechanical strength

Although mechanical strength of the PS blend was not checked in this study, a certain level of mechanical strength would be required to utilize the PS blend as a practical optical material. As mentioned in 3.3.3 Orientation birefringence, impact strength of

the film sample made from PS-BBP alone was too brittle to be processed into the desired rectangular sample. This implies that blends with a higher ratio of PS-BBP have weaker impact strength than linear PS. However, high impact strength is not really a prerequisite for its use as lens elements in lens systems. Because optical glass, which has long been used as lens elements, is also very fragile, while can be used for such applications. Therefore, the required impact strength of the PS blend depends on its manufacturing process. Since most lens elements made from polymers are processed by injection molding, the PS blend must have at least the impact strength to withstand the process. Specifically, it is necessary that the PS blend can withstand the force of ejection during release from the mold in the injection molding. Since the specific value for this impact resistance is not clear, it would need to be confirmed through prototyping in an injection molding process using the PS blend. In addition, the PS blend should have a tensile modulus (Young's modulus) that can withstand the external forces exerted by the lens assembly. Specifically, it would be preferrable for the PS blend to possess the Young's modulus higher than 2.1×10^3 MPa, which is the same value as that of PC for optical applications and is the lowest Young's modulus in optical polymers. To improve such mechanical strength of the PS blend, it can be very effective to increase the main-chain length of PS-BBP. Also, since the PS blend is a blended material, it may be effective to increase the main-chain length of linear PS mixed with PS-BBP.

b) Mass production of bottlebrush polymers

To apply the PS blend to practical optical applications, it is necessary to mass-produce PS-BBP with low cost while maintaining its quality. In this study, ATRP, which is a method in precise radical polymerizations, was adopted to synthesize PS side chains of PS-BBP. This was because the side-chain length of PS-BBP and the polydispersity of the side chains had to be precisely controlled to achieve reliable compensation for orientation birefringence with PS-BBP. However, it may not be realistic to mass-produce the side chains of PS-BBP using the precise radical polymerization such as ATRP. Because such procedure tends to be high cost in mass production due to its complicated process. Therefore, a method to more easily produce the side chains of

PS-BBP in the mass production should be found. In that case, it may be difficult to control the side-chain length of PS-BBP and the polydispersity of the side chains, leading to decrease in rigidity of the main chain of PS-BBP. Nevertheless, if the PS-BBP still retains enough functionality to compensate for birefringence of linear PS, it should be preferable to utilize the procedure for mass production of PS-BBP. Thus, it would be desirable to find a synthesis process for the side chains suitable for mass production and to optimize the degree of polymerization and the polydispersity of the side chains through the process.

c) Optimization of the material for injection molding

Since most lens elements made from polymers are manufactured through injection molding process, the PS blend must be optimized for the process when utilizing the material in mass production of lens elements. In particular, flowability during melting, which is called melt-flow-rate, is very important in the injection molding process and must be adjusted. This can be addressed by optimizing the length of the main chains of linear PS and PS-BBP as well as the method to improve mechanical strength. In addition, additives such as mold release agents and antioxidants, which play important roles in the injection molding process, should be properly selected for compatibility with the PS blend.

d) Further enhancement of thermal properties

As mentioned in 3.3.2 Thermal properties, the PS blend exhibited both T_g derived from linear PS and PS-BBP. It was not so critical to using the PS blend as an optical polymer. Because the difference of T_g between linear PS and PS-BBP was only about 15°C and can be addressed by selecting appropriate thermal condition in the manufacturing process. However, since less difference enhances flexibility of adjustment for process conditions in practical manufacture, it is desirable that T_g of PS-BBP is almost identical to that of linear PS. To increase in T_g of PS-BBP, it can be effective to select the monomer unit of the main chain in PS-BBP with T_g, which is higher than that of the norbornene unit used in this study and is close to that of linear PS. It may also be useful to increase the length of the grafted side chains while maintaining the elongation of the main chain in the BBP.

e) Further improvement of transparency

As mentioned in 3.3.6 Light Transmittance, the PS blend with low birefringence accomplished over 77% of light transmittance at 420nm by adopting the revised synthesis and purification process of PS-BBP. This transparency is sufficient for use in lens elements for lens systems in digital still cameras and smartphone cameras. Because such cameras possess a digital image device that converts the optical image formed by the imaging lens system into an electric signal and enables color correction. However, considering the use of the PS blend as an eyepiece lens for AR/VR devices, it may be necessary to further improve the transparency. The human eye, unlike such imaging devices, is not equipped with color correction and requires higher transmittance over the visible light range of 400 – 800 nm, hopefully over 80% transmittance. Therefore, it is preferable to further improve the transmittance in the short wavelength range of the PS blend. An effective method to reach such high transparency can be hydrogenation to the double bonds of norbornenes constituting the main chains of PS-BBP. Since the double bonds may be oxidized at high temperatures and cause a decrease in transmittance at the short wavelengths, elimination of the double bonds by the hydrogenation would be very promising. In addition, another promising approach may be the thorough reduction of halogens such as bromine to hydrogen using organotin compounds such as tributyltin in the synthesis of bottle brush polymers.

Finally, future perspectives of this study are discussed. This method of compensation for birefringence by blending a linear polymer with related bottlebrush polymers is not limited to materials with negative birefringence such as PMMA and PS. Actually, it is applicable to a wide variety of materials as long as the side chains of the bottlebrush polymer are composed of the same material as the original polymer. Therefore, it is also effective to optical materials with positive birefringence such as COP and PC, if the side chains of the bottlebrush polymer can be synthesized in the materials with positive birefringence. In addition, this approach can produce polymers with any birefringence which is less than the absolute value of birefringence the linear polymer

possesses. Thus, it can be very promising for production of optical elements that require arbitrary birefringence, such as quarter-wave plates and half-wave plates, which are optical elements to control polarization. Namely, this method is expected to be applicable not only to compensation for birefringence of various optical polymers but also to their polarization control. This new polymer blend will enable optical elements such as optical lenses with low birefringence or films with controlled polarization, and bring excellent optical properties to optical devices including these elements.

List of publications

Chapter 2

- Tamura, M.; Kurokawa, N.; Hotta, A. Compensation for orientation birefringence of PMMA by blending bottlebrush polymers composed of well-controlled graft chains. *ACS Macro Letters* **2022**, *11* (6), 799-804.

Chapter 3

- Tamura, M.; Kurokawa, N.; Hotta, A. Blending bottlebrush polymers for compensation of orientation birefringence of polystyrene for use as an optical polymer. *ACS Applied Polymer Materials* **2023**, *5* (12), 10245-10255.

Chapter 4

- Tamura, M.; Kurokawa, N.; Hotta, A. Application of low-birefringence polystyrene in high-resolution imaging-lens systems. *Optical Review* **2024**, *31* (4), 430-439.

International conference

- Tamura, M.; Kurokawa, N.; Hotta, A. Compensation for orientation birefringence of PMMA by bottlebrush polymers with high graft density, 37th International Conference of the Polymer Processing Society (PPS-37), Fukuoka, Apr.11-15 (**2022**).

Acknowledgements

This research was conducted under the supervision of Professor Atsushi Hotta, while the author was a doctoral student at the Graduate School of Science and Technology, Keio University.

First of all, I would like to express my deepest gratitude to my supervisor, Professor Atsushi Hotta, for giving me the opportunity to do research at the university and for his kind support in advancing my research. I would also like to thank him for his careful guidance in revising the papers and responding to peer review.

In addition to my supervisor, I would like to greatly thank Professor Tetsuya Suzuki, Professor Hiroaki Onoe, and Associate Professor Noriyoshi Arai for giving me the opportunity to discuss my research and for reviewing my doctoral dissertation.

Next, I would like to express my sincere appreciation to Dr. Naruki Kurokawa for closely giving me direction and advice on my research. Thanks to his guidance, I was able to accomplish my research.

I would also like to thank Dr. Tomoki Maeda for his advice on my research through the classes in the Hotta group and for refining my doctoral dissertation.

My appreciation also goes to the member of Hotta Group: Dr. Yusei Kobayashi, Dr. Shunsuke Tazawa, Dr. Koichiro Tashiro, Yuya Oyama, Kosaku Yano, Shuhei Takamura, Mu Kawashima, Kenta Hashimoto, Shoichiro Mori, Masatoshi Moriguchi, Kosuke Yoshimura, Junichi Asakuma, Iku Ota, Kei Matsumoto, Naoki Kamezaki, Manami Sato, Tomoyuki Nomura, Kai Hiraga, Takumi Koike, Hiromu Hiramatsu, Sei Yoshioka, Adriana Saikali, Shunsuke Ishizuka, Shigeki Okada, Suguru Morikaku, Shusaku Yoshinaka, Naoki Shioya, Yuya Yokogi, Gabin Goy, Satoshi Uchida, Rikuto Uchida, Mitsuru Onishi, Yuki Shinoda, Yutaro Takeuchi, Ryuya Hangai, Sena Asano, Nolwenn Rodriguez, Hibiki Ikawa, Ryota Kasai, Manato Teraoka, Shunsuke Yamamura, Daigo Odaka, Kanji Niimi, Taishi Fujiwara, Yasuaki Honda, Kotaro Yamaura, Kenshin Yamada, Celestin Brisset.

I am also grateful to Apple Inc. where I work for understanding that I do my

research at the university while working for the company. I am especially grateful to my team members at Yokohama Technology Center in Apple. In addition, I would like to thank Daisuke Yamada in Apple for his advice on molding optical polymers.

Finally, I would like to thank my family for their understanding and support for my research at graduate school, and I would like to thank my father who passed away in October 2021 while supporting me in my doctoral research.

References

[1] Muranaka, M. *Technology and application of plastic lens system*; CMC Publishing, **2003**.

[2] Kudo, H. *Control and improvement of high-refractive-index property of transparent polymers*; CMC Publishing, **2019**.

[3] Tanio, N. *Development and application of high-performance transparent polymers*; CMC Publishing, **2022**.

[4] Kidger, M. J. *Fundamental optical design*; SPIE Press, **2002**.

[5] Ward, I. M. *Structure and properties of oriented polymers*; Springer Science & Business Media, **2012**.

[6] Hermans, J.; Hermans, P.; Vermaas, D.; Weidinger, A. Quantitative evaluation of orientation in cellulose fibres from the X‐ray fibre diagram. *Recueil des Travaux Chimiques des Pays‐Bas* **1946**, *65* (6), 427-447.

[7] Kragh, H. The Lorenz-Lorentz formula: Origin and early history. *Substantia* **2018**, *2* (2), 7-18.

[8] Okada, Y.; Urakawa, O.; Inoue, T. Reliability of intrinsic birefringence estimated via the modified stress-optical rule. *Polymer Journal* **2016**, *48* (11), 1073-1078.

[9] Shafiee, H.; Tagaya, A.; Koike, Y. Mechanism of generation of photoelastic birefringence in methacrylate polymers for optical devices. *Journal of Polymer Science Part B: Polymer Physics* **2010**, *48* (19), 2029-2037.

[10] Inoue, T.; Kuwada, S.; Ryu, D.-S.; Osaki, K. Effects of wavelength on strain-induced birefringence of polymers. *Polymer journal* **1998**, *30* (11), 929-934.

[11] Hahn, B. R.; Wendorff, J. H. Compensation method for zero birefringence in oriented polymers. *Polymer* **1985**, *26* (11), 1619-1622.

[12] Saito, H.; Inoue, T. Chain orientation and intrinsic anisotropy in birefringence‐free polymer blends. *Journal of Polymer Science Part B-Polymer Physics* **1987**, *25* (8), 1629-1636.

[13] Nishio, Y.; Haratani, T.; Takahashi, T. Miscibility and orientation behavior of poly

(vinyl alcohol)/poly (vinyl pyrrolidone) blends. *Journal of Polymer Science Part B-Polymer Physics* **1990**, *28* (3), 355-376.

[14] Nishio, Y.; Suzuki, H.; Sato, K. Molecular orientation and optical anisotropy induced by the stretching of poly (vinyl alcohol) poly (N-vinyl pyrrolidone) blends. *Polymer* **1994**, *35* (7), 1452-1461.

[15] Uchiyama, A.; Yatabe, T. Analysis of extraordinary birefringence dispersion of uniaxially oriented poly(2,6-dimethyl 1,4-phenylene oxide)/atactic polystyrene blend films. *Japanese Journal of Applied Physics* **2003**, *42* (Part 1, No. 6A), 3503-3507.

[16] Ohno, T.; Nishio, Y. Molecular orientation and optical anisotropy in drawn films of miscible blends composed of cellulose acetate and poly(N-vinylpyrrolidone-co-methyl methacrylate). *Macromolecules* **2007**, *40* (9), 3468-3476.

[17] Yamaguchi, M.; Masuzawa, K. Birefringence control for binary blends of cellulose acetate propionate and poly(vinyl acetate). *European Polymer Journal* **2007**, *43* (8), 3277-3282.

[18] Iwata, S.; Tsukahara, H.; Nihei, E.; Koike, Y. Compensation for birefringence of oriented polymers by random copolymerization method. *Japanese Journal of Applied Physics Part 1-Regular Papers Short Notes & Review Papers* **1996**, *35* (7), 3896-3901.

[19] Iwata, S.; Tsukahara, H.; Nihei, E.; Koike, Y. Transparent zero-birefringence copolymer and its optical properties. *Applied Optics* **1997**, *36* (19), 4549-4555.

[20] Tagaya, A.; Harada, T.; Koike, K.; Koike, Y.; Okamoto, Y.; Teng, H.; Yang, L. Improvement of the physical properties of poly(methyl methacrylate) by copolymerization with pentafluorophenyl methacrylate. *Journal of Applied Polymer Science* **2007**, *106* (6), 4219-4224.

[21] Ban, H. T.; Hagihara, H.; Nishii, K.; Tsunogae, Y.; Nojima, S.; Shiono, T. A new approach for controlling birefringent property of cyclic olefin copolymers. *Journal of Polymer Science Part A: Polymer Chemistry* **2008**, *46* (22), 7395-7400.

[22] Kojo, T.; Tagaya, A.; Koike, Y. Mechanism of generation of birefringence in poly(methyl methacrylate/styrene). *Polymer Journal* **2011**, *44* (2), 167-173.

[23] Shafiee, H.; Tagaya, A.; Koike, Y. Design and synthesis of a zero-photoelastic birefringence polymer with a high glass-transition temperature by a random copolymerization method. *Polymer Journal* **2011**, *43* (3), 306-312.

[24] Iwasaki, S.; Satoh, Z.; Shafiee, H.; Tagaya, A.; Koike, Y. Design and synthesis of zero-zero-birefringence polymers in a quaternary copolymerization system. *Polymer* **2012**, *53* (15), 3287-3296.

[25] Lou, L. P.; Tagaya, A.; Ide, Y.; Koike, Y.; Okamoto, Y. Copolymers of methyl methacrylate with N-trifluorophenyl maleimides: High glass transition temperature and low birefringence polymers. *Journal of Polymer Science Part a-Polymer Chemistry* **2012**, *50* (17), 3530-3536.

[26] Tagaya, A.; Lou, L.; Ide, Y.; Koike, Y.; Okamoto, Y. Improvement of the physical properties of poly(methyl methacrylate) by copolymerization with N-pentafluorophenyl maleimide; zero-orientational and photoelastic birefringence polymers with high glass transition temperatures. *Science China Chemistry* **2012**, *55* (5), 850-853.

[27] Iwasaki, S.; Satoh, Z.; Shafiee, H.; Tagaya, A.; Koike, Y. Design of zero-zero-birefringence polymers in methacrylate copolymer systems containing trichloroethyl methacrylate. *Journal of Applied Polymer Science* **2013**, *130* (1), 138-144.

[28] Beppu, S.; Iwasaki, S.; Shafiee, H.; Tagaya, A.; Koike, Y. Design and synthesis of zero–zero‐birefringence polymers using N‐methylmaleimide. *Journal of Applied Polymer Science* **2014**, *131* (12).

[29] Beppu, S.; Hotta, H.; Shafiee, H.; Tagaya, A.; Koike, Y. Investigation of optical and thermal properties of N-(alkyl-substituted) maleimides for use in zero-zero-birefringence polymer. *Appl Opt* **2015**, *54* (4), 779-788.

[30] Shafiee, H.; Beppu, S.; Iwasaki, S.; Tagaya, A.; Koike, Y. Mechanisms of orientational and photoelastic birefringence generation of methacrylates for the design of zero-zero-birefringence polymers. *Polymer Engineering and Science* **2015**, *55* (6), 1330-1338.

[31] Tagaya, A.; Iwata, S.; Kawanami, E.; Tsukahara, H.; Koike, Y. Zero-birefringence

polymer by the anisotropic molecule dope method. *Applied Optics* **2001**, *40* (22), 3677-3683.

[32] Tagaya, A.; Iwata, S.; Kawanami, E.; Tsukahara, H.; Koike, Y. Anisotropic molecule dopant method for synthesizing a zero-birefringence polymer. *Japanese Journal of Applied Physics Part 1-Regular Papers Short Notes & Review Papers* **2001**, *40* (10), 6117-6123.

[33] Ohkita, H.; Ishibashi, K.; Tanaka, R.; Tagaya, A.; Koike, Y. Compensation of photoelastic birefringence of polymers by anisotropic molecules and analysis of compensation mechanism. *Japanese Journal of Applied Physics* **2005**, *44* (6R).

[34] Ohkita, H.; Ishibashi, K.; Tsurumoto, D.; Tagaya, A.; Koike, Y. Compensation of the photoelastic birefringence of a polymer by doping with an anisotropic molecule. *Applied Physics A* **2005**, *81* (3), 617-620.

[35] Abd Manaf, M. E.; Miyagawa, A.; Nobukawa, S.; Aoki, Y.; Yamaguchi, M. Incorporation of low-mass compound to alter the orientation birefringence in cellulose acetate propionate. *Optical Materials* **2013**, *35* (7), 1443-1448.

[36] Songsurang, K.; Shimada, H.; Nobukawa, S.; Yamaguchi, M. Control of three-dimensional refractive indices of uniaxially-stretched cellulose triacetate with low-molecular-weight compounds. *European Polymer Journal* **2014**, *59*, 105-112.

[37] Kiyama, A.; Nobukawa, S.; Yamaguchi, M. Birefringence control of solution-cast film of cellulose triacetate. *Optical Materials* **2017**, *72*, 491-495.

[38] Tagaya, A.; Ohkita, H.; Mukoh, M.; Sakaguchi, R.; Koike, Y. Compensation of the birefringence of a polymer by a birefringent crystal. *Science* **2003**, *301* (5634), 812-814.

[39] Ohkita, H.; Tagaya, A.; Koike, Y. Preparation of a zero-birefringence polymer doped with a birefringent crystal and analysis of its characteristics. *Macromolecules* **2004**, *37* (22), 8342-8348.

[40] Koike, Y.; Yamazaki, K.; Ohkita, H.; Tagaya, A. Zero‐birefringence optical polymer by birefringent crystal and analysis of the compensation mechanism. *Macromolecular Symposia* **2006**, *235* (1), 64-70.

[41] Tagaya, A.; Ohkita, H.; Koike, Y. Zero-birefringence optical polymers by nano-

birefringent crystals for liquid crystal displays. *Materials Science and Engineering: C* **2006**, *26* (5-7), 966-970.

[42] Yamada, Y.; Tagaya, A.; Koike, Y. Birefringence analysis of a photonics polymer doped with a birefringent crystal. In *Conference on Organic Photonic Materials and Devices XI*, San Jose, CA, Jan 27-29, **2009**; Vol. 7213.

[43] Shafiee, H.; Shikama, K.; Tagaya, A.; Hardinghaus, F.; Miyaji, T.; Köhler, K.; Koike, Y. Control of the birefringence dispersion of an optical polymer by doping with an inorganic crystal. *Japanese Journal of Applied Physics* **2011**, *50* (3R).

[44] Unohara, T.; Teramoto, Y.; Nishio, Y. Molecular orientation and optical anisotropy in drawn films of cellulose diacetate-graft-PLLA: comparative investigation with poly(vinyl acetate-co-vinyl alcohol)-graft-PLLA. *Cellulose* **2011**, *18* (3), 539-553.

[45] Yamanaka, H.; Teramoto, Y.; Nishio, Y. Orientation and birefringence compensation of trunk and graft chains in drawn films of cellulose acetate-graft-PMMA synthesized by ATRP. *Macromolecules* **2013**, *46* (8), 3074-3083.

[46] Nobukawa, S.; Enomoto-Rogers, Y.; Shimada, H.; Iwata, T.; Yamaguchi, M. Effect of acetylation site on orientation birefringence of cellulose triacetate. *Cellulose* **2015**, *22* (5), 3003-3012.

[47] Nobukawa, S.; Nakao, A.; Songsurang, K.; Pulkerd, P.; Shimada, H.; Kondo, M.; Yamaguchi, M. Birefringence and strain-induced crystallization of stretched cellulose acetate propionate films. *Polymer* **2017**, *111*, 53-60.

[48] Hatamoto, K.; Shimada, H.; Kondo, M.; Nobukawa, S.; Yamaguchi, M. Effect of acetyl substitution on the optical anisotropy of cellulose acetate films. *Cellulose* **2018**, *25* (8), 4453-4462.

[49] Nobukawa, S.; Shimada, H.; Aoki, Y.; Miyagawa, A.; Doan, V. A.; Yoshimura, H.; Tachikawa, Y.; Yamaguchi, M. Extraordinary wavelength dispersion of birefringence in cellulose triacetate film with anisotropic nanopores. *Polymer* **2014**, *55* (15), 3247-3253.

[50] Shimada, H.; Nobukawa, S.; Yamaguchi, M. Development of microporous structure and its application to optical film for cellulose triacetate containing diisodecyl adipate. *Carbohydr Polym* **2015**, *120*, 22-28.

[51] Beers, K. L.; Gaynor, S. G.; Matyjaszewski, K.; Sheiko, S. S.; Möller, M. The synthesis of densely grafted copolymers by atom transfer radical polymerization. *Macromolecules* **1998**, *31* (26), 9413-9415.

[52] Venkatesh, R.; Yajjou, L.; Koning, C. E.; Klumperman, B. Novel brush copolymers via controlled radical polymerization. *Macromolecular Chemistry and Physics* **2004**, *205* (16), 2161-2168.

[53] Matyjaszewski, K.; Wang, J.-L.; Grimaud, T.; Shipp, D. A. Controlled/"living" atom transfer radical polymerization of methyl methacrylate using various initiation systems. *Macromolecules* **1998**, *31* (5), 1527-1534.

[54] Tsukahara, Y.; Mizuno, K.; Segawa, A.; Yamashita, Y. Study on the radical polymerization behavior of macromonomers. *Macromolecules* **1989**, *22* (4), 1546-1552.

[55] Jha, S.; Dutta, S.; Bowden, N. B. Synthesis of ultralarge molecular weight bottlebrush polymers using Grubbs' catalysts. *Macromolecules* **2004**, *37* (12), 4365-4374.

[56] Xia, Y.; Kornfield, J. A.; Grubbs, R. H. Efficient Synthesis of Narrowly Dispersed Brush Polymers via Living Ring-Opening Metathesis Polymerization of Macromonomers. *Macromolecules* **2009**, *42* (11), 3761-3766.

[57] Deng, G.; Chen, Y. Cylindrical molecular brushes with a loose grafting density. *Journal of Polymer Science Part A: Polymer Chemistry* **2009**, *47* (20), 5527-5533.

[58] Moughton, A. O.; Sagawa, T.; Gramlich, W. M.; Seo, M.; Lodge, T. P.; Hillmyer, M. A. Synthesis of block polymer miktobrushes. *Polym. Chem.* **2013**, *4* (1), 166-173.

[59] Zhang, M.; Müller, A. H. E. Cylindrical polymer brushes. *Journal of Polymer Science Part A: Polymer Chemistry* **2005**, *43* (16), 3461-3481.

[60] Zhang, Y.; He, H.; Gao, C. Clickable macroinitiator strategy to build amphiphilic polymer brushes on carbon nanotubes. *Macromolecules* **2008**, *41* (24), 9581-9594.

[61] Verduzco, R.; Li, X.; Pesek, S. L.; Stein, G. E. Structure, function, self-assembly, and applications of bottlebrush copolymers. *Chem Soc Rev* **2015**, *44* (8), 2405-2420.

[62] Chen, P. B.; Gao, X. Y. Optical design of the 13 mega-pixels mobile phone camera. In *3rd International Conference on Materials Engineering, Manufacturing Technology and Control (ICMEMTC)*, Taiyuan, PEOPLES R CHINA, Feb 27-28, **2016**; Vol. 67, pp 835-840.

[63] Ryu, T.-S.; Park, S.-C. Achromatic and athermal design of a mobile-phone camera lens by redistributing optical first-order quantities. *Current Optics and Photonics* **2023**, *7* (3), 273-282.

[64] Dalsin, S. J.; Hillmyer, M. A.; Bates, F. S. Linear rheology of polyolefin-based bottlebrush polymers. *Macromolecules* **2015**, *48* (13), 4680-4691.

[65] Kurokawa, N.; Kimura, S.; Hotta, A. Mechanical properties of poly(butylene succinate) composites with aligned cellulose‐acetate nanofibers. *Journal of Applied Polymer Science* **2017**, *135* (24).

[66] Wang, J. S.; Matyjaszewski, K. Controlled/" living" radical polymerization. atom transfer radical polymerization in the presence of transition-metal complexes. *Journal of the American Chemical Society* **1995**, *117* (20), 5614-5615.

[67] Kato, M.; Kamigaito, M.; Sawamoto, M.; Higashimura, T. Polymerization of methyl methacrylate with the carbon tetrachloride/dichlorotris-(triphenylphosphine) ruthenium (II)/methylaluminum bis (2, 6-di-tert-butylphenoxide) initiating system: possibility of living radical polymerization. *Macromolecules* **1995**, *28* (5), 1721-1723.

[68] Shen, D. W.; Yong, H. The synthesis of CDA-g-PMMA copolymers through atom transfer radical polymerization. *Polymer* **2004**, *45* (21), 7091-7097.

[69] Verma, H.; Kannan, T. Atom transfer radical polymerization of methyl methacrylate using telechelic tribromo terminated polyurethane macroinitiator. *Journal of Macromolecular Science Part a-Pure and Applied Chemistry* **2010**, *47* (5), 407-415.

[70] Liu, H.; Zhou, W. Z.; Ye, H. Q.; Han, K.; Hou, S. C.; Zhang, X. Y. Effect of catalyst on formation of poly(methyl methacrylate) brushes by surface initiated atom transfer radical polymerization. *Journal of Central South University* **2014**, *21* (8), 3049-3056.

[71] Zhao, Y.; Jasse, B.; Monnerie, L. Fourier transform infrared study of orientation and relaxation in poly (methyl methacrylate). In *Makromolekulare Chemie. Macromolecular Symposia*, Sep, **1986**; Wiley Online Library: Vol. 5, pp 87-97.

[72] Tagaya, A.; Ohkita, H.; Harada, T.; Ishibashi, K.; Koike, Y. Zero-birefringence optical polymers. *Macromolecules* **2006**, *39* (8), 3019-3023.

[73] Ban, H. T.; Hagihara, H.; Tsunogae, Y.; Cai, Z.; Shiono, T. Highly thermostable and low birefringent norbornene-styrene copolymers with advanced optical properties: A potential plastic substrate for flexible displays. *Journal of Polymer Science Part A: Polymer Chemistry* **2011**, *49* (1), 65-71.

[74] Riedl, M. J. *Optical Design : Applying the Fundamentals*; SPIE, **2009**.

[75] Malacara, D.; Malacara, Z. *Handbook of optical design*; CRC Press, **2013**.

[76] Tagaya, A.; Koike, K.; Koike, Y.; Okamoto, Y. Effect of trifluoromethyl substituents on birefringence of polystyrene. *Polymers for Advanced Technologies* **2017**, *28* (8), 994-999.

[77] Takamatsu, K.; Suzuki, S.; Nishimura, Y.; Saito, H. Reduction of birefringence by dynamic asymmetry in miscible blends of dissimilar polycarbonates. *Polymer* **2021**, *222*.

[78] Inoue, T. Strain-induced birefringence of amorphous polymers and molecular design of optical polymers. *ACS Applied Polymer Materials* **2021**, *3* (5), 2264-2273.

[79] Fu, Q.; Lin, W.; Huang, J. A new strategy for preparation of graft copolymers via "graft onto" by atom transfer nitroxide radical coupling chemistry: Preparation of poly(4-glycidyloxy-2,2,6,6-tetramethylpiperidine-1-oxyl-co-ethylene oxide)-graft-polystyrene and poly(tert-butyl acrylate). *Macromolecules* **2008**, *41* (7), 2381-2387.

[80] Morandi, G.; Heath, L.; Thielemans, W. Cellulose nanocrystals grafted with polystyrene chains through surface-initiated atom transfer radical polymerization (SI-ATRP). *Langmuir* **2009**, *25* (14), 8280-8286.

[81] Degirmenci, M.; Alter, S.; Genli, N. Synthesis and characterization of well-defined mid-chain functional macrophotoinitiators of polystyrene by combination

of ATRP and “click” chemistry. *Macromolecular Chemistry and Physics* **2011**, *212* (15), 1575-1581.

[82] Coffin, R. C.; Diamanti, S. J.; Hotta, A.; Khanna, V.; Kramer, E. J.; Fredrickson, G. H.; Bazan, G. C. Pseudo-tetrablock copolymers with ethylene and a functionalized comonomer. *Chem Commun (Camb)* **2007**, (34), 3550-3552.

[83] Shultz, A. R.; Flory, P. J. Phase equilibria in polymer-solvent systems. *Journal of the American Chemical Society* **1952**, *74* (19), 4760-4767.

[84] Hariharan, A.; Kumar, S. K.; Russell, T. P. A lattice model for the surface segregation of polymer chains due to molecular weight effects. *Macromolecules* **1990**, *23* (15), 3584-3592.

[85] Tanaka, K.; Takahara, A.; Kajiyama, T. Effect of polydispersity on surface molecular motion of polystyrene films. *Macromolecules* **1997**, *30* (21), 6626-6632.

[86] Okayama, Y.; Nakahara, K.; Arouette, X.; Ninomiya, T.; Matsumoto, Y.; Orimo, Y.; Hotta, A.; Omiya, M.; Miki, N. Characterization of a bonding-in-liquid technique for liquid encapsulation into MEMS devices. *Journal of Micromechanics and Microengineering* **2010**, *20* (9).

[87] Mahmoudi, P.; Matsen, M. W. Entropic segregation of short polymers to the surface of a polydisperse melt. *Eur Phys J E Soft Matter* **2017**, *40* (10), 85.

[88] Hill, J. A.; Endres, K. J.; Mahmoudi, P.; Matsen, M. W.; Wesdemiotis, C.; Foster, M. D. Detection of surface enrichment driven by molecular weight disparity in virtually monodisperse polymers. *ACS Macro Lett* **2018**, *7* (4), 487-492.

[89] Stein, G. E.; Laws, T. S.; Verduzco, R. Tailoring the attraction of polymers toward surfaces. *Macromolecules* **2019**, *52* (13), 4787-4802.

[90] Lojkowski, M.; Chlanda, A.; Choinska, E.; Swieszkowski, W. Water vapor induced self-assembly of islands/honeycomb structure by secondary phase separation in polystyrene solution with bimodal molecular weight distribution. *Sci Rep* **2021**, *11* (1), 13299.

[91] Rizzo, P.; Albunia, A. R.; Guerra, G. Negatively birefringent polymer films. *Macromolecular Chemistry and Physics* **2009**, *210* (24), 2148-2152.

[92] Jeong, J.; Park, D.; Lee, J. H. Simultaneous retardation compensation during bending of plastic film coated with a polymer layer of opposite birefringence. *Appl Opt* **2016**, *55* (31), 8738-8742.

[93] Ryu, H. J.; Hwang, J.; Kim, J.; Lee, J. H. Dependence of the birefringence of polystyrene film on the stretching conditions. *Appl Opt* **2018**, *57* (2), 268-272.

[94] Kolsky, H. Stress-birefringence in polystyrene. *Nature* **1950**, *166* (4214), 235-236.

[95] Steinich, T.; Blahnik, V. Optical design of camera optics for mobile phones. *aot* **2012**, *1* (1-2), 51-58.

[96] Ji-Yan, Z.; Yuan-qing, H.; Fei-bing, X.; Xian-guo, M. Design of 10 mega-pixel mobile phone lens. In *2013 Third International Conference on Instrumentation, Measurement, Computer, Communication and Control*, **2013**; pp 569-573.

[97] Kohara, T. Development of new cyclic olefin polymers for optical uses. *Macromolecular Symposia* **1996**, *101* (1), 571-579.

[98] Yamazaki, M. Industrialization and application development of cyclo-olefin polymer. *Journal of Molecular Catalysis A: Chemical* **2004**, *213* (1), 81-87.

[99] Khanarian, G. Optical properties of cyclic olefin copolymers. *Optical Engineering* **2001**, *40* (6), 1024.

[100] Yoon, K.-b.; Choi, J. S.; Lee, D.-h.; Hur, Y.; Noh, S. K. Synthesis and optical properties of cycloolefin copolymers for plastic substrates. *Molecular Crystals and Liquid Crystals* **2006**, *459* (1), 27/[307]-334/[314].

[101] Hasegawa, T.; Koyama, Y.; Seto, R.; Kojima, T.; Hosokawa, K.; Takata, T. Diphenolic 9,9-diarylfluorene trimers and derivatives possessing flexible alkylene chain spacers: Synthesis of the monomers, their polymerization, and properties of the resulting polymers. *Macromolecules* **2009**, *43* (1), 131-136.

[102] Nakazono, K.; Yamashita, C.; Ogawa, T.; Iguchi, H.; Takata, T. Synthesis and properties of pendant fluorene moiety-tethered aliphatic polycarbonates. *Polymer Journal* **2015**, *47* (5), 355-361.

[103] Sakurai, K.; Fuji, M. Optical properties of a low birefringence polyester containing fluorene side chain I. *Polymer Journal* **2000**, *32* (8), 676-682.

[104] Seesukphronrarak, S.; Kawasaki, S.; Kobori, K.; Takata, T. Fluorene-rich high

performance polyesters: Synthesis and characterization of 9,9-fluorenylidene and 2,7-fluorenylene-based polyesters with excellent optical property. *Journal of Polymer Science Part A: Polymer Chemistry* **2008**, *46* (7), 2549-2556.

[105] Tanio, N. Improvement of transparency of optical polymers. *Kobunshi Ronbunshu* **2004**, *61* (1), 12-21.

[106] Tanio, N.; Obata, H.; Okada, A.; Segawa, S.; Takemura, Y.; Kaneko, M. Improvement of transparency of optical polymer by amorphous structure control. *Kobunshi Ronbunshu* **2009**, *66* (1), 1-9.

[107] Tanio, N.; Nakanishi, T. Physical aging and refractive index of poly(methyl methacrylate) glass. *Polymer Journal* **2006**, *38* (8), 814-818.

[108] Tanio, N.; Momono, Y.; Hosoi, K.; Okura, M.; Matuhara, J. Refractive index prediction system of optical polymers. *Kobunshi Ronbunshu* **2009**, *66* (1), 24-30.

[109] Tanio, N.; Tukahara, N. Physical aging and refractive index of optical polymer glass. *Kobunshi Ronbunshu* **2009**, *66* (1), 31-35.

[110] Kato, N.; Ikeda, S.; Hirakawa, M.; Ito, H. Relationship between degree of polymerization and optical and thermal properties of fluorene in polycarbonate polymers. *Journal of Applied Polymer Science* **2017**, *134* (30), 45042.

[111] Kato, N.; Ikeda, S.; Hirakawa, M.; Ito, H. Correlation of the Abbe number, the refractive index, and glass transition temperature to the degree of polymerization of norbornane in polycarbonate polymers. *Polymers (Basel)* **2020**, *12* (11), 2484.

[112] Higashihara, T.; Ueda, M. Recent progress in high refractive index polymers. *Macromolecules* **2015**, *48* (7), 1915-1929.

[113] Tamura, M.; Katsuragi, D.; Nihei, Y.; Kanai, F.; Sakae, K. Imaging unit and imaging apparatus with rotatable lens group for optical vibration isolation. United States US 10491825 B2, **2019**.

[114] Kim, D.; Chang, S.; Kwon, H.-S. Wide field-of-view, high-resolution endoscopic lens design with low F-number for disposable endoscopy. *Photonics* **2021**, *8* (4), 89.